Università degli Studi di Padova

Dipartimento di Fisica e Astronomia "Galileo Galilei"

Master Degree in Physics

Final Dissertation

Scattering Processes via Tensor Network Simulations

Candidate:

Marco Rigobello

Supervisor:

Prof. Simone Montangero

Academic Year 2019–2020

Abstract

Scattering processes are a crucial ingredient for the investigation of fundamental interactions. The ever-increasing amount of data produced at particle colliders has fuelled recent progresses in the field of scattering amplitudes computation. To date, on the numerical side, the results achieved are mainly based on Monte-Carlo simulations. In this Thesis the problem is attacked with a different approach: a real-time simulation of the dynamics of a $1+1$ dimensional quantum field theory is performed, exploiting the powerful tensor network methods from many-body theory. A matrix product state representation of the asymptotic input states is identified, allowing for the preparation of the initial momentum wave packets. This initial state is then evolved and we aim to compute the S-matrix elements from the knowledge of the final state. We focus on a specific fermionic $U(1)$ gauge model, developing a set of tools which are relevant for a broader class of $1 + 1$ dimensional quantum field theories with global or local symmetries.

Contents

Introduction

Gauge theories are the cornerstone of our current understanding of the fundamental laws of nature. Apart from the Standard Model of particle physics, gauge theories and more in general the framework of quantum field theory, have found important applications in condensed matter physics [43, 75], e.g., in the study of superconductivity [10, 64]. Motivated by the extreme relevance of the topic, the investigation of quantum field theories has played a central role in physics research since their introduction. This has lead to outstanding results and countless experimentally tested predictions, mostly coming from a perturbative expansion around well known free theories [49]. Nevertheless, because of its nature, the perturbative approach is viable only in weak coupling regimes. Even in this regime the perturbative series is known to be generally ill defined and plagued by divergencies that have to be cured order by order via regularization and renormalization procedures [50, 77]. On the other hand, despite all the efforts put forward by the physics community over the last fifty years, we still lack non-perturbative control of any $1 + 3$ dimensional interacting quantum field theory [77]. Lattice quantum field theory poses itself as a candidate solution of both the aforementioned problems. It does this by reformulating the theory as a quantum many-body system. On a conceptual level, this approach might provide an alternative, non-perturbative, way of defining quantum field theories [68]. On a more practical level, the lattice has proven to be a successful framework for the numerical computation of quantities of physical interest, especially in theories or regimes outside the domain of application of the perturbative expansion [102]. In particle physics, the paradigmatic way of probing the properties of elementary particles are scattering experiments [49]. It follows that numerical simulations of these processes are a crucial tool for the comparison of the measurements carried out at particle colliders with the predictions of theoretical models.

The numerical simulation of many-body systems, and thus lattice field theories, is an extremely demanding task [87]. Its complexity stems from the exponential growth of the Hilbert space dimension with the size of the system. To circumvent this obstacle, most numerical investigations have been based on Monte-Carlo methods, which evaluate of phase space integrals by stochastic sampling [102]. However, integrals involving fermions often exhibit an highly oscillatory behaviour that causes a severe increase in the sampling complexity. This is the infamous sign problem [102]. A complementary approach to the study of many-body systems, proposed by Feynman in 1982 [37], is quantum computation. The basic idea is that of emulat-

ing the system of interest with another, more controllable, quantum system, called simulator. Exploiting quantum phenomena such as interference and entanglement, these devices can potentially perform many-body calculations with resources that scale polynomially with the system size [100]. Quantum simulators are synthetic quantum systems made of, e.g., trapped ions, ultra-cold atoms in optical lattices or superconducting circuits. They are divided in two classes, analog and digital simulators [97], that differ in how the emulation is achieved. Analog simulators are engineered specifically to reproduce the degrees of freedom and the dynamics of the investigated system, while in digital simulators the dynamics of the target system is obtained by applying sequence of short quantum operations or gates. In the recent years there have been some experimental realizations [76, 88, 92] of various simulating platforms. Moreover, some studies and platforms target specifically the simulation of lattice gauge theories [81, 84, 87–89, 97, 104]. Together with the implementation of quantum computation techniques, the development of efficient classical numerical methods still remains an important research topic [97], at least for two reasons. The first being that classical methods can be used to benchmark quantum simulators [87]. The second reason is that recent feasibility studies [101, 103] have shown that the technologies currently available are not yet capable of reliable large scale quantum computations, especially for simulations tackling the complicated dynamics of lattice gauge theories. It is thus important to develop quantum-inspired numerical techniques able to reproduce closely both the theory of interest and the behaviour of a quantum simulator. The state-of-the-art in this regard are tensor network methods [87, 95]. For many important physical systems, tensor networks overcome the exponential growth of the Hilbert space dimension by discarding the irrelevant information contained in an exact representation of the many-body Hilbert space [80]. In this way they allow to represent the state and the operators of the many-body system and solve standard quantum mechanical problems, e.g., evaluate ground states and time evolutions. This is achieved without resorting to stochastic methods and thus avoiding the sign problem [90].

In this thesis we lay out the ingredients that are needed to set up a tensor network simulation of a scattering process. To this aim we present the Hamiltonian lattice formulation of abelian and nonabelian gauge theories and study some tensor network methods. We focus on $1 + 1$ dimensional problems and implement the relevant numerical codes. We demonstrate the applicability of the methods we have presented, and partly developed, by reporting the simulation of meson-meson scatterings in the lattice Schwinger model [9]. In particular, we show that tensor networks are capable of simulating these processes for various coupling strenghts, discuss the role played entanglement generation and characterize the numerical convergence of the simulations.

This Thesis is organized as follows.

Continuum Theories. In the first Chapter the foundations of relativistic quantum field theory are recalled. A definition of particle is given and an idealized scattering process is characterized. We put forward a strategy to extract S-matrix elements from transition amplitudes evaluated on a finite spacetime.

The Lagrangian formalism is reviewed and used to construct the relativistic theories of Dirac and Yang-Mills fields. We expose the geometric structure behind gauge theories, which will allow a smooth transition to the lattice setting. The Hamiltonian formalism is reviewed as it provides the natural language for the implementation of tensor network simulations, as well as quantum simulations. The Hamiltonian description of Dirac and Yang-Mills fields is developed following the Dirac-Bergmann theory of constrained systems and the Yang-Mills Gauss law constraint is derived. The Chapter terminates with a review of the canonical quantization prescription.

Lattice Theories. In the second Chapter the principles of Hamiltonian lattice quantum field theory are outlined. The plan for the reminder of the Chapter is the following: we first reformulate the theories introduced in the continuum as classical Hamiltonian systems with a finite number of degrees of freedom and, afterwards, quantize them. In this way, the mathematical inconsistencies typically encountered in the quantization of continuum field theories are avoided. The first step is partially covered introducing a discretization prescription. The quantization formally follows the same procedure introduced at the end of the previous Chapter.

In the implementation of the above plan, some peculiarities emerge for both matter and gauge fields. Matter fields are affected by the fermion doubling problem, which we solve introducing Kogut-Susskind staggered fermions. The quantized theory of free staggered fermions is analyzed in detail. We solve its equations of motion, find the particle spectrum and show it reproduces that of a well-defined free quantum field theory. Gauge fields are discretized adopting a compact formulation, where the fundamental degrees of freedom are group valued comparators and representatives for the electric field.

We specialize to the quantized lattice Schwinger model. We introduce three strategies to cope with the infinite dimensional photon Hilbert space. The first one exploits Gauss law to integrate the gauge field degrees of freedom; the others are truncation prescriptions. Finally, we discuss the confining properties of the model and put forward a proposal for the construction of its asymptotic meson states.

Tensor Networks.   In the third Chapter the general properties of quantum many-body systems are discussed. We emphasize the exponential scaling of the dimension of the Hilbert space with the system size. The entanglement entropy is introduced and some far reaching results, known as area laws, are recalled. These identify tensor networks as an efficient classical method for the simulation of one dimensional lattice systems. Two tensor network ansatze, namely matrix product states and operators, are presented; ground state search and time evolution algorithms are outlined.

Scattering Simulations.   In the last Chapter we present the results of our numerical simulations. We first test the numerical tools developed in this Thesis simulating the kinematics of free staggered fermions wave packets and verifying it complies with the analytic results obtained in the second Chapter. Then, we investigate the lattice Schwinger model in a moderately weak coupling regime. We attack the scattering problem with approaches, either integrating out the gauge field or with tensor networks, and discuss their feasibility. The outcome of some proof of principle scattering simulations is reported, together with a study of their numerical convergence.

Notations and Conventions

We use natural units, so that the speed of light and the Planck constant are set to one, $c = \hbar = 1$. The dimension of spacetime is $D = 1 + d$, d being space dimension. In the first chapter the spacetime coordinate is denoted by $x = (x^\mu) = (x^0, x^i) = (t, \mathbf{x})$. We adopt the mostly minuses metric signature, $(+, -, \ldots, -)$.

The following families of indices are implicitly contracted:

  ∗ Lorentz vector indices μ, ν, ρ, σ (and sometimes α, β);

  ∗ Lorentz spinor indices α, β (generally omitted);

  ∗ internal symmetry algebra indices $a, b, c, \ldots$;

  ∗ internal symmetry group indices r, s (denoting an irreducible representation);

  ∗ generic indices m, n transforming under both the Lorentz and internal group.

More specific contraction conventions are introduced in some Sections of the Thesis. We use the Feynman slash notation $v^\mu \gamma_\mu = \slashed{v}$, where γ_μ are the gamma matrices defined in (1.43).

For Grassmann variables we always use left derivatives and complex conjugation is defined by $(FG)^* = G^* F^*$. The (super) Poisson bracket $\{\,\cdot\,,\,\cdot\,\}$ is defined in (1.61).

We use the Dirac $\langle$bra$|$ket$\rangle$ notation to represent pure quantum states. From the second Chapter we omit the hat on operators and denote the graded commutator $[\,\cdot\,,\,\cdot\,]_\pm$ defined in Section 1.5 by $[\,\cdot\,,\,\cdot\,]$.

Lattice Conventions.

We represent Euclidean space as d-dimensional hypercubic lattice Λ with lattice spacing ℓ and linear size ℓL. The position coordinate is $x = (x^i)$, $x^i = \ell, 2\ell, \ldots, L\ell$. Summations involving space coordinates x, y, z, w always extend over Λ. Summations involving momenta k, p, q are over the reciprocal lattice defined in (2.2); unless the starred sum $\sum^\star$ symbol is used, in which case they are restricted to the sublattice (2.42). We typically work in lattice units, $\ell = 1$.

The same notation, either by index or by argument, is used to denote the variable of discrete and continuous functions. This applies also to δ functions which can be either Kronecker deltas or Dirac deltas. The symbol ∂ is used for both the continuous derivative and the discrete central derivative defined in (2.3). For all these objects the distinction should be clear from the context.

$$\text{(A)} \quad \begin{aligned} \varphi(\omega, k) &= \frac{1}{2\pi L^d} \int \mathrm{d}\omega \sum_x e^{+i\omega t - i\sum_j k^j x^j} \varphi(t, x) \\ \varphi(t, x) &= \int \mathrm{d}\omega \sum_k e^{-i\omega t + i\sum_j k^j x^j} \varphi(\omega, k) \end{aligned}$$

$$\text{(B)} \quad \begin{aligned} \varphi(k) &= \frac{1}{L^{d/2}} \sum_x e^{-i\sum_j k^j x^j} \varphi(x) \\ \varphi(x) &= \frac{1}{L^{d/2}} \sum_k e^{+i\sum_j k^j x^j} \varphi(k) \end{aligned}$$

$$\text{(C)} \quad \begin{aligned} \Gamma(x, y) &= \int_{-\pi}^{+\pi} \mathrm{d}p \, \mathrm{d}q \, e^{+ip_\mu x^\mu + iq_\mu y^\mu} \Gamma(p, q) \\ (2\pi)^D \delta(p + q)\Gamma(p, q) &= \sum_{xy} e^{-ip_\mu x^\mu - iq_\mu y^\mu} \Gamma(x, y) \end{aligned}$$

Table 1: Normalization and sign conventions for Fourier transforms. (A) is adopted for functions of discrete space and continuous time and in Appendix B also for functions of space only. (B) is adopted for functions of space only, notice it is an isometry. (C) is adopted in Subsection 2.3A to compute a propagator on an infinite and discrete spacetime, in this case only x, y and p, q are D-vectors rather than d-vectors.

In Chapter 2 and Appendix B we compute various continuous and discrete Fourier transforms. Functions and their Fourier transforms are generally denoted with the same symbol and distinguished by their argument. Different normalizations are used for Fourier transforms of different objects. These are summarized in Table 1.

Tensor Networks Acronyms.

In Chapter 3 various acronyms for tensor network related concepts are introduced. These are reported below, together with their meaning.

SVD	Singular Value Decomposition
SV	Singular Value
TN	Tensor Network
MPS	Matrix Product State
MPO	Matrix Product Operator
DMRG	Density Matrix Renormalization Group
TEBD	Time Evolving Block Decimation

1

Continuum Theories

In this Chapter the basic principles of quantum field theory are presented. Some concepts of scattering theory, relevant for the numerical simulations of Chapter 4, are discussed. Classical Lagrangian and Hamiltonian gauge theories are reviewed with the aim of developing a description that naturally fits in the lattice framework introduced in Chapter 2. Finally, a quantization prescription appropriate for the numerical tools introduced in Chapter 3 is elaborated.

1.1 Relativistic Quantum Mechanics

Quantum field theories (QFTs) have emerged as the natural way to reconcile the principles of *quantum mechanics* with those of *special relativity*. The quantum mechanical interpretation of the theory requires that when "maximal information" about the configuration of the system is available, this information is identified with a pure state, i.e. a *ray* in a Hilbert space $\mathscr{H}$. A ray is an equivalence class of normalized Hilbert space vectors that differ only by a phase[1]. Relativistic covariance requires that $\mathscr{H}$ carries a *representation* of the Poincaré group of spacetime symmetries. The quantum mechanical description mandates this representation to be *projective* and *unitary*. Namely, that it is realized by unitary operators defined only up to a group element dependent phase[2]. Besides spacetime (or external) symmetries, the theory may posses other (internal) symmetries that have to be represented on $\mathscr{H}$ as well. Anyhow, under some reasonable assumptions, the *Coleman-Mandula* no-go theorem [14] states that continuous external and internal symmetries have to be combined in the "trivial" way, in the sense that the overall symmetry algebra must be the direct sum of the Poincaré algebra and another Lie algebra $\mathfrak{g}$. This result greatly simplifies the tractation as it allow to study the two symmetries separately.

---

[1] Measurable quantities, namely expectation values of observables $\langle \Psi | \hat{\mathcal{O}} | \Psi \rangle$ and transition probabilities $|\langle \Phi | \Psi \rangle|^2$, are clearly representative independent. The phase is void of physical significance.

[2] This is the most general well-defined action of a continuous symmetry transformation on Hilbert space rays. If the phase can be reabsorbed the representation is equivalent to an ordinary unitary representation, otherwise it is said to be intrinsically projective. Discrete symmetries may also be implemented by antiunitary operators, this is the case of time reversal [50].

In the light of these observations, we now focus on some consequences of spacetime symmetries, which are a mandatory feature of every relativistic theory. A more specific qualification of the internal symmetry group is postponed to the next Sections.

Spacetime symmetries. By spacetime here it is meant the Minkowski $D = 1 + d$ dimensional affine space equipped with the "mostly-minus" metric tensor $\eta_{\mu\nu}$,

$$\mathbb{R}^{1,d} = \left\{ x^\mu = (x^0, x^i) = (t, \mathbf{x}) , \ i = 1, \ldots, d \right\}, \qquad \eta = \text{diag}(+, - \ldots, -) . \quad (1.1)$$

The group of spacetime symmetries is the Poincaré or inhomogeneous Lorentz group[3]

$$\text{IO}(1, d) = \text{O}(1, d) \ltimes \mathbb{R}^{1,d} \tag{1.2}$$

of isometries of Minkowski spacetime. Namely, affine transformations consisting of an homogeneous Lorentz group $\text{O}(1, d)$ transformation $\Lambda^\mu{}_\nu$ and a translation a^μ,

$$(\Lambda, a) \colon x^\mu \mapsto \Lambda^\mu{}_\nu x^\nu + a^\mu , \qquad \eta_{\mu\nu} \Lambda^\mu{}_\rho \Lambda^\nu{}_\sigma = \eta_{\rho\sigma} . \tag{1.3}$$

Other than the physical space $d = 3$ case, hereafter also $d = 1$ is considered as the tensor network methods studied in this Thesis have been employed in the study of gauge theories only for spacetime dimension lower than $1 + 3$ and, until very recently [98], only in $1 + 1$. It should be kept in mind that not all the results that hold for $d = 3$ extend straightforwardly to lower dimensions, e.g., the Coleman-Mandula theorem holds only for $d > 1$ [59]. In such cases we proceed by analogy.

Particles. The aim of this Thesis is to lay the foundations for a numerical simulation of the scattering of particles. It is thus important to define what a particle is in the context of in high energy physics and, more generally, relativistic QFT. According to Wigner's classification [3] particles are identified with subspaces of $\mathscr{H}$ carrying an *irreducible* (projective, unitary) representation of the symmetry group of the theory[4]. These are labeled by some symmetry invariant quantum numbers, to be identified. Translations commute thus their generators on $\mathscr{H}$, namely the components $\hat{P}^\mu$ of the *energy-momentum* operator, can be simultaneously diagonalized. The $\hat{P}^\mu$ are not Lorentz invariant but the mass squared operator $\hat{M}^2 = \hat{P}_\mu \hat{P}^\mu$ is. Its eigenvalues m^2 provide a first quantum number. In general the *mass spectrum* might include both of a discrete and a continuous part. It is only the discrete part orthog-

---

[3] In this Thesis we take parity and time reversal as valid spacetime symmetries, see Appendix A.

[4] An overview of these representations for $d = 3$ as well as $d = 1$ is given in Appendix A.

onal to the *vacuum* $|\Omega\rangle$, $\hat{P}^\mu |\Omega\rangle = 0$, that can be related to single particle states[5]. The continuous part corresponds to multi-particle states [52]. In $d = 3$ there is also a quantum number $j \in \mathbb{N}/2$ associated with the generators of rotations, the spin or, for $m = 0$, the magnitude of the helicity. Finally, other quantum numbers related to the internal symmetry group might be present.

1.2 Particle Scattering

The paradigmatic particle physics experiment consists in preparing the system by specifying its content in localized and far-distant regions of space to resemble that of a single particle. This initial state of, typically two, effectively non-interacting particles is then let evolve, the particles approach each other and interact. During the interaction the multi-particle state interpretation is lost. It is recovered when the products of the collision are again well separated, making their description independent one from the others. The observer may then measure transition probabilities by comparing the appearance of this final state with that of the initial one. We shall now make this picture more precise and concrete, mostly following [50].

It has been observed that particles are irreducible symmetry-invariant subspaces of the Hilbert space $\mathscr{H}$ that correspond to an isolated mass shell. Inside such a subspace, a state can be singled out specifying its spatial momentum $\mathbf{p}$ and possibly a spin projection σ (in $d = 3$) and some other discrete labels related to the internal group. States specified in this way are called *single particle states* or *bound states* and denoted $|p\sigma\alpha\rangle$, were α collects all the remaining labels including one identifying the particle specie. By definition, under Poincaré transformations $\hat{U}(\Lambda, a)$, these states transform as

$$\hat{U}(\Lambda, a) |p\sigma\alpha\rangle = \sqrt{\frac{(\Lambda p)^0}{p^0}} \exp(-ia_\mu p^\mu) \sum_{\sigma'} W^{(\alpha)}_{\sigma'\sigma}(\Lambda, p) |(\Lambda p)\sigma'\alpha\rangle \ . \qquad (1.4)$$

Here $W^{(\alpha)}(\Lambda, p)$ is a representative of the little group[6] of particle type α and the coefficient in front of the right hand side serves to make the normalization

$$\langle q\tau\beta | p\sigma\alpha \rangle = \delta^d(\mathbf{q} - \mathbf{p})\delta_{\tau\sigma}\delta_{\beta\alpha} \qquad (1.5)$$

consistent under Poincaré transformation.

An important point is that in the definition of particle there is no reference to it

---

[5] Complications here ignored arise if no sharp mass eigenvalues are present, as it happens in $1 + 3$ dimensional quantum electrodynamics. In such cases one speaks of *infraparticles* [52, 77].

[6] See Appendix A. In one space dimension $D(\Lambda, p) \equiv 1$ for all particle types.

being elementary with respect to the degrees of freedom of the theory. This is crucial in confined theories, such as quantum chromodynamics. There, at sufficiently low energies, the particles are internal group singlets (mesons, baryons and glueballs) and correspond to composite operators rather than to the colour charged quark and gluon fields that appear in the Hamiltonian of the theory [49]. An analogous phenomenon is present in the theory of $1+1$ dimensional quantum electrodynamics (QED$_2$) that we will introduce at the end of Chapter 2.

Free multi-particle states are defined to be states that transform as a tensor product of single particle states (1.4). In particular, for spacetime translations we have

$$\hat{U}(1,a)\,|\{p_k\,\sigma_k\alpha_k\}\rangle = e^{-ia_\mu\hat{P}^\mu}\,|\{p_k\,\sigma_k\alpha_k\}\rangle = \exp\left(-ia_\mu\sum_k p_k^\mu\right)|\{p_k\,\sigma_k\alpha_k\}\rangle\;,\quad(1.6)$$

where k indexes the particles in the state. Multi-particle states are normalized via a condition analogous to (1.5) but that also takes into account the indistinguishability of identical particles and their bosonic or fermionic statistics,

$$\langle\{q_k\tau_k\beta_k\}_{k=1}^N|\{p_j\,\sigma_j\alpha_j\}_{j=1}^M\rangle = \delta_{NM}\sum_{\mathfrak{S}}\mathrm{sgn}\,\mathfrak{S}\prod_i\delta^d(\mathbf{q}_{\mathfrak{S}i}-\mathbf{p}_i)\delta_{\tau_{\mathfrak{S}i}\sigma_i}\delta_{\beta_{\mathfrak{S}i}\alpha_i}\;,\quad(1.7)$$

where $\mathfrak{S}$ is a permutation of $1,2,\ldots,N$ and $\mathrm{sgn}\,\mathfrak{S}$ is -1 if an odd number of fermions exchanges is involved, $+1$ otherwise. It follows from transformation law (1.6) that these states are energy and momentum eigenstates belonging in the continuous part of the mass spectrum. Their total energy equates the sum of the energies of their "constituents", whence the "free" attribute. It also implies that multi-particle states cannot be localized and are time translation invariant. These states are clearly an idealization and are not actually realized in interacting theories. Nevertheless, superpositions of free multi-particle states can be localized and are realized as asymptotic configurations in nontrivial scattering processes. At least, this happens when the theory has a *mass gap*, namely when in the mass spectrum there is a finite separation between the vacuum and the lowest-lying single particle state. This guarantees that the interaction decays sufficiently fast [52, 77] and asymptotically particles are effectively non-interacting. In the following we always assume a mass gap is present.

We work in the Schrödinger picture[7] and assume that the instant $t=0$ occurs during the collision. The scattering experiment is described through a state

$$|\Psi(t)\rangle = e^{-itH}\,|\Psi\rangle\;,\quad(1.8)$$

---

[7]   The Schrödinger picture is not well suited for non-perturbative continuum QFT because it requires sharp time localization [77]. Yet, the aim of this presentation is to prepare the ground for the description of scattering in a lattice theory with a finite and discrete spacetime.

called scattering solution. At asymptotic times $|\Psi(t)\rangle$ approaches the "trajectories" of wave packets $w_\pm(\{p_k, \sigma_k, \alpha_k\})$ of free multi-particle states

$$|\Psi(t)\rangle \xrightarrow{t \to \pm\infty} \sum_{\{\sigma_k, \alpha_k\}} \int d\{\mathbf{p}_k\} \, w_\pm(\{p_k, \sigma_k, \alpha_k\}) \, \exp\left(-it \sum_k p_k^0\right) |\{p_k \sigma_k \alpha_k\}\rangle \ .$$

(1.9)

We assume that scattering solutions are completely determined by either their infinite past or their infinite future asymptote. Otherwise stated, given one of the wave packets $w_\pm$ the state $|\psi\rangle$ is uniquely identified. We can use this fact to label it,

$$|\Psi\rangle = |w_-, \text{in}\rangle = |w_+, \text{out}\rangle \ .$$

(1.10)

That is, $|w_-, \text{in}\rangle$ denotes the state that approaches the trajectory of the $t = 0$ wave packet w_- at $t \to -\infty$; $|w_+, \text{out}\rangle$ approaches the trajectory described by w_+ at $t \to +\infty$. Scattering theory is concerned precisely with the relation between the two "bases" $|\cdot, \text{in}\rangle$ and $|\cdot, \text{out}\rangle$.

If the probability amplitudes that a state approaching a generic asymptotic configuration w_- in the far past will approach another generic configuration w'_+ in the distant future are given, the outcome of any scattering experiment is known. These amplitudes are called *S-matrix* elements and denoted

$$S\left(\{p_k \sigma_k \alpha_k\} \to \{q_k \tau_k \beta_k\}\right) = \langle\{q_k \tau_k \beta_k\}, \text{out}|\{p_k \sigma_k \alpha_k\}, \text{in}\rangle \ ,$$

(1.11)

where a limiting procedure of narrow wave packets is implied [50]. Notice that the S-matrix elements are precisely the coefficients of the expansion of the $|\cdot, \text{in}\rangle$ states in terms of $|\cdot, \text{out}\rangle$ states. Transition probabilities are the absolute square of the S-matrix elements. Often spin polarizations are not measured experimentally; then the relevant probability is obtained averaging over the initial polarizations σ_k and summing over final ones τ_k [49].

Clearly the $t \to \pm\infty$ limits are an idealization. In real world experiments the states are measured at times that precede and follow the collision by a time lapse much larger than the microscopic time scale of the collision itself, but still finite. If the wave packets are localized in a energy range ΔE then $t \to \infty$ should read $t \gg 1/\Delta E$. Measurements done at these finite times should reveal a state that approximates a free multi-particle state with a degree of precision related to that of the time limit. The same criterion applies if the scattering takes place in a finite spacetime, such as a lattice. Consider a finite spacetime with a time direction spanning the interval $t \in [-T, T]$. A state can be prepared as an *approximate* free multi-particle wave packet w_{-T} at the initial time $-T$, let evolve until time T, and finally compared with another approximate wave packet w'_{+T}.

The transition amplitudes obtained in this way, namely

$$\langle w'_{+T}|e^{-2iTH}|w_{-T}\rangle \ , \tag{1.12}$$

can be related to S-Matrix elements. To this aim the free evolution of the wave packets w_{-T} and w_{+T} from time $t = 0$ to $t = \pm T$ has to be compensated[8]. In this way approximate (due to the finite T) and smeared (due to the finite momentum spread of the wave packets) S-matrix are obtained. Increasing T and, simultaneously, the precision with which the wave packets approximate a single free multi-particle state, the S-matrix elements (1.11) are recovered.

1.3 Lagrangian Formalism

A common starting point for the construction of a quantum field theory is the Lagrangian description of the associated classical field theory. This approach makes it particularly easy to write down theories that respect the symmetry requirements of Section 1.1 [53]. The degrees of freedom of the theory are functions of spacetime: the fields $\varphi = \{\varphi^n\}_{n=1}^N$ and their derivatives. Under a Poincaré transformation:

$$(\Lambda, a): \ \varphi^m(x) \to D(\Lambda)^m{}_n \, \varphi^n(\Lambda^{-1}(x-a)) \tag{1.13}$$

where $D(\Lambda)$ is a finite-dimensional representation of the Lorentz group[9] $\mathrm{O}(1,d)$. In this Thesis we only consider vector fields and Dirac fields. The former transform in the defining representation of $\mathrm{O}(1,d)$ while the latter belong to the Dirac spinor representation, introduced in Subsection 1.3B. If a non-trivial internal symmetry group G is also present, we denote $V(g)$, $g \in G$, the finite-dimensional unitary representation under which the fields transform:

$$g: \ \varphi^m(x) \to V(g)^m{}_n \, \varphi^n(x) \ . \tag{1.14}$$

The dynamics of the classical theory is specified by a variational principle as the stationary point $\delta S = 0$ of an action functional $S(\varphi)$. We always assume that the action can be written as the spacetime integral of a *local* Lagrangian density $\mathcal{L}(\varphi(x), \partial_\mu \varphi(x))$ (or simply Lagrangian for the reminder of this Section) in the form

$$S(\varphi) = \int \mathrm{d}^D x \, \mathcal{L}(\varphi(x), \partial_\mu \varphi(x)) \ . \tag{1.15}$$

---

[8] Recall that the reference wave packet states in (1.10) are defined at time $t = 0$.

[9] Actually of its covering group, see Appendix A. The requirement of $D(\Lambda)$ being finite-dimensional is that of having a finite number of fields.

The Lagrangian must be real, of mass dimension[10] D and a scalar under Poincaré and internal group transformations[11]. Invariance is ensured if all the Lorentz and internal group indices appearing in the Lagrangian terms are appropriately contracted via invariant tensors. Finally, if power-counting renormalizability[12] of the quantum theory is required, $\mathcal{L}$ must be a polynomial with coefficients of positive mass dimension [32].

Symmetries and conservation laws. *Noether theorem* associates a conserved quantity to every infinitesimal transformation $\varphi \mapsto \varphi + \delta\varphi$ that leaves the action invariant. Suppose that the internal symmetry group G is a *compact* reductive[13] Lie group and that the representation $V(g)$ has generators $\{T^a\}_{a=1}^{\dim G}$, namely

$$V(g) = \exp(\theta^a T^a) \ , \tag{1.16}$$

for g in a neigbourhood of the identity and some $\theta^a \in \mathbb{R}$. The generators satisfy

$$(T^a)^\dagger = -T^a \ , \qquad [T^a, T^b] = f^{abc} T^c \ , \tag{1.17}$$

where f^{abc} are the completely antisymmetric structure constants of the Lie algebra of G. The infinitesimal symmetry transformations of the fields read

$$\delta_\theta \varphi^m = \theta^a (T^a)^m{}_n \varphi^n \ , \qquad \theta^a \ll 1 \ . \tag{1.18}$$

Noether theorem provides as (independent) conserved currents and charges,

$$j^{a\,\mu} = (T^a)^m{}_n \varphi^n \frac{\partial \mathcal{L}}{\partial(\partial_\mu \varphi^m)} \ , \qquad Q^a(t) = \int \mathrm{d}^d \mathbf{x}\, j^{a\,0}(t, \mathbf{x}) \ . \tag{1.19}$$

On the solutions of the equations of motion,

$$\partial_\mu j^{a\,\mu} = 0 \ , \qquad \mathrm{d}Q^a/\mathrm{d}t = 0 \ . \tag{1.20}$$

---

[10] A quantity Z is said to have (classical) scaling dimension or mass dimension Δ if, under spacetime dilations $x \to \lambda x$, it transform as $Z \to \lambda^{-\Delta} Z$. Obviously $\Delta(\partial/\partial x^\mu) = 1$ and $\Delta(\mathrm{d}x^\mu) = -1$. In natural units the action is adimensional $\Delta(S) = 0$, whence $\Delta(\mathcal{L}) = -\Delta(\mathrm{d}^D x) = D$.

[11] That is, $(\Lambda, a, g)\colon \mathcal{L}(x) \equiv \mathcal{L}(\varphi(x), \partial_\mu \varphi(x)) \to \mathcal{L}(\Lambda x + a)$.

[12] Renormalizability is not necessary if the theory is an effective theory, but the requirement is at least of historical importance as it greatly constrained the terms allowed in the Lagrangian.

[13] Compactness ensures the existence of finite dimensional unitary representations, necessary since we want to construct a unitary quantum theory with a finite number of fields. Reductiveness is here assumed only to lighten the notation. The Lie algebra of a reductive Lie group is a direct sum of one-dimensional (abelian) $\mathfrak{a}_j$ and simple (nonabelian) $\mathfrak{h}_k$ factors $\mathfrak{g} = \mathfrak{a}_1 \oplus \cdots \oplus \mathfrak{a}_J \oplus \mathfrak{h}_1 \oplus \cdots \oplus \mathfrak{h}_K$.

1.3A   Gauge Theories

A gauge theory is a redundant description of a physical system, typically due to an arbitrariness in the choice of some "frame of reference" in which the system configuration is specified. This redundancy turns out to be necessary to achieve a local and Lorentz covariant formulation of an interacting quantum theory that includes massless particles of helicity ± 1 [50], such as quantum electrodynamics.

Gauge theories originate from the requirement of the invariance of the action $S(\varphi)$ under *gauge transformations*: internal group G transformations assigned independently at each spacetime point. In the notations introduced above,

$$\varphi(x) \mapsto ({}^{g}\varphi)(x) = V(g(x))\,\varphi(x) \;, \qquad S(\varphi) = S({}^{g}\varphi) \;, \tag{1.21}$$

for smooth $g\colon \mathbb{R}^{1,d} \to G$ such that $g(x) \xrightarrow{|\mathbf{x}|\to\infty} 1_{G}$. Gauge theories built out of nonabelian groups are called *Yang-Mills* theories after Yang and Mills who first considered this possibility in 1954 [6]. In the following we will sometime use the expression Yang-Mills also to refer to the abelian case.

Geometrical viewpoint. Transformation law (1.21) can be interpreted stating that the image of field φ at different spacetime points belongs to different copies of the internal group representation space, with no canonical identification between them. In order to compare field values at different spacetime points, e.g., when taking a derivative, such an identification has to be provided explicitly. This is usually done introducing the (differential) notion of covariant derivative which allows to define the (integral) notion of parallel transport. Here we proceed the other way round [49] and start from the parallel transport. This will provide useful insights on how to build a lattice Yang-Mills Hamiltonian (see Section 2.4).

Let $\gamma\colon I \to \mathbb{R}^{1,d}$ be a smooth curve defined on an open interval $I \subset \mathbb{R}$. To each γ and $s,t \in I$ we associate a unitary matrix $U_{\gamma}(t,s)$ in the V representation of G, requiring

(i)   the association to be smooth[14];

(ii) $U_{\gamma}(s,s) = 1_{V}$, the V representation space identity;

(iii) $U_{\gamma}(t,u)\,U_{\gamma}(u,s) = U_{\gamma}(t,s)$, in particular $U_{\gamma}(s,t) = U_{\gamma}^{\dagger}(t,s)$;

(iv) $U_{\gamma}(t,s) \mapsto V(g(\gamma(t)))\,U_{\gamma}(t,s)\,V^{\dagger}(g(\gamma(s)))$ under gauge transformations (1.21).

The *parallel transport* $U_{\gamma}(t,s)$ maps the representation space attached to $x = \gamma(s)$

---

[14] This is better qualified deriving the parallel transport from the connection but this presentation is not aimed at strict rigor.

to the one at $y = \gamma(t)$, in such a way that the difference

$$U_\gamma^\dagger(t,s)\,\varphi(y) - \varphi(x) \xrightarrow{\;(1.21)\,+\,\text{(iv)}\;} V(g(x))\left[U_\gamma^\dagger(t,s)\,\varphi(y) - \varphi(x)\right] \qquad (1.22)$$

makes sense and transforms covariantly (and independently of t) by construction[15].

Due to locality, we are interested in derivatives rather than finite differences[16]. A notion of covariant derivative along the curve γ, D_γ, is retrieved taking the $t \to s$ limit of (1.22):

$$D_\gamma\varphi(s) := \lim_{t \to s} \frac{U_\gamma^\dagger(t,s)\varphi(\gamma(t)) - \varphi(\gamma(s))}{t - s} = \left.\frac{\mathrm{d}}{\mathrm{d}t}U_\gamma^\dagger(t,s)\varphi(\gamma(t))\right|_{t=s} . \qquad (1.23)$$

Recalling properties (i) and (ii), $U_\gamma(t,s)$ can be expanded for small $\epsilon = t - s$ via the generators T^a of the V representation. Let us assume a γ dependence of the form

$$U_\gamma(t,s) = 1 + \epsilon\dot\gamma^\mu(0)\,A_\mu(x) + \mathcal{O}(\epsilon^2) , \quad A_\mu(x) = A_\mu^a(x)\,T^a , \quad A_\mu^a(x) \in \mathbb{R} , \quad (1.24)$$

where the *connection* 1-form A has been introduced. Setting $\eta = \dot\gamma(0)$, $x = \gamma(0)$,

$$D_\gamma\varphi(s) = \lim_{\epsilon \to 0} \frac{(1 - \epsilon\eta^\mu A_\mu)(\varphi + \epsilon\eta^\mu\partial_\mu\varphi)(x) - \varphi(x)}{\epsilon} = \eta^\mu(\partial_\mu - A_\mu)\varphi(x) , \quad (1.25)$$

which defines the *covariant derivative* of φ in x along η. Symbolically,

$$D = \partial - A , \qquad D \xrightarrow{\;(1.21)\;} V D V^\dagger . \qquad (1.26)$$

This (adjoint) transformation law is a consequence of (1.21) and (1.22) and ensures that φ and $D\varphi$ belong to the same G representation. Moreover, it implies

$$A \xrightarrow{\;(1.21)\;} V A V^\dagger - V \partial V^\dagger ; \qquad (1.27)$$

or, under infinitesimal transformations $V = \exp(\theta T^a)$ [32],

$$\delta_\theta A_\mu^a = D_\mu\theta^a = \partial_\mu\theta^a - f^{abc}A_\mu^b\theta^c = f^{abc}\theta^b A_\mu^c + \partial_\mu\theta^a \qquad (1.28)$$

Because of the inhomogeneous term, A is not a tensor under gauge transformations[17].

---

[15] It is anyway path dependent.

[16] At least in theories defined on a continuous spacetime. When we will reformulate gauge theories on the lattice in Chapter 2 the situation will be different.

[17] Otherwise stated, it does not transform covariantly. It is nevertheless well defined, in the sense that the transformed connection is still algebra representation valued and its components A_μ^a are independent from the representation V chosen, as shown by the infinitesimal transformation (1.28).

The ingredients introduced above allow to convert a Lagrangian invariant under global G transformations into a Lagrangian invariant under local transformations via the *minimal substitution*

$$\partial \rightarrow D \ . \tag{1.29}$$

Pure Yang-Mills Lagrangian.   The last step to obtain a proper gauge theory is to promote the connection components A_μ^a to propagating degrees of freedom, termed *gauge fields* or *gauge bosons*. In order to do so, a kinetic term has to be introduced. Recalling transformation rule (1.26) a covariant term containing derivatives of the connection components is its *curvature* or *field strength*

$$F_{\mu\nu} = F_{[\mu\nu]} = -\left[D_\mu, D_\nu\right] = F_{\mu\nu}^a T^a \ , \quad F_{\mu\nu}^a = \partial_\mu A_\nu^a - \partial_\nu A_\mu^a - f^{abc} A_\mu^b A_\nu^c \ . \tag{1.30}$$

As a consequence of (1.26), the field strength also transforms in the adjoint

$$F_{\mu\nu} \xrightarrow{\ (1.21)\ } V F_{\mu\nu} V^\dagger \ . \tag{1.31}$$

A valid kinetic term for gauge bosons should be local, Poincaré and internal group invariant, renormalizable (by our requirement) and quadratic (by definition). It is now evident that such a term is provided by

$$\mathcal{L} \propto \mathrm{tr}\left(F_{\mu\nu} F^{\mu\nu}\right) \ ; \tag{1.32}$$

together with cubic and quartic self-interactions whenever the group is nonabelian ($f^{abc} \neq 0$). It is nevertheless worth it pursuing an alternative, easily discretizable, derivation of Lagrangian (1.32). It can be proven that the parallel transport is the unique solution to the initial value problem [49]

$$\frac{\mathrm{d}}{\mathrm{d}t} U_\gamma(t,0) = \dot{\gamma}^\mu(t) A_\mu(\gamma(t)) \, U_\gamma(t,0) \ , \qquad U_\gamma(0,0) = 1 \ ; \tag{1.33}$$

and can be expressed as a path ordered exponential[18]

$$U_\gamma(t,0) = \mathcal{P} \exp\left\{\int_0^t \mathrm{d}s \, \dot{\gamma}^\mu(s) \, A_\mu(\gamma(s))\right\} \ . \tag{1.34}$$

For every closed curve γ, the *holonomy* or *Wilson loop* [20]

$$W_\gamma = \mathrm{tr}\, U_\gamma := \mathrm{tr}\, \mathcal{P} \exp \oint_\gamma A \tag{1.35}$$

---

[18] Path ordering $\mathcal{P}$ is needed when G is nonabelian. The path ordered product of a one-parameter family of operators is here defined as the product of the operators ordered from right to left by increasing parameter. For functions, the ordering is done on the terms of their Taylor expansion.

is gauge invariant as a consequence of the transformation law (iv) of the parallel transport. For abelian gauge groups this is easily recast into a surface integral via Stokes theorem. Considering the abelian case[19] $G = \mathrm{U}(1)$,

$$U_\gamma = \exp \oint_\gamma A = \exp \int_\Sigma F \ . \tag{1.36}$$

where Σ is a surface enclosed by $\partial\Sigma = \gamma$ and the 2-form F is the field strength. Since we want a local action term, given any point x, vectors $\sigma_1^\mu, \sigma_2^\mu$ and $\epsilon \ll 1$, consider the infinitesimal surface $\Sigma = (\epsilon\sigma_1) \wedge (\epsilon\sigma_2)$ with origin in x, then

$$U_{\partial\Sigma} = \exp\big(\epsilon^2 \sigma_1^\mu \sigma_2^\nu F_{\mu\nu}(x) + \mathcal{O}(\epsilon^3)\big) \ . \tag{1.37}$$

In the nonabelian case (1.36) is more involved [31] but for the infinitesimal path $\partial\Sigma$ the result is again (1.37) [49]. Assume now G is either $\mathrm{U}(1)$, or a simple[20] nonabelian Lie group, such as $\mathrm{SU}(N)$. Suppose also that the representation $V(g)$ is irreducible, of dimension d_V and that the generators are normalized via

$$\mathrm{tr}\{T^a T^b\} = -2D_V \delta^{ab} \ , \quad D_V \in \mathbb{R} \ . \tag{1.38}$$

Then[21], by (1.37) and $(T^a)^\dagger = -T^a$,

$$\begin{aligned}
\frac{1}{2}\left[W_{\partial\Sigma} + W_{\partial\Sigma}^\dagger\right] &= \mathrm{tr}\left[\mathbb{1}_V + \frac{\epsilon^4}{2}\, \sigma_1^\mu \sigma_1^\rho \sigma_2^\nu \sigma_2^\sigma \, F_{\mu\nu}^a F_{\rho\sigma}^b(x)\, T^a T^b + \mathcal{O}(\epsilon^5)\right] \\
&= d_V - \epsilon^4\, D_V\, \sigma_1^\mu \sigma_1^\rho \sigma_2^\nu \sigma_2^\sigma \, F_{\mu\nu}^a F_{\rho\sigma}^a(x) + \mathcal{O}(\epsilon^5) \ . \tag{1.39}
\end{aligned}$$

In principle higher order terms may be considered but their coefficients have negative mass dimension and are thus ruled out by renormalizability. In the lattice theory they will however play a role. No intrinsic preferred directions $\sigma_1^\mu, \sigma_2^\mu$ are available, thus the last step to obtain a valid kinetic term is to replace them with an invariant tensor in the same Lorentz group representation; the only possibility is

$$\sigma_1^\mu \sigma_1^\rho \sigma_2^\nu \sigma_2^\sigma \to \eta^{\mu\rho}\eta^{\nu\sigma} \ . \tag{1.40}$$

Introducing a last bit of notation, this replacement can be achieved directly at the level of Wilson loops. Let $W_{\alpha\beta}(x;\epsilon)$ be the infinitesimal square Wilson loop with

---

[19] To comply with the above conventions A is pure imaginary here, $A = A^1 T^1 = A^1(-i)$.

[20] A simple Lie group is a Lie group which does not have nontrivial connected normal subgroups, namely subgroups invariant under conjugation by elements of the group.

[21] The $\mathcal{O}(\epsilon^3)$ terms in (1.37) (and its nonabelian generalization) do not contribute up to $\mathcal{O}(\epsilon^6)$. To see this, recall that $U_{\partial\Sigma}$ is a matrix in the V representation of G. Then, order by order in ϵ, all the terms in the exponent in (1.37) are of the form $c^a T^a$ for some real c^a. In the first order expansion of the exponential they cancel with the contribution of the Hermitian conjugate.

origin in x and $\sigma_1^\mu = \delta_\alpha^\mu$ and $\sigma_2^\mu = \delta_\beta^\mu$, $(\alpha, \beta = 0, \dots, d)$. Then,

$$\sum_{\alpha\beta} \eta^{\alpha\alpha}\eta^{\beta\beta} \frac{W_{\alpha\beta}(x;\epsilon) + W_{\alpha\beta}^\dagger(x;\epsilon)}{2} = \sum_{\alpha\beta} \eta^{\alpha\alpha}\eta^{\beta\beta}\Big[d_V - \epsilon^4\, D_V F_{\alpha\beta}^a F_{\alpha\beta}^a(x)\Big] + \mathcal{O}(\epsilon^5) \ ,$$

$$(1.41)$$

and the general[22] *pure Yang-Mills* (no matter fields) Lagrangian is

$$\mathcal{L} = \frac{1}{4g^2} \lim_{\epsilon\to 0} \sum_{\alpha\beta} \frac{\eta^{\alpha\alpha}\eta^{\beta\beta}}{D_V \epsilon^4} \left[\frac{W_{\alpha\beta}(\epsilon) + W_{\alpha\beta}^\dagger(\epsilon)}{2} - d_V \right] = -\frac{1}{4g^2} F_{\mu\nu}^a F^{a\,\mu\nu} \ . \qquad (1.42)$$

Here a coupling constant g has been introduced. This coupling is typically reabsorbed in the gauge fields via $A_\mu^a \to g A_\mu^a$ in order to obtain canonically normalized kinetic terms and explicit coupling dependence in front of the interactions. Observe also that, remarkably, gauge invariance forbids a gauge boson mass term $A_\mu^a A^{a\,\mu}$. When the Lie algebra is not simple but is reductive a sum of Lagrangians of type (1.42) is obtained, one for each algebra factor, each with its independent coupling. This happens, e.g., for the Standard Model of particle physics which has gauge group $\mathrm{SU}(3) \times \mathrm{SU}(2) \times \mathrm{U}(1)$.

1.3B   Three Models

Lagrangian (1.42) has been obtained without any specific choice of matter fields. We now want to couple the theory to some Dirac fields. To this scope it is sufficient to identify a valid Dirac field Lagrangian with some internal (global) symmetries and perform the minimal substitution (1.29). Before doing so, we review the basic properties of the Dirac spinor representation.

Free Dirac fermions.   A way to construct Dirac spinors in arbitrary spacetime dimensions[23] is through the gamma matrices, namely matrices generating an irreducible representation of the Clifford algebra

$$\gamma_\mu \gamma_\nu + \gamma_\nu \gamma_\mu = 2\eta_{\mu\nu} \ . \qquad (1.43)$$

In D spacetime dimensions the gamma matrices are $2^{\lfloor D/2 \rfloor} \times 2^{\lfloor D/2 \rfloor}$ dimensional [61], $\lfloor \cdot \rfloor$ denoting the integer part. In particular, for $d = 1$ they are 2×2 matrices. Now,

$$\Sigma_{\rho\sigma} := \frac{1}{4}\big[\gamma_\rho, \gamma_\sigma\big] \qquad (1.44)$$

---

[22] At least imposing renormalizability and parity or time-reversal invariance. Fixing an orientation of spacetime a topological θ-term can enter the action [21, 25].

[23] The problem of how spinors arise in $d = 1$ where there is no spin is addressed in Appendix A.

obey the Lorentz algebra (A.2a) and thus generate a representation $D(\Lambda)$,

$$D(\Lambda)^\alpha{}_\beta := \exp\left[\frac{1}{2}\omega^{\rho\sigma}(\Sigma_{\rho\sigma})^\alpha{}_\beta\right] , \quad \omega^{\rho\sigma} = -\omega^{\sigma\rho} . \tag{1.45}$$

A multiplet of fields ψ^α transforming with $D(\Lambda)$ is a Dirac spinor field; the conjugate spinor $\overline{\psi}_\alpha := \psi_\beta^\dagger(\gamma_0)^\beta{}_\alpha$ is in the dual representation; and $(\gamma^\mu)^\alpha{}_\beta$ are invariant tensors,

$$\Lambda^\mu{}_\nu \, D(\Lambda)^\alpha{}_\gamma \, (\gamma^\nu)^\gamma{}_\delta \, D(\Lambda^{-1})^\delta{}_\beta = (\gamma^\mu)^\alpha{}_\beta . \tag{1.46}$$

They have one vector, one spinor and one conjugate spinor index and thus allow to write down a Lorentz invariant expression containing a derivative of ψ^α. From now on spinor indices will be usually omitted and when gamma matrices are contracted with a vector we will sometimes write $\not{v}$ in place of $v^\mu \gamma_\mu$.

For a single Dirac fermion ψ the simplest kinetic Lagrangian that can written down, complying with the conditions on the action imposed at the beginning of this Section, is[24]

$$\mathcal{L} = \overline{\psi}\,(i\not{\partial} - m)\,\psi . \tag{1.47}$$

It describes a free Dirac field. Its equation of motion, namely

$$\delta S / \delta\overline{\psi} = (i\not{\partial} - m)\,\psi = 0 , \tag{1.48}$$

is the *Dirac equation.* This equation can be solved exactly, also at the quantum level. With this particle content no other Lagrangian term satisfying our requirements can be built in more than two spacetime dimensions[25]. In $D = 2$ the spinors have mass dimension $1/2$ thus a four-fermion interaction is also allowed by renormalizability. Here we neglect it but it appears, e.g., in the Thirring and Gross-Neveu models [59].

As will be clear in Section 1.5, when the theory is quantized, the fields $\psi^\alpha, \overline{\psi}_\alpha$ become operators $\hat{\psi}^\alpha, \hat{\overline{\psi}}_\alpha$ that have to satisfy anticommutation relations[26]. In order to have a consistent quantization procedure, the classical variables $\psi^\alpha(x)$ and $\overline{\psi}_\alpha(x)$ should be treated as anticommuting Grassmann numbers [46]. In doing so, here we define derivatives and complex conjugation by

$$\delta F(\psi,\overline{\psi}) = \delta\psi^\alpha\,\frac{\partial F}{\partial\psi^\alpha} + \delta\overline{\psi}_\alpha\,\frac{\partial F}{\partial\overline{\psi}_\alpha} , \qquad (FG)^* = G^* F^* ; \tag{1.49}$$

following the conventions of [46].

---

[24] If equations of motion are to be first order (1.47) is the only possible kinetic Lagrangian; it is not real but its imaginary part is a total derivative (see the Grassmann number conventions below).

[25] Even adding other Dirac fields, $\mathcal{L}$ is a sum of (1.47) copies, possibly with different masses.

[26] This consequence of the spin-statistic theorem holds also in $D = 2$, see Appendix A.

Electrodynamics. Lagrangian (1.47) is invariant under the *particle number* U(1)

$$\psi \mapsto e^{-i\theta}\psi \ , \quad \overline{\psi} \mapsto e^{+i\theta}\overline{\psi} \ , \qquad \theta \in \mathbb{R} \ . \tag{1.50}$$

Promoting this U(1) to a gauge symmetry via the minimal substitution we obtain the abelian gauge theory of *electrodynamics*, also known in two spacetime dimensions as *Schwinger model* [9, 18]. In this context the field ψ is called *electron*. The Lagrangian is

$$\mathcal{L} = -\frac{1}{4}F_{\mu\nu}F^{\mu\nu} + \overline{\psi}(i\slashed{D} - m)\psi \ , \tag{1.51}$$

where the gauge field $A_\mu = A_\mu^1$, called *photon*, has been canonically normalized. The the Noether current[27] and the Euler-Lagrange equations of (1.51) read

$$j^\mu = g\overline{\psi}\gamma^\mu\psi \ , \qquad \partial_\mu F^{\mu\nu} = j^\nu \ , \qquad (i\slashed{D} - m)\,\psi = 0 \ . \tag{1.52}$$

Chromodynamics. Considering a theory of N fermions $\{\psi^s\}$ all with the same mass, the global symmetry group becomes the nonabelian U(N), with the fermions transforming in the defining representation: $V \in$ U(N). Any of its continuous subgroups may be used to build a gauge theory. For ease of notation we pick its largest simple subgroup, SU(N). The minimal substitution provides immediately a Lagrangian similar in form to (1.51),

$$\mathcal{L} = -\frac{1}{4}F_{\mu\nu}^a F^{a\,\mu\nu} + \overline{\psi}_r(i\slashed{D}^r{}_s - m\delta^r{}_s)\psi^s \ , \tag{1.53}$$

This Lagrangian describes *chromodynamics*[28], the theory of *quarks* ψ and *gluons* A. Expanding and isolating kinetic and interaction terms $\mathcal{L} = \mathcal{L}_{\text{kin}} + \mathcal{L}_{\text{int}}$ yields

$$\mathcal{L}_{\text{kin}} = -\frac{1}{2}(\partial_\mu A_\nu^a - \partial_\nu A_\mu^a)\,\partial^\mu A^{a\,\nu} + \overline{\psi}_s(i\gamma^\mu\partial_\mu - m)\psi^s \tag{1.54}$$

$$\mathcal{L}_{\text{int}} = -ig\overline{\psi}_r\gamma^\mu A_\mu^a(T^a)^r{}_s\psi^s + gf^{abc}\partial_\mu A_\nu^a A^{b\,\mu}A^{c\,\nu} - \frac{1}{4}g^2 f^{abc}f^{ade}A_\mu^b A_\nu^c A^{d\,\mu}A^{e\,\nu} \ . \tag{1.55}$$

Noether theorem provides a particle number conserved current associated to $\mathfrak{u}(1)$ transformations, but also a conserved but not gauge invariant current for $\mathfrak{su}(N)$,

$$j_{\mathfrak{u}(1)}^\mu = \overline{\psi}_r\gamma^\mu\psi^r \ , \qquad j_{\mathfrak{su}(N)}^{a\,\mu} = ig\overline{\psi}_r\gamma^\mu(T^a)^r{}_s\psi^s + gf^{abc}A_\mu^b F^{c\,\mu\nu} \ . \tag{1.56}$$

---

[27] The coupling in front due to the rescaling of the generator $(-i) \to g(-i)$ in (1.50).

[28] Clearly Lagrangian (1.53) is not exactly that describing the strong interactions observed in nature but the structure is exactly the same. Both theories involve massive Dirac fermions matter fields transforming in the defining representation of a special unitary gauge group.

The latter receives a contribution from the gluons, reflecting their self-interactions. The Euler-Lagrange equation for the gluons reads

$$\partial_\mu F^{a\,\mu\nu} = j^{a\,\nu} \ , \tag{1.57}$$

and clearly shows that the Noether current is conserved.

1.4 Hamiltonian Formalism

The numerical simulations implemented in this Thesis rely on the Hamiltonian formalism. Contrarily to the manifestly covariant Lagrangian approach of the previous section, in the Hamiltonian formulation the time coordinate plays a privileged role. A choice of time direction has to be made, then the fields are taken to be functions of the space coordinates only[29].

Consider again the generic theory of the fields $\varphi = \{\varphi^n\}$ introduced in Section 1.3. In the Hamiltonian formalism the degrees of freedom are the fields $\{\varphi^n\}$ and their conjugate field momenta $\{\pi_n\}$. To lighten the notation here the indices n, m not only label the different fields but also run over the space coordinate $\mathbf{x}$ when the space dependence of the field is not indicated explicitly. Their contraction involves summation over different fields as well as integration over space. This convention facilitates the parallelism with the case of a finite number of degrees of freedom.

The mapping from $(\varphi, \dot\varphi)$ space to phase space (φ, π) is the Legendre transform:

$$\pi_n = \delta L/\delta \dot\varphi^n \ , \tag{1.58}$$

where L is the Lagrangian, defined as the space integral of the lagrangian density,

$$L(\varphi, \dot\varphi) = \int \mathrm{d}\mathbf{x} \, \mathcal{L}(\varphi(\mathbf{x}), (\dot\varphi(\mathbf{x}), \partial_i \varphi(\mathbf{x}))) \ . \tag{1.59}$$

The Hamiltonian is

$$H(\varphi, \pi) = \dot\varphi^n(\varphi, \pi)\,\pi_n - L(\varphi, \dot\varphi(\varphi, \pi)) \ . \tag{1.60}$$

Grouping the fields in commuting $\{\varphi^{n_e}\}$ and anticommuting $\{\varphi^{n_o}\}$ ones, the (super) Poisson bracket of two functionals $F(\varphi, \pi)$, $G(\varphi, \pi)$ is defined as [46]

$$\{F, G\} = \left[\frac{\delta F}{\delta \varphi^{n_e}} \frac{\delta G}{\delta \pi_{n_e}} - \frac{\delta F}{\delta \pi_{n_e}} \frac{\delta G}{\delta \varphi^{n_e}} \right] + \eta \left[\frac{\delta F}{\delta \varphi^{n_o}} \frac{\delta G}{\delta \pi_{n_o}} + \frac{\delta F}{\delta \pi_{n_o}} \frac{\delta G}{\delta \varphi^{n_o}} \right] \ ; \tag{1.61}$$

---

[29] Their time dependence is fixed by time evolution.

where $\eta = +1$ if F is commuting, -1 otherwise. The properties of (1.61) reproduce those of commutators or anticommutators. The fundamental brackets read

$$\{\varphi^{m_e}, \pi_{n_e}\} = -\{\pi_{n_e}, \varphi^{m_e}\} = \delta^{m_e}{}_{n_e} \ , \qquad \{\varphi^{m_o}, \pi_{n_o}\} = +\{\pi_{n_o}, \varphi^{m_o}\} = -\delta^{m_o}{}_{n_o} \ .$$
$$(1.62)$$

As in the Lagrangian formalism, the dynamics descends from an action principle [46]

$$\delta S = \delta \int_{-\infty}^{+\infty} \mathrm{d}t \left[\dot{\varphi}^n \pi_n - H(\varphi, \pi) \right] = 0 \ . \tag{1.63}$$

The equation of motion deriving from (1.63) can be written in terms of the Poisson brackets. For a generic functional of the canonical variables $F(\varphi, \pi)$ it reads

$$\dot{F} = \{F, H\} \ . \tag{1.64}$$

Symmetries and conservation laws. The Hamiltonian formalism provides an elegant description of continuous symmetries. Suppose the theory has again the internal symmetry group G of Section 1.3. The Noether charges together with the Poisson bracket form a representation of the Lie algebra,

$$Q^a = \int \mathrm{d}\mathbf{x} \, (T^a)^m{}_n \, \varphi^n(\mathbf{x}) \, \pi_m(\mathbf{x}) \ , \qquad \{Q^a, Q^b\} = f^{abc} Q^c \ . \tag{1.65}$$

Most importantly, the charges realize the internal symmetry transformations (1.18) as infinitesimal canonical transformations. Considering again a generic $F(\varphi, \pi)$

$$\delta_\theta F = \theta^a \{F, Q^a\} \ , \qquad \delta_\theta \varphi^m = \theta^a \{\varphi^m, Q^a\} = \theta^a (T^a)^m{}_n \varphi^n \ . \tag{1.66}$$

1.4A   Gauge Theories

The canonical variables describing the configuration of a gauge theory in its Hamiltonian formulation satisfy relations that constrain them to a submanifold of phase space [46]. To see this, observe that the invertibility of the Legendre transform (1.58) is equivalent to the invertibility of the Hessian

$$\mathcal{W}_{mn} = \frac{\delta \pi_m}{\delta \dot{\varphi}^n} = \frac{\delta^2 L}{\delta \dot{\varphi}^m \, \delta \dot{\varphi}^n} \ . \tag{1.67}$$

Provided $\mathcal{W}_{mn}$ is invertible, Euler-Lagrange equations can be put in standard form and thus the existence and uniqueness theorems applies to their solutions. On the other hand, the solutions of the equations of motion of a gauge theory are only determined up to gauge transformations, whence the original claim that the Legen-

dre transform cannot be invertible, its image being a submanifold of phase space[30]. It can be shown that it is still possible to introduce an Hamiltonian which is well defined on this submanifold and freely extensible elsewhere[31] [46]. Nevertheless, in order to allow the description of constrained systems, the traditional Hamiltonian formalism requires some adjustments, originally developed by Bergmann and Dirac [4, 5]. The core ideas of the formalism are now sketched; for an exhaustive and rigorous treatment see [46]. In the following we assume that all the fields are commuting, the extension to the anticommuting case is a matter of keeping track of the correct signs.

The initial ingredients are the Hamiltonian $H(\varphi, \pi)$ and some (*primary*) constraints

$$\kappa^{u_1}(\varphi, \pi) = 0 , \qquad u_1 = 1, \dots, U_1 \tag{1.68}$$

These can be enforced by the method of Lagrange multipliers, introducing auxiliary variables (functions) $\lambda_u(t, \mathbf{x})$ and a modified version of the action principle (1.63),

$$\delta S = \delta \int_{-\infty}^{+\infty} \mathrm{d}t \left[\dot{\varphi}^n \pi_n - H(\varphi, \pi) - \lambda_{u_1} \kappa^{u_1}(\varphi, \pi) \right] = 0 , \tag{1.69}$$

where the implicit integration over repeated indices has been extended con the constraints. Moreover the canonical and auxiliary variables are implicitly evaluated along a trajectory $t \to (\varphi, \pi, \lambda)(t)$, an abuse of notation that will be reiterated in the following. The time evolution of $F(\varphi, \pi)$ along such trajectories is then

$$\dot{F} = \{F, H + \lambda_{u_1} \kappa^{u_1}\} . \tag{1.70}$$

Consistency algorithm. We now show that, in order for the primary constraints (1.68) to be preserved by the time evolution, a new set of constraints as well as some restrictions on the Lagrange multipliers might have to be enforced. Via (1.70) the condition (1.68) can be recast as an initial value problem. Namely, we require that the constraints are satisfied by the initial system configuration $(\bar{\varphi}, \bar{\pi})$ and that they are respected by time evolution:

$$\kappa^{u_1}(\bar{\varphi}, \bar{\pi}) = 0 , \qquad \dot{\kappa}^{u_1}(\varphi, \pi) = \{\kappa^{u_1}, H\} + \lambda_{u'_1}\{\kappa^{u_1}, \kappa^{u'_1}\} = 0 . \tag{1.71}$$

Each of the right equations results either in a restriction on the auxiliary variables or, when the λ dependence cancels, in a (possibly new, *secondary*) constraint. The same

---

[30] At least under some assumptions better formulated in the finite dimensional case and here omitted.

[31] This arbitrariness in the definition of the Hamiltonian is unsurprisingly related to gauge freedom in a way that will be made precise below.

equation is then imposed on the U_2 newly obtained constraints and so on, until no new independent condition is generated. In the end we are left with an enlarged set of constraints κ^u and a system of linear equations for the auxiliary variables $\{\lambda_{u_1}\}$. The former, here assumed to be all independent, identify the *constraint surface*

$$\Sigma = \{(\varphi, \pi) : \kappa^u(\varphi, \pi) = 0 , \ u = 1, \ldots, U = U_1 + U_2 + \ldots\} ; \qquad (1.72)$$

the latter read

$$\{\kappa^u, H\} + \lambda_{u_1}\{\kappa^u, \kappa^{u_1}\} \approx 0 \qquad \forall \ u = 1, \ldots, U , \qquad (1.73)$$

where "$\approx$" denotes equality on Σ. Inserting a solution A_{u_1} of (1.73) in (1.69) provides a refined time evolution generated by $H' = H + A_{u_1}\kappa^{u_1}$ which automatically preserves the constraints, all is left to do is to choose valid initial conditions $(\overline{\varphi}, \overline{\pi}) \in \Sigma$.

Gauge invariance. This refined time evolution has also the advantage of isolating and making manifest the eventual "ambiguity" in the dynamics of the system. Indeed A_{u_1} (and thus H') is only determined up to solutions $\{B^v{}_{u_1}\}_{v=1}^V$ of the homogeneous system associated to (1.73). Let $\eta^v = B^v{}_{u_1}\kappa^{u_1}$, then (1.69) is equivalent to

$$\delta S = \delta \int_{-\infty}^{+\infty} dt \left[\dot{\varphi}^n\pi_n - H'(\varphi, \pi) - \lambda_v\eta^v(\varphi, \pi)\right] = 0 , \qquad \kappa^u(\overline{\varphi}, \overline{\pi}) = 0 , \quad (1.74)$$

where the remaining multipliers λ_v are completely arbitrary. Two Hamiltonian flows that differ by the choice of $\lambda_v = \lambda_v(t, \mathbf{x})$ are *gauge equivalent*. We may include this gauge freedom in the Hamiltonian defining the *total Hamiltonian*

$$H_T = H' + \lambda_v\eta^v . \qquad (1.75)$$

The relation between constraints and gauge invariance suggests that it might be difficult or impossible to completely remove the constraints by solving them explicitly. Nevertheless, not all constraints reflect a gauge freedom and while gauge symmetries imply the existence of constraints, the reverse is not true[32]. An $F(\varphi, \pi)$ such that $\{\kappa^u, F\} \not\approx 0$ for some u cannot generate a valid canonical transformation because this would violate the constraints. In Dirac's terminology [5] it is said to be *second-class*, as opposed to *first-class*[33]. Second-class constraints do not generate gauge transformations and are thus just relations between the canonical variables; they can be removed restricting phase space to their zero locus Σ^*, which inherits a symplectic structure from the original phase space. Conversely, the remaining

---

[32] Indeed, it may happen that (1.73) completely fixes the auxiliary variables.

[33] H' and η^v are first-class by construction.

first-class constraints can generate gauge transformations. They may be converted to second-class ones by imposing gauge-fixing conditions; nevertheless, this is not always convenient or even doable (due to Gribov's obstructions [46]).

Dirac Bracket. As a last ingredient it should be mentioned how the symplectic structure of Σ^* is defined. This is done introducing a modified bracket [5], called Dirac bracket. Let $\{\chi^w\}_{w=1}^W$ be the second-class constraints. The Dirac bracket is

$$\{F, G\}^* = \{F, G\} - \{F, \chi^w\}(\Delta^{-1})_{ww'}\{\chi^{w'}, G\} \ , \quad \Delta^{ww'} = \{\chi^w, \chi^{w'}\} \ . \quad (1.76)$$

It has all the properties of the Poisson bracket [46]; moreover it vanishes when F or G are second-class constraints, its restriction to $\Sigma^* = \{\chi^w(\varphi, \pi) = 0\}$ is thus well defined. It also reduces to the Poisson bracket for first-class functionals.

1.4B Three Models

Three theories of increasing complexity, whose Lagrangian description has been given in the previous Section, are now translated to the Hamiltonian formalism.

Free Dirac Fermions. As a first example consider the Dirac Lagrangian (1.47). The conjugate momenta to the matter fields ψ, $\psi^\dagger$ are

$$\pi = \frac{\partial \mathcal{L}}{\partial(\partial_0 \psi)} = -i\psi^\dagger \ , \qquad \pi^\dagger = \frac{\partial \mathcal{L}}{\partial(\partial_0 \psi^\dagger)} = 0 \ ; \quad (1.77)$$

Recalling $\overline{\psi} = \psi^\dagger \gamma^0$ and $(\gamma^0)^2 = 1$ the Hamiltonian is[34]

$$H = \int \mathrm{d}\mathbf{x} \left[\dot{\psi}(-i\psi^\dagger) - \psi^\dagger \gamma^0 \left(i\gamma^\mu \partial_\mu - m\right)\psi \right] = \int \mathrm{d}\mathbf{x}\, \overline{\psi} \left(-i\gamma^i \partial_i + m\right)\psi \quad (1.78)$$

Equation (1.77) provides two primary second-class constraints,

$$\kappa^1 = \pi + i\psi^\dagger = 0 \ , \qquad \kappa^2 = \pi^\dagger = 0 \ ; \quad (1.79)$$

$$\{\kappa^1(\mathbf{x}), \kappa^2(\mathbf{y})\} = \{i\psi^\dagger(\mathbf{x}), \pi^\dagger(\mathbf{y})\} = -i\delta(\mathbf{x} - \mathbf{y}) \ . \quad (1.80)$$

The consistency algorithm just fixes the Lagrange multipliers. We have therefore an example of a constrained but not gauge invariant theory; κ^1 and κ^2 can be consistently solved introducing the Dirac bracket (1.76). There is nothing particularly instructive in the computation thus we just state the well known result,

$$\{\psi(\mathbf{x}), \psi^\dagger(\mathbf{y})\}^* = -i\delta(\mathbf{x} - \mathbf{y}) \ ; \quad (1.81)$$

---

[34] Space dependence of the integrands is omitted when this does not creates confusion.

while π and $\pi^\dagger$ can be safely eliminated solving the constraints.

Pure Yang-Mills. We now turn to the pure Yang-Mills theory, described by the Lagrangian (1.42) (here we adopt canonically normalized kinetic terms). Due to the space-time splitting, in the Hamiltonian formalism it is convenient to parametrize the field strength by electric and magnetic fields

$$F_{0i}^a = E_i^a \ , \quad F_{ij}^a = B_{ij}^a \ . \tag{1.82}$$

For the reminder of this Chapter $(X_{ij...}^{ab...})^2$ represents $\sum_{i<j<...,\,ab...}(X_{ij...}^{ab...})^2$ and repeated spatial $i, j \ldots$ indices are summed over independently from their position.

The conjugate momenta associated to the gluons A_μ^a read

$$\Pi^{a\mu} = \frac{\partial \mathcal{L}}{\partial(\partial_0 A_\mu^a)} = -\frac{1}{2} F^{b\,\rho\sigma} \frac{\partial F_{\rho\sigma}^b}{\partial(\partial_0 A_\mu^a)} = -F^{a\,0\mu} = \delta_i^\mu E_i^a \ ; \tag{1.83}$$

providing a family of primary constraints

$$\kappa^{1a} = \Pi^{a0} \approx 0 \ . \tag{1.84}$$

The invertibility of the Legendre transform is lost because $\dot{A}_0^a$ is not specified by the canonical coordinates A_μ^a and $\Pi^{a\mu}$; but the Hamiltonian is still unambiguously defined on the constraint surface,

$$\begin{aligned}
H &= \int \mathrm{d}\mathbf{x} \left[\dot{A}_\mu^a \Pi^{a\mu} - \mathcal{L} \right] \\
&= \int \mathrm{d}\mathbf{x} \left[\dot{A}_i^a E_i^a + \frac{1}{4} \left(F_{0i}^a F^{a\,0i} + F_{i0}^a F^{a\,i0} + F_{ij}^a F^{a\,ij} \right) \right] \\
&= \int \mathrm{d}\mathbf{x} \left[\dot{A}_i^a E_i^a + \frac{1}{4} \left(-2(E_i^a)^2 + 2(B_{ij}^a)^2 \right) \right] \ .
\end{aligned} \tag{1.85}$$

Integrating by parts (assuming appropriate behavior at spatial infinity) we have

$$\begin{aligned}
\dot{A}_i^a E_i^a &= \left[F_{0i}^a + \partial_i A_0^a + g f^{abc} A_0^b A_i^c \right] E_i^a \\
&= (E_i^a)^2 - A_0^a (\partial_i E_i^a) + g f^{abc} A_0^b A_i^c E_i^a \\
&= (E_i^a)^2 - A_0^a \left[\partial_i E_i^a - g f^{abc} A_i^b E_i^c \right] \\
&= (E_i^a)^2 - A_0^a (D_i E_i^a) \ ,
\end{aligned} \tag{1.86}$$

where in the last step the fact that E_i^a transforms in the group adjoint was used.

Inserting in the expression of H

$$H = \int d\mathbf{x} \left[\frac{1}{2}(E_i^a)^2 + \frac{1}{2}(B_{ij}^a)^2 - A_0^a(D_i E_i^a) \right] . \tag{1.87}$$

Making use of the modified time evolution (1.70), the consistency of $\kappa^{1a} \approx 0$ implies[35]

$$\dot{\kappa}^{1a}(t,\mathbf{x}) = \{\Pi^{a0}(\mathbf{x}), H\}_t + \int d\mathbf{y}\, \lambda_1^b(t,\mathbf{y})\, \{\Pi^{a0}(\mathbf{x}), \Pi^{b0}(\mathbf{y})\}_t = D_i E_i^a(t,\mathbf{x}) \approx 0 ; \tag{1.88}$$

thus giving *Gauss Law* as a secondary constraint:

$$\kappa^{2a} = \mathcal{G}^a = D_i E_i^a \approx 0 . \tag{1.89}$$

It can be shown [36, 47] that the consistency algorithm stops here, namely that no new independent conditions are obtained imposing $\dot{\kappa}^{2a} \approx 0$. Moreover, the $\mathcal{G}^a$ satisfy the algebra

$$\{\mathcal{G}^a(\mathbf{x}), \mathcal{G}^b(\mathbf{y})\} = g f^{abc}\, \mathcal{G}^c(\mathbf{x})\, \delta(\mathbf{x} - \mathbf{y}) \approx 0 . \tag{1.90}$$

Obviously we also have

$$\{\kappa^{1a}, \kappa^{2b}\} = \{\Pi^{a0}, D_i E_i^b\} = 0 , \tag{1.91}$$

therefore all constraints are first-class and the auxiliary functions λ_1^a are free. This has the immediate consequence that the solution $A_0^a(t,\mathbf{x})$ is an arbitrary function:

$$\dot{A}_0^a(t,\mathbf{x}) = \{A_0^a(\mathbf{x}), H\}_t + \int d\mathbf{y}\, \lambda_1^b(t,\mathbf{y})\, \{A_0^a(\mathbf{x}), \Pi^{b0}(\mathbf{y})\}_t = \lambda_1^a(t,\mathbf{x}) . \tag{1.92}$$

We can use it to express λ_1^a. Summarizing all the above, the total Hamiltonian is

$$H_T = H + \int d\mathbf{x}\, \lambda_1^a \kappa^{1a} = \int d\mathbf{x} \left[\frac{1}{2}(E_i^a)^2 + \frac{1}{2}(B_{ij}^a)^2 - A_0^a(D_i E_i^a) + \dot{A}_0^a \Pi^{a0} \right] . \tag{1.93}$$

Hamiltonian flows that differ by the choice of the arbitrary $A_0^a(t,\mathbf{x})$ must be gauge equivalent thus we can almost[36] read off the generator of gauge transformations from (1.93). Calling $\theta^a(t,\mathbf{x})$ the A_0^a parametrizing the transformation,

$$\int d\mathbf{x} \left[-\theta^a(t)(D_i E_i^a) + \dot{\theta}^a(t)\Pi^{a0} \right] = \int d\mathbf{x} \left[(D_i \theta^a(t)) E_i^a + \dot{\theta}^a(t)\Pi^{a0} \right] , \tag{1.94}$$

---

[35] Here $\{\ ,\ \}_t$ means that, after the Poisson bracket has been computed, is evaluated along the solutions of the equations of motion, at time t.

[36] The generator given below is incomplete, it does not give the correct transformation laws of the arbitrary variables A_0^a. While it can be completed by a standard procedure [36] to $(D_\mu \theta)^a \Pi^{\mu a}$, we do not need this result because we will completely remove A_0^a by gauge fixing.

where we moved the covariant derivative as in (1.86).

For our purposes it is convenient to impose the *temporal* gauge fixing $A_0^a \approx 0$. Since

$$\{A_0^a(\mathbf{x}), \Pi^{b0}(\mathbf{y})\} = \delta^{ab}\delta(\mathbf{x} - \mathbf{y}) , \tag{1.95}$$

the gauge fixing converts Π^{a0} and A_0^a in second-class constraints. On the other hand, $\mathcal{G}^a$ is still first-class and we expect it to generate residual gauge transformations. Having introduced a new condition we must check its consistency; recalling (1.92) this fixes the multipliers λ_1^a:

$$\dot{A}_0^a(t, \mathbf{x}) = \lambda_1^a(t, \mathbf{x}) \approx 0 \quad \Rightarrow \quad \lambda_1^a = 0 \quad \Rightarrow \quad A_0^a(t, \mathbf{x}) = A_0^a(\mathbf{x}) . \tag{1.96}$$

Then the last term of the total Hamiltonian (1.93) is removed and the residual gauge transformations are time independent; they are generated by $-\mathcal{G}^a$:

$$-\int \mathrm{d}\mathbf{x}\, \theta^a \left(D_i E_i^a \right) = +\int \mathrm{d}\mathbf{x}\, (D_i \theta^a)\, E_i^a , \qquad \theta^a(t, \mathbf{x}) = \theta^a(\mathbf{x}) . \tag{1.97}$$

This gives the correct transformation (1.28) of A_i^a, indeed

$$\delta_\theta A_i^a(\mathbf{x}) = \int \mathrm{d}\mathbf{y} \left\{ A_i^a(\mathbf{x}), (D_j^b \theta^b)(\mathbf{y})\, E_j^b(\mathbf{y}) \right\} \tag{1.98}$$

$$= \int \mathrm{d}\mathbf{y}\, \mathrm{d}\mathbf{z}\, \frac{\delta A_i^a(\mathbf{x})}{\delta A_k^c(\mathbf{z})} \frac{\delta((D_j \theta^b)(\mathbf{y})\, E_j^b(\mathbf{y}))}{\delta E_k^c(\mathbf{z})} \tag{1.99}$$

$$= D_i \theta^a(\mathbf{x}) . \tag{1.100}$$

Furthermore, E_i^a transforms in the adjoint, as expected from its definition (1.82),

$$\delta_\theta E_i^a(\mathbf{x}) = \int \mathrm{d}\mathbf{y} \left\{ E_i^a(\mathbf{x}), (D_j^b \theta^b)(\mathbf{y})\, E_j^b(\mathbf{y}) \right\} \tag{1.101}$$

$$= \int \mathrm{d}\mathbf{y}\, \mathrm{d}\mathbf{z} \left[-\frac{\delta E_i^a(\mathbf{x})}{\delta E_k^c(\mathbf{z})} \frac{\delta((\partial_j \theta^b - g f^{bde} A_i^d \theta^e)(\mathbf{y})\, E_i^b(\mathbf{y}))}{\delta A_k^c(\mathbf{z})} \right] \tag{1.102}$$

$$= g f^{abc} \theta^b E_i^c(\mathbf{x}) . \tag{1.103}$$

At this point we can introduce the Dirac brackets and then restrict the phase space by removing A_0^a and Π^{a0}. All the fundamental Dirac brackets coincide with the Poisson ones, except for $\{A_0^a, \Pi^{a0}\}^* = 0$ that allows the removal of A_0^a and Π^{a0}. Finally,

$$H(A_i^a, \partial_i A_j^a, \Pi^{ai}) = \int \mathrm{d}\mathbf{x} \left[\frac{1}{2}(E_i^a)^2 + \frac{1}{2}(B_{ij}^a)^2 \right] . \tag{1.104}$$

Electrodynamics and Chromodynamics.   The matter coupled Yang-Mills theory (1.51)-(1.53) is obtained combining the two previous ones. Here we just state some results (see, e.g., [77]), working directly in the temporal gauge. The Hamiltonian is the sum of (1.78) (eventually generalized to many flavours) and (1.104), plus the potential accounting for the interaction between fermions and gauge fields:

$$H = \int \mathrm{d}\mathbf{x} \left[\frac{1}{2}(E_i^a)^2 + \frac{1}{2}(B_{ij}^a)^2 + \overline{\psi}_r \left(-i\gamma^i \partial_i + m \right) \psi^r + ig\overline{\psi}_r \gamma^i A_i^a (T^a)^r{}_s \psi^s \right] \quad (1.105)$$

$$= \int \mathrm{d}\mathbf{x} \left[\frac{1}{2}(E_i^a)^2 + \frac{1}{2}(B_{ij}^a)^2 + \overline{\psi}_r \left(-i(\gamma^i D_i)^r{}_s + m\delta^r{}_s \right) \psi^s \right] \;. \quad (1.106)$$

Observe that, in temporal gauge, the minimal coupling (1.29) (here involving space derivatives only) gives precisely the interaction term between gauge and matter fields.

As expected, matter fields give an additional contribution to Gauss law:

$$\begin{aligned}
\mathcal{G}^a &= D_i E_i^a - ig\overline{\psi}_r \gamma^0 (T^a)^r{}_s \psi^s \\
&= \partial_i E_i^a - gf^{abc} A_i^b E_i^c - ig\overline{\psi}_r \gamma^0 (T^a)^r{}_s \psi^s \\
&= \partial_i E_i^a - j^{a\,0} \approx 0 \;;
\end{aligned} \quad (1.107)$$

where we used the definitions (1.86) of $D_i E_i^a$ and (1.56) of the Noether current. The $\mathcal{G}^a$ smeared with a time independent parameter $\theta^a(\mathbf{x})$ are still the generators of gauge transformations. If the parameters θ^a are taken also space independent the generators of global transformations are recovered: integrating by parts we have

$$-\int \mathrm{d}\mathbf{x}\, \theta^a \mathcal{G}^a(\mathbf{x}) = -\int \mathrm{d}\mathbf{x}\, \theta^a (\partial_i E_i^a - j^{a\,0}) = \int \mathrm{d}\mathbf{x}\, \theta^a j^{a\,0} = \theta^a Q^a \;. \quad (1.108)$$

1.5   Canonical Quantization

Among the various quantization prescriptions, *canonical quantization* is the most suited for the application of the tensor network techniques of Chapter 3. Consider a generic theory with canonical fields $(\varphi, \pi) = (\{\varphi^n\}, \{\pi_n\})$ and Hamiltonian $H(\varphi, \pi)$.

Canonical quantization [2] "maps" the classical Hamiltonian theory in a quantum one promoting the canonical fields φ^n, π_n as well as their functionals $F(\varphi, \pi)$ to field operators $\hat{\varphi}^n$, $\hat{\pi}_n$, $\hat{F}(\varphi, \pi) = F(\hat{\varphi}, \hat{\pi})$. Namely operator valued functions[37] of space acting on an Hilbert space $\mathscr{H}$, where the state of the system is defined. The field operators are imposed to satisfy

$$[\hat{F}, \hat{G}]_{\pm} = i\, \widehat{\{F, G\}} \;, \qquad \hat{F}^\dagger = \widehat{F^*} \;; \quad (1.109)$$

---

[37] Actually distributions; but we do not pursue this level of mathematical rigor in this work.

where the graded commutator $[\hat{F}, \hat{G}]_\pm$ is equal to the commutator $\hat{F}\hat{G} - \hat{G}\hat{F}$ unless F and G are both Grassmann odd, in which case the anticommutator $\hat{F}\hat{G} + \hat{G}\hat{F}$ is used [46]. As a consequence of (1.109), canonical field operators $\hat{\varphi}, \hat{\pi}$ obey the *canonical commutation* (or *anticommutation*) *relations*

$$[\hat{\varphi}^m(\mathbf{x}), \hat{\pi}_n(\mathbf{y})]_\pm = \mp i \delta^m{}_n \delta(\mathbf{x} - \mathbf{y}) \hat{1} \; . \tag{1.110}$$

Another consequence of (1.109) is that, in the Heisenberg picture, the time evolution of the system is specified by

$$\frac{\mathrm{d}}{\mathrm{d}t} \hat{F} = i [\hat{H}, \hat{F}]_- \; . \tag{1.111}$$

Alternatively, working in the Schrödinger picture field operators remain time independent while the state $|\Psi(t)\rangle$ evolves according to the Schrödinger equation

$$i \frac{\mathrm{d}}{\mathrm{d}t} |\Psi(t)\rangle = \hat{H} |\Psi(t)\rangle \; . \tag{1.112}$$

Ordering of operators.   The above quantization prescription leaves an ambiguity. Consider for simplicity a theory of a single field φ. Classically $\varphi(\mathbf{x})\pi(\mathbf{x}) = \pi(\mathbf{x})\varphi(\mathbf{x})$ but due to (1.110) $\hat{\varphi}(\mathbf{x})\hat{\pi}(\mathbf{x}) \neq \hat{\pi}(\mathbf{x})\hat{\varphi}(\mathbf{x})$ in the quantum theory. This makes the expression $\hat{F}(\varphi, \pi) = F(\hat{\varphi}, \hat{\pi})$ not completely well defined unless an ordering prescription for the operators can be identified; an example will be given in Subsection 2.3C.

Quantum symmetries.   Recall that the Noether charges associated to an internal symmetry form, with the Poisson bracket, a representation of the symmetry algebra (1.65)-(1.66). By (1.109), a representation of the algebra is now realized on $\mathscr{H}$ through the charge operators[38] $\hat{Q}^a$ and the commutator,

$$[\hat{Q}^a, \hat{Q}^b]_- = i f^{abc} \hat{Q}^c \; , \qquad \delta_\theta \hat{F} = i\theta^a [\hat{Q}^a, \hat{F}]_- \quad \text{or} \quad \delta_\theta |\Psi\rangle = i\theta^a \hat{Q}^a |\Psi\rangle \; . \tag{1.113}$$

Moreover, the conservation of the charges $\hat{Q}^a$ reads,

$$[H, Q]_- = 0 \; . \tag{1.114}$$

Analogous results hold for the generators of spacetime symmetries. Finally, using the representatives $\hat{U}(\Lambda, a)$ of the Poincaré group on $\mathscr{H}$, the transformation (1.13) of the classical fields can be recast in [50]

$$\hat{U}(\Lambda, a) \, \hat{\varphi}^m \, \hat{U}^\dagger(\Lambda, a) = D(\Lambda^{-1})^m{}_n \, \hat{\varphi}^n(\Lambda x + a) \; . \tag{1.115}$$

---

[38] Here we assume that all the charges are bosonic, i.e. Grassmann even at the classical level.

In the following we omit the hat on operators and the $\pm$ in the graded commutator.

1.5A Quantization of Gauge Theories

The constraints that appear in the Hamiltonian formulation of gauge theories require some care during quantization and the prescription given above has to be integrated with further conditions. In classical Hamiltonian gauge theories, only the subspace of phase space that satisfies the constraints corresponds to physical configurations. A similar result holds for the Hilbert space of the quantum theory. However, it is important to distinguish between first-class and second-class constraint.

In Subsection 1.4B second-class constraints have been solved; they correspond to null operators in the quantum theory obtained using the Dirac bracket in (1.109) [46]. First-class constraints have been recognized as generators of gauge transformations. It seems reasonable not to impose their vanishing in the operatorial sense. Still, physics is expected to be invariant under gauge transformation. Therefore, following Dirac [5, 46], we impose the weaker condition that only the gauge-invariant states annihilated by first-class constraints are physical and identify the subspace

$$\mathscr{H}_{\text{phys}} = \{\mathcal{G} \left|\Psi_{\text{phys}}\right\rangle = 0\} \subset \mathscr{H} \, , \tag{1.116}$$

where $\mathcal{G}$ denotes symbolically the set of all first-class constraint operators.

An attempt at the quantization of the photon. Even in the simplest scenario, the quantization of pure electromagnetism, the prescription just presented encounters a difficulty. This emerges when we try to impose the physical condition on the states

$$\mathcal{G} \left|\Psi_{\text{phys}}\right\rangle = \partial_i \Pi^i \left|\Psi_{\text{phys}}\right\rangle = 0 \, . \tag{1.117}$$

Then, for any operator O we have

$$\left\langle\Psi_{\text{phys}}\right| [O, \partial_j \Pi^j] \left|\Psi_{\text{phys}}\right\rangle = 0 \, ; \tag{1.118}$$

a result that clashes with the canonical commutation relations [27], giving

$$\left\langle\Psi_{\text{phys}}\right| [A_i^a(\mathbf{x}), \partial_j \Pi^j(\mathbf{y})] \left|\Psi_{\text{phys}}\right\rangle = -i\frac{\partial}{\partial x^i}\delta(\mathbf{x} - \mathbf{y}) \left\langle\Psi_{\text{phys}}|\Psi_{\text{phys}}\right\rangle \, . \tag{1.119}$$

It has been suggested [40] to circumvent the problem assuming that the states satisfying Gauss law are not normalizable. Yet, among these states there must be the vacuum $\left|\Omega\right\rangle$. As pointed out by Strocchi [77], an unormalizable vacuum may lead to inconsistencies from the perspective of a rigorous non-perturbative quantization. We do not discuss this problem any further because it is beyond the scope of this Thesis and, interestingly, will disappear when we formulate the theory on the lattice.

2

Lattice Theories

In this Chapter the general principles of Hamiltonian lattice quantum field theory are discussed. A discretization prescription is elaborated and applied to theories of Dirac and gauge fields. Then the lattice Schwinger model is studied in more detail and some numerically tractable reformulations of the theory are put forward, paving the way for the application of the methods presented in Chapter 3.

2.1 Lattice as a Regulator

Applying the canonical quantization prescription to a classical Hamiltonian is not enough to completely define a QFT. The theory obtained in this way produces divergent results that must be cured by also specifying a *regularization* prescription. A possible strategy is to start from a theory with a finite number of degrees of freedom defined on a lattice: a discrete and finite spacetime and then *defined* the QFT as the *continuum* and *thermodynamic limits* of this finite theory. This is the paradigm of lattice quantum field theory. The lattice provides both an ultraviolet (UV) cutoff, due to the finite spacing between lattice points, and an infrared (IR) cutoff, because of the finite extent of the lattice. The continuum and thermodynamic limits consists in sending the spacing to zero and the volume to infinity[1]; in doing so a *renormalization* procedure is necessary to ensure that the relevant observables remain finite in the limits. In the following we will use the expression continuum limit to refer to both the above limits. There are many reasons to choose the lattice as a regulator and study lattice quantum field theories, both technical and conceptual [102].

Technical motivations.   The first observation is that the lattice regularization is genuinely *non-perturbative.* Moreover, prior to taking the continuum limit, the theory is really a *many-body quantum mechanical system.* Avoiding the problem of dealing directly with an infinite number of degrees of freedom has important advantages: (i) many far-reaching exact statements can be made quite rigorous in the framework of quantum mechanics and thus of lattice quantum field theories; (ii) the finiteness of the problem makes it accessible, at least in principle, to numerical

---

[1] It should be noted that the two limits do not in general commute and care has to be taken.

simulation on the computer. Clearly, some difficulties are just postponed to the delicate task of taking the continuum limit. This obviously can not be performed directly on a computer (as the amount of available resources is always finite) and other techniques, such as finite-size scaling analysis [19, 95], are necessary for its extrapolation. Furthermore, whether the exact results mentioned above continue to hold in the continuum limit is often not clear for interacting theories and positive answers are generally based on circumstantial evidence [102].

Conceptual motivations. Depending on personal taste, the problem of having a rigorous continuum limit might not be perceived as relevant as the previous statements make it appear to be. Without dwelling too much on topics that go beyond the scope of this Thesis and partially attain to philosophy of science [74], if the universe is assumed to be finite and quantum gravity appears at some ultraviolet scale, any theory on flat Minkowski spacetime is to be considered an effective field theory, only relevant over a finite distance and up to a finite energy. Consequently a finite and discrete theory might actually even be a better approximation of nature than its continuum counterpart.

Hamiltonian approach. Lattice field theories are most commonly quantized in Euclidean[2] spacetime using the path integral formalism; and numerically simulated via Monte-Carlo methods. This approach provided remarkable results in the past decades. Here a different but promising path [23, 30] is followed and a canonical quantization of the (finite) lattice degrees of freedom is preformed. In this framework there is no need to analytically continue to imaginary times; for this reason, when performing dynamical studies this approach is referred to as *real-time* simulation. The Hamiltonian formalism requires to choose a time direction thus spoiling manifest Lorentz boost invariance, which is nevertheless already broken by the lattice itself. On the other hand, it is particularly well suited to compute physically interesting quantities such as ground states, masses, properties of bound states and phase diagrams, that are sometimes hard to extract from the path integral formulation [62]. Notably, Hamiltonian numerical simulations do not suffer from the sign problem often found in Monte-Carlo simulations [90, 102]. Finally, the numerical analysis performed in this Thesis relies on classical simulation techniques from many-body and quantum information theory (introduced in Chapter 3). However, the canonical formulation is also the natural one for the study of analog and digital quantum simulation [58, 87, 97] of quantum field theories.

---

[2] The presence of the oscillatory phase in the path integral partition function requires a Wick rotation (analytic continuation of the time coordinate to imaginary values) for formal convergence.

2.2 Discretization Prescription

Some key ingredients for the discretization of a $(1 + d)$-dimensional Hamiltonian field theory are now briefly outlined. As mentioned in Section 1.4, Hamiltonian fields are functions of Euclidean space $\mathbb{R}^d$ rather than Minkowski spacetime $\mathbb{R}^{1,d}$. It is thus Euclidean space that has to be truncated and discretized in order to obtain the discrete domain on which the Hamiltonian lattice field theory degrees of freedom are defined. The time direction is not involved in this procedure. The lattice theories here studied are thus formulated in continuous time[3] and discrete space [62].

Lattice and reciprocal lattice. In this Thesis an homogeneous lattice[4] with spacing ℓ and linear size ℓL,

$$\Lambda := \ell \left\{ 1, \dots, L \right\}^d \ , \tag{2.1}$$

is always used. Analytic derivations are carried out assuming *periodic boundary conditions*, $\Lambda \cong \ell(\mathbb{Z}_L)^d$. Continuous spacetime symmetries cannot be implemented on the lattice but are recovered in the continuum limit [68]. On the lattice, space rotations are broken down to the finite rotation group of the d-hypercube while only translations by multiples of the lattice step ℓ are available, the group of residual space translations being Λ itself. There are still conserved charges associated to these symmetries, such as the momentum, but they take discrete values [102].

The UV and IR regulators provided by the lattice are ℓ and $1/L$ respectively. By removing these regulators $\ell \to 0$ and $1/L \to 0$ (after a renormalization procedure) the continuum theory is defined. The cutoff role played by ℓ and L is even clearer in momentum space. The frequency spectrum of a function defined on Λ cannot contain modes of wavelength shorter than ℓ or longer than ℓL.[5] Explicitly, the momentum space or reciprocal lattice of the theory on which discrete Fourier transforms of spatial functions are defined is (even L is here assumed for ease of notation),

$$\Lambda^* := \frac{2\pi}{\ell L} \left\{ -\frac{L}{2}, -\frac{L}{2} + 1, \dots, \frac{L}{2} - 1 \right\}^d \simeq \frac{2\pi}{\ell L} (\mathbb{Z}_L)^d \ . \tag{2.2}$$

---

[3] If numerical simulations are performed the time direction has to be discretized anyway. However, this discretization is not part of the definition of the theory and is not present in analytical studies.

[4] As a slight generalization, hyperrectangular lattices may be considered. More exotic geometries have been explored in the past but did not provide manifest benefits [102].

[5] Let $d = 1$ (the generalization is obvious). Since x is a multiple of ℓ, Fourier modes e^{ikx} with momenta differing by $2\pi/\ell$ are identified. In addition, due to periodic boundary conditions, a function defined on Λ is equivalent to a ℓL-periodic function on $\ell\mathbb{Z}$, thus only momenta multiple of $2\pi/\ell L$ are allowed.

This is the discrete subset of the Brillouin zone of solid state physics on which Fourier transforms of ℓL-periodic functions are supported. For $L \to \infty$ the full Brillouin zone is recovered. The correspondence is due to periodicity and translation invariance of the lattice Λ, that make it equivalent to a hypercubic Bravais lattice with primitive cell of side ℓ and whose Brillouin zone is the d-torus $\mathbb{T}^d \simeq [-\pi/\ell, \pi/\ell[^d$ [63].

Discrete analysis. Loosely speaking, limiting procedures ($\epsilon \to 0$) that appear in analytic operations, such as (Riemann) integration and derivation, have to be reverted on the lattice ($\epsilon \sim \ell$). In fact they are incorporated in the continuum limit of the lattice theory. This operation is not always uniquely determined but the various implementations must yield the same $\ell \to 0$ limit.

More concretely, integrals and derivatives will be replaced by Riemann sums and finite difference operators, such as the central derivative,

$$\int \mathrm{d}^D x \, \phi(x) \; \to \; \ell^d \sum_{x \in \Lambda} \phi(x) \, , \qquad \partial_k \phi(x) \; \to \; \frac{\phi(x + \ell\hat{k}) - \phi(x - \ell\hat{k})}{2\ell} \qquad (2.3)$$

where $\hat{k}$ is the k-th element of the canonical basis of $\mathbb{R}^d$. Analogous substitutions apply in momentum space with Λ and ℓ replaced by Λ^* and $2\pi/\ell L$.

Lattice units. Most of the work in lattice field theory is done at finite spacing, in which case ℓ provides a convenient length unit. If not otherwise stated, *lattice units* $\ell = 1$ are assumed in the following.

2.3 Matter Fields

The mapping of continuum fermionic theories into their lattice equivalent requires particular care. The most striking consequence of a naïve discretization is the infamous doubling problem: a proliferation of propagating degrees of freedom on the lattice. This problem is now discussed and a possible solution, *staggered fermions*, is introduced and adopted throughout the remainder of the Thesis. The discussion in then specialized to $1 + 1$ spacetime dimensions and the general solution of the discretized Dirac equation is found. Upon quantization the general solution provides the free theory creation and annihilation operators that allow to build particle wave packet states. Finally, the normal ordered Hamiltonian and particle number charge operators are given. Apart from the doubling problem, the results here obtained reproduce most of the features of the continuum ones [49]; some peculiarities of the lattice description are emphasized.

2.3A   Doubling problem

To adhere to the presentations of the doubling problem commonly found in the literature [57, 63, 73], in this introduction discretized fermions are studied from the prespective of the action rather than that of the Hamiltonian. Space and time are momentarily taken to be both discrete and are modeled by an infinite lattice $x, y \in \ell\mathbb{Z}^D$. Similar results hold on a finite lattice or working with only space discretized. The "naïve" discretization of the action of free Dirac fermions (1.47),

$$S = \int \mathrm{d}x\, \overline{\psi} \left(i\slashed{\partial} - m \right) \psi \ , \tag{2.4}$$

following the recipe of Section 2.2 provides

$$S = \sum_{xy} \overline{\psi}_x \Gamma^x{}_y \psi^y \ , \qquad \Gamma^x{}_y = i\slashed{\partial}^x{}_y - m\delta^x{}_y \ . \tag{2.5}$$

Here spinor indices are left implicit and the derivative is the central derivative

$$(\partial_\mu)^x{}_y := \frac{1}{2\ell} \left[\delta^{x+\ell\hat{\mu}}{}_y - \delta^{x-\ell\hat{\mu}}{}_y \right] \ . \tag{2.6}$$

The cinematic of the free theory is contained in the propagator Γ^{-1}. This is easily obtained in momentum space. The only non-trivial term of $\Gamma(k)$ is the derivative:

$$\sum_{xy} e^{-i(px+qy)} (\partial_\mu)^x{}_y = \left[\sum_x e^{-i(p+q)x} \right] \frac{e^{-i\ell p_\mu} - e^{+i\ell p_\mu}}{2\ell} = (2\pi)^D \delta^D(p+q) \frac{-i\sin(\ell p_\mu)}{\ell} \tag{2.7}$$

Therefore

$$\Gamma(k) = \gamma^\mu \frac{1}{\ell} \sin(\ell k_\mu) - m \ . \tag{2.8}$$

and the propagator reads

$$\Gamma^{-1}(k) = \frac{\gamma^\mu \tilde{k}_\mu + m}{\tilde{k}^2 - m^2} \ , \qquad \tilde{k}_\mu = \frac{1}{\ell} \sin(\ell k_\mu) \ . \tag{2.9}$$

The denominator of $\Gamma^{-1}(k)$ is invariant under $k_\mu \to k_\mu + \pi n_\mu$ with $n \in \{0,1\}^D$ and thus has 2^D zeros. On its turn, this implies that our lattice version of a continuum theory with one fermion specie has a propagator with 2^d poles, and hence propagating fermion species. Even if an initial state composed by excitations corresponding only to one of the poles is prepared, as soon as some interaction is included the additional fermions can be produced just as easily as the original ones [96]. The problem clearly does not fade away in the continuum limit $\ell \to 0$, nor it is a peculiarity of the followed discretization prescription.

The problem presented above is the manifestation of a general result [35, 38, 96], the Nielsen-Ninomiya no-go theorem (1981), which states that for even spacetime dimensions[6] there cannot exist a Γ satisfying

(i) $\Gamma(k) = \gamma^\mu k_\mu - m + \mathcal{O}(\ell k)^2$, to reproduce the continuum theory for momenta small compared to the ultraviolet cutoff;

(ii) $\Gamma(k)$ is analytic in $k \in \mathbb{T}^D$, to ensure the locality of the continuum limit theory;

(iii) $\Gamma(k)$ anticommutes with $\gamma_0 \gamma_1 \dots \gamma_{D-1}$, to preserve chiral symmetry for $m = 0$;

(iv) $\Gamma^{-1}(k)$ has a single pole, to avoid doublers (violated by naïve fermions).

Therefore there cannot exist a translation invariant, local, hermitian lattice theory of Dirac fermions with chiral symmetry and no doublers.

The doubling problem is essentially a consequence of the first derivative nature of fermionic actions (there is no doubling problem for bosons) and is also strictly related to chiral symmetry (absence of axial anomaly [15, 16, 41] on the lattice [34, 73]). These aspects are not discussed here. We turn instead to one of the possible (partial) solutions: *staggered fermions*, proposed in 1975 by Kogut and Susskind [23, 24, 26].

2.3B   Staggered Fermions

The staggered formulation stems from a procedure of spin-diagonalization [57, 63] of the action. At each lattice site a unitary transformation of the spinor allows to put the action in a diagonal and degenerate form with respect to the $2^{D/2}$ spinor components (even D is assumed here). Finally the contribution of only one component is kept. In this way the number of doublers is reduced, but $2^{D/2} - 1$ of them still presist: like naïve fermions, staggered fremions verify (i), (ii) and (iii) but not (iv).

In $1 + 1$ dimensions with only space discretized the staggerization corresponds to a complete removal of the doublers. In the following we focus on this case and stagger directly the naïvely discretized ($\ell = 1$) Dirac Hamiltonian (1.78)

$$H = \sum_x \left[-i\overline{\psi}_x \gamma^1 \partial_1 \psi^x + m\overline{\psi}_x \psi^x \right] \; ; \tag{2.10}$$

where $\partial_1 \equiv \partial$ is the spatial central derivative. A possible choice of γ matrices is

$$\gamma^0 = \begin{bmatrix} 1 & 0 \\ 0 & -1 \end{bmatrix} , \qquad \gamma^1 = \begin{bmatrix} 0 & 1 \\ -1 & 0 \end{bmatrix} . \tag{2.11}$$

We now use these to make explicit the spinor components $\psi^x = (\psi^{1,x}, \psi^{2,x})$. With

---

[6] A similar result holds for odd spacetime dimensions, with chiral symmetry replaced by parity.

a summation over the repeated position indices x implied,

$$H = \left[-i\psi^\dagger_{1,x} \partial \psi^{2,x} + (1 \leftrightarrow 2) \right] + \left[m \psi^\dagger_{1,x} \psi^{1,x} - (1 \leftrightarrow 2) \right] \; . \tag{2.12}$$

Here "$1 \leftrightarrow 2$" denotes symbolically the terms on its left with 1 and 2 exchanged. Similar notations are used in the following. Introducing

$$\xi^x = \begin{cases} \psi^{1,x} & x \text{ even} \\ \psi^{2,x} & x \text{ odd} \end{cases}, \qquad \tilde{\xi}^x = \xi^x|_{1 \leftrightarrow 2} \; ; \tag{2.13}$$

the kinetic terms become (via periodic boundary conditions)

$$-\frac{i}{2}\, \xi^\dagger_x(\xi^{x+1} - \xi^{x-1})\Big|_{x \text{ even}} + (\xi \to \tilde{\xi})\Big|_{x \text{ odd}} + (\xi \leftrightarrow \tilde{\xi}) = \frac{i}{2}\xi^\dagger_{x+1}\xi^x + \text{H.c.} + (\xi \to \tilde{\xi}) \; . \tag{2.14}$$

An identical procedure applies to the mass term

$$\xi^\dagger_x \xi^x\Big|_{x \text{ even}} + (\xi \to \tilde{\xi})\Big|_{x \text{ odd}} - (\xi \leftrightarrow \tilde{\xi}) = (-1)^x \xi^\dagger_x \xi^x - (\xi \to \tilde{\xi}) \; ; \tag{2.15}$$

where an alternating sign, peculiar of staggered fermions, has appeared. In both terms the contributions of ξ and $\tilde{\xi}$ decouple; moreover, via the field redefinition $\tilde{\xi}^x \to i(-1)^x\tilde{\xi}^x$ the Hamiltonian becomes also manifestly degenerate in ξ and $\tilde{\xi}$ and the spin-diagonalization procedure is complete. Finally, only one of the two identical contributions is kept and the Hamiltonian describing a free staggered fermion field is obtained

$$H = \frac{i}{2} \sum_x \left(\xi^\dagger_{x+1}\xi^x - \xi^\dagger_x \xi^{x+1} \right) + m \sum_x (-1)^x \xi^\dagger_x \xi^x \; . \tag{2.16}$$

The Poisson bracket between ψ^x and $\psi^\dagger_y$, discrete analogous of (1.81), implies

$$\{\xi^x, \xi^\dagger_y\} = -i\delta^x{}_y \; . \tag{2.17}$$

Staggered lattice. The mass term in Hamiltonian (2.16) is invariant only under $x \to x + 2\ell$ shifts (ℓ has been reintroduced for clarity). Accordingly, the lattice of staggered fermions can be thought of as the union of two even and odd site sublattices with doubled spacing and thus halved Brillouin zone. Specularly, the reciprocal lattice can be thought of as the union of two halved effective Brillouin zones of width π/ℓ, one for each pole of Section 2.3A. In some cases encountered in the following it will be convenient to introduce *staggered functions*, i.e. functions defined separately on the even and odd sublattices. Some machinery that will prove useful for this scope is introduced in Appendix B. The main message is that the even site and odd site parts of the position space staggered function correspond respectively to the π/ℓ-periodic and π/ℓ-antiperiodic part of its momentum space

representation.

Quantization and Jordan-Wigner representation. The quantization prescription of Section 1.5 applies straightforwardly to the theory of free staggered fermions. The Poisson bracket (2.17) results in the canonical anticommutation relations

$$[\xi^x, \xi_y^\dagger] = \delta^x{}_y \;, \qquad [\xi^x, \xi^y] = 0 \;, \qquad [\xi_x^\dagger, \xi_y^\dagger] = 0 \;. \tag{2.18}$$

We now aim to find an explicit irreducible representation of (2.18). These imply

$$[\xi_x^\dagger \xi^x, \xi_y^\dagger] = \xi_x^\dagger \delta^x{}_y \;, \qquad (\xi^x)^2 = 0 \;, \qquad (\xi_x^\dagger \xi^x)^2 = \xi_x^\dagger \xi^x \;. \tag{2.19}$$

The first shows that ξ^x is a raising operator for the *occupation number* operator $n_x = \xi_x^\dagger \xi^x$. The others that there can be only two occupation levels, $|0\rangle$ and $|1\rangle$. Hence, for a one site chain and working in the $\{|1\rangle, |0\rangle\}$ basis, a representation of (2.18) is in terms of the spin-1/2 raising and lowering matrices,

$$\xi^\dagger = \sigma^+ = \begin{bmatrix} 0 & 1 \\ 0 & 0 \end{bmatrix} \;, \qquad \xi = \sigma^- = \begin{bmatrix} 0 & 0 \\ 1 & 0 \end{bmatrix} \;, \qquad n = \sigma^+ \sigma^- = \begin{bmatrix} 1 & 0 \\ 0 & 0 \end{bmatrix} \;. \tag{2.20}$$

When dealing with more sites, as many-body Hilbert space basis we choose

$$\left\{ \bigotimes_x |n_x\rangle \;:\; n_x = 1, 0 \right\} \;. \tag{2.21}$$

In order to achieve anticommutation between fermionic operators acting on different sites we adopt the *Jordan-Wigner* representation [1]

$$\xi_x^\dagger = \sigma_x^+ \prod_{y<x} (-1)^{n_y} = \sigma_x^+ \, e^{i\Theta_x} \;, \qquad \Theta_x = \pi \sum_{y<x} n_y \;; \tag{2.22}$$

which corresponds the convention that ξ^x and $\xi_x^\dagger$ pick up a minus sign for every filled site on their left. Notice that in the (quantized) Hamiltonian (2.16) all the non-local Jordan-Wigner strings $e^{i\Theta_x}$ cancel out in the case of open or infinite boundaries. For periodic boundary conditions, observing that $\sigma^+ = -(-1)^n \sigma^+$ we have

$$\xi_L^\dagger \xi^1 = (-1)^{\sum_{x<L} n_x} \sigma_L^+ \sigma_1^- = (-1)^{N-1} \sigma_L^+ \sigma_1^- \;, \qquad N = \sum_x n_x \;. \tag{2.23}$$

While the explicit representation of the staggered fermions operators outlined above is needed for the implementation of numerical simulations, it will not be relevant for the analytic investigations carried out in the following Sections.

2.3C Particle Spectrum

In continuum free quantum field theories the particle picture of Sections 1.1–1.2 can be constructed explicitly. Particle quanta are excitations of modes of an infinite system of Harmonic oscillators, and generate the Fock space of the free theory. The previous statements become manifest through a Fourier decomposition of the general solution of the equations of motion. Here we follow the same procedure to show that analogous results hold for the lattice theory of free staggered fermions.

Solution of the equation of motion. Let $\xi(t,x) \equiv \xi^x(t)$ be a classical trajectory. The Hamilton equations of the staggered fermion Hamiltonian (2.16) read[7]

$$i\dot{\xi}(t,x) = i\frac{\partial H}{\partial(i\xi_x^\dagger)}\bigg|_{\xi(t,x)} = -\frac{i}{2}\left[\xi(t,x+1) - \xi(t,x-1)\right] + m\,(-1)^x\xi(t,x) \ . \quad (2.24)$$

Equations (2.24) imply the second order condition

$$-\ddot{\xi}(t,x) = -\frac{1}{4}\left[\xi(t,x+2) - \xi(t,x-2) - 2\xi(t,x)\right] + m^2\,\xi(t,x) \ . \quad (2.25)$$

Writing $\xi(t,x)$ in terms of its Fourier transform

$$\xi(t,x) = \int d\omega \sum_k e^{-i\omega t + ikx}\,\xi(\omega,k) \quad (2.26)$$

and inserting it in (2.25)

$$\int d\omega \sum_k \left[\omega^2 - \frac{1}{4}\left(e^{+2ik} + e^{-2ik} - 2\right) + m^2\right]\xi(\omega,k) = 0 \ , \quad (2.27)$$

yields the on-shell condition, namely

$$\xi(\omega,k) = \delta(\omega^2 - \sin^2(k) - m^2)\,\zeta(\omega,k) \quad (2.28)$$

for some function $\zeta(\omega,k)$. This result is the lattice equivalent of the observation that the general solution of the Dirac equation also satisfies Klein-Gordon's and thus verifies the relativistic dispersion relation $\omega_k = \sqrt{m^2 + k^2}$. Nevertheless, this dispersion relation and the related group velocity are modified by lattice artifacts to

$$\omega_k = \sqrt{m^2 + \frac{\sin^2(\ell k)}{\ell^2}} \ , \qquad \omega_k' = \frac{\sin(\ell k)\cos(\ell k)}{\ell\omega_k} \ ; \quad (2.29)$$

---

[7] Here we work at the classical level but the equations are linear thus their solution provides also a solution of the Heisenberg equation for the ξ^x operator.

where the lattice spacing ℓ has been reintroduced for clarity. The continuum relations are reproduced in a neighbourhood of each pole $\ell k \sim 0, \pi$. This modification has nevertheless important consequences on the propagation of staggered fermions, see Figure 2.1.
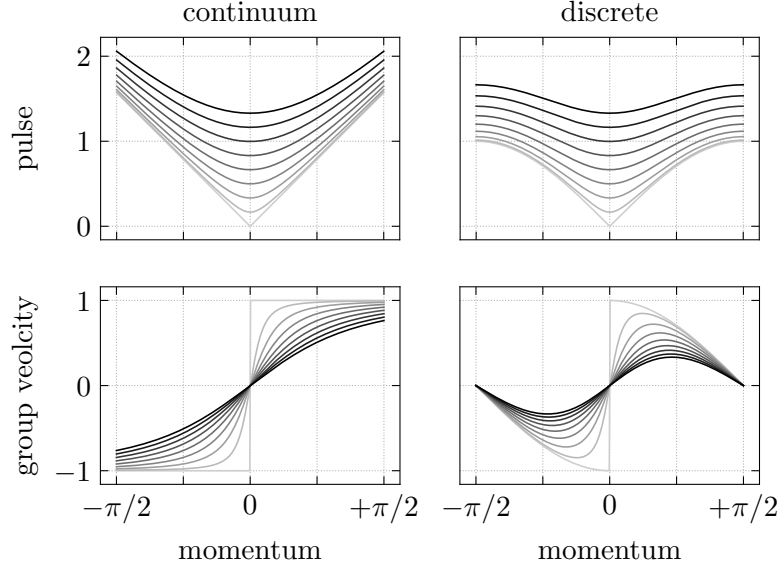

Figure 2.1: Dispersion relation and propagation speed in the continuum (left) and on the lattice (right, $L = \infty$, $\ell = 1$) for different values of the mass m (lighter colours correspond to lighter particles) and momenta in one of the two effective Brillouin zones of staggered fermions (the other being an identical copy).

Before pressing on and imposing the first order equations (2.24) two observations are in order. Firstly, these equations are different in form for the ξ degrees of freedom living on even and odd sublattices, it is then convenient to write them in terms of two independent functions ξ^{E} and ξ^{O}, as per (B.2). Secondly, (2.28) can be further expanded isolating the contribution of positive and negative frequency solutions

$$\xi(\omega, k) = \xi_+(\omega, k) + \xi_-(\omega, k) = \frac{\delta(\omega - \omega_k)\, \zeta_+(k) + \delta(\omega + \omega_k)\, \zeta_-(k)}{2\omega_k} \ , \qquad (2.30)$$

with $\zeta_\pm(k) = \zeta(\pm\omega_k, k)$. Bearing all this in mind,

$$\xi_\pm^{\mathrm{E,O}}(t, x) = \sum_k \frac{1}{2\omega_k}\, e^{\mp i\omega_k t + ikx}\, \zeta_\pm^{\mathrm{E,O}}(k) \ . \qquad (2.31)$$

Recalling that the Fourier transform of $(-1)^x$ is $\delta(k - \pi)$ and the shift symmetry

properties (B.7), (2.24) imply

$$\pm \omega_k \left[\zeta_\pm^{\mathrm{E}}(k) + \zeta_\pm^{\mathrm{O}}(k) \right] = \sin(k) \left[\zeta_\pm^{\mathrm{E}}(k) + \zeta_\pm^{\mathrm{O}}(k) \right] + m \left[\zeta_\pm^{\mathrm{E}}(k) - \zeta_\pm^{\mathrm{O}}(k) \right] . \qquad (2.32)$$

These must hold for every k, combining them with the equations for $k + \pi$ provides

$$\begin{bmatrix} \pm\omega_k - m & -\sin(k) \\ -\sin(k) & \pm\omega_k + m \end{bmatrix} \begin{bmatrix} \zeta_\pm^{\mathrm{E}}(k) \\ \zeta_\pm^{\mathrm{O}}(k) \end{bmatrix} = 0 . \qquad (2.33)$$

The solutions are

$$\begin{bmatrix} \zeta_+^{\mathrm{E}}(k) \\ \zeta_+^{\mathrm{O}}(k) \end{bmatrix} = a(k) \begin{bmatrix} \omega_k + m \\ \sin(k) \end{bmatrix} , \qquad \begin{bmatrix} \zeta_-^{\mathrm{E}}(-k) \\ \zeta_-^{\mathrm{O}}(-k) \end{bmatrix} = b^\dagger(k) \begin{bmatrix} \sin(k) \\ \omega_k + m \end{bmatrix} ; \qquad (2.34)$$

where the Grassman odd $a(k)$ and $b(k)$ are the Fourier weights of the positive and negative frequency plane wave solutions of momentum k. These are completely determined by their behaviour on half of the Brillouin zone,

$$a(k) = a(k + \pi) , \qquad b^\dagger(k) = -b^\dagger(k + \pi) ; \qquad (2.35)$$

confirming that the two poles of the propagator (2.9) are related to the same "wave" component and making the counting of position space and momentum space degrees of freedom consistent.

Introducing some normalization conventions, the general solution reads

$$\xi(t,x) = \frac{1}{\sqrt{L}} \sum_k \frac{1}{\sqrt{2\omega_k}} (f_k + g_k) \left[a(k) \, e^{-ik_\mu x^\mu} + b^\dagger(k) \, e^{+ik_\mu x^\mu} \right] \Big|_{k^\mu = (\omega_k, k)} , \qquad (2.36)$$

where

$$f_k = \sqrt{\omega_k + m} , \quad g_k = \sin(k)/\sqrt{\omega_k + m} ;$$
$$f_k^2 + g_k^2 = 2\omega_k , \quad f_k^2 - g_k^2 = 2m ;$$
$$f_{-k} = f_{k+\pi} = +f_k , \quad g_{-k} = g_{k+\pi} = -g_k ;$$
$$g_k \to 0 , \ f_k^2 \sim 2m \ \text{ for } \ m \to \infty , \quad f_k^2 \sim g_k^2 \sim \omega_k \ \text{ for } \ m \to 0 .$$
$$\qquad (2.37)$$

Using these, even and odd site contributions are recovered; at $t = 0$

$$\xi(0,x) = \frac{1}{\sqrt{L}} \sum_k \frac{e^{+ikx}}{\sqrt{2\omega_k}} \left[(f_k + g_k)a(k) + (f_k - g_k)b^\dagger(-k) \right] \qquad (2.38a)$$

$$= \frac{1}{\sqrt{L}} \sum_k \frac{e^{+ikx}}{\sqrt{2\omega_k}} \begin{cases} f_k \, a(k) - g_k \, b^\dagger(-k) & x \text{ even} \\ g_k \, a(k) + f_k \, b^\dagger(-k) & x \text{ odd} \end{cases} . \qquad (2.38b)$$

Finally,

$$a(k) = \frac{1}{\sqrt{L}} \sum_x \frac{e^{-ikx}}{\sqrt{2\omega_k}} \xi(0,x) \begin{cases} f_k & x \text{ even} \\ g_k & x \text{ odd} \end{cases} \; , \tag{2.39a}$$

$$b^\dagger(k) = \frac{1}{\sqrt{L}} \sum_x \frac{e^{+ikx}}{\sqrt{2\omega_k}} \xi(0,x) \begin{cases} g_k & x \text{ even} \\ f_k & x \text{ odd} \end{cases} \; . \tag{2.39b}$$

We now check (2.39a) explicitly, an identical procedure applies to (2.39b),

$$(2.39\text{a}) = \sum_q \frac{1}{\sqrt{2\omega_k 2\omega_q}} \left[f_k(f_q a_q - g_q b^\dagger_{-q}) \sum_{x \text{ even}} + g_k(g_q a_q + f_q b^\dagger_{-q}) \sum_{x \text{ odd}} \right] \frac{e^{-ikx+iqx}}{L} \; . \tag{2.40}$$

Recalling (B.5) the space sums of the phases yield $(\delta_{kq} \pm \delta_{k,q+\pi})/2$. Yet, given (2.35) and (2.37), the summand is symmetric under $q \to q+\pi$. If we restrict the summation on the half of the domain containing p, only the first delta contributes,

$$(2.39\text{a}) = \sum_q \frac{f_k(f_q a_q - g_q b^\dagger_{-q}) + g_k(g_q a_q + f_q b^\dagger_{-q})}{\sqrt{2\omega_k 2\omega_q}} \delta_{kq} = \frac{f_k^2 + g_k^2}{2\omega_k} a_k = a_k \; . \tag{2.41}$$

As just found, sometimes the π-periodicity of the integrand in (2.38b) makes it convenient to work only with momenta contained in one half of the full Brillouin zone, e.g., with the effective reciprocal lattice

$$\Lambda^* \cap [-\pi/2, +\pi/2[\; . \tag{2.42}$$

This is not always the case; in particular this choice does not allow to to write the Fourier decomposition of the general solution of the equation of motion (2.24) in terms of a unique function of the momentum, as in (2.36). To exploit the best of both approaches, alongside $a(k)$ and $b(k)$ we introduce two new "effective" Fourier coefficients $\tilde{a}(k)$ and $\tilde{b}(k)$ related to the previous by[8]

$$\tilde{a}(k) = \sqrt{2}a(k) \; , \qquad \tilde{b}(k) = \sqrt{2}b(k) \; , \qquad k \in [-\pi/2, +\pi/2[\; ; \tag{2.43}$$

but defined only on the effective reciprocal lattice. In terms of these (2.38b) becomes

$$\xi(0,x) = \sqrt{\frac{2}{L}} \sum_k^\star \frac{e^{+ikx}}{\sqrt{2\omega_k}} \begin{cases} f_k \tilde{a}(k) - g_k \tilde{b}^\dagger(-k) & x \text{ even} \\ g_k \tilde{a}(k) + f_k \tilde{b}^\dagger(-k) & x \text{ odd} \end{cases} \; ; \tag{2.44}$$

---

[8]   Conversely, due to (2.35) $a(k)$ and $b(k)$ are completely specified by $\tilde{a}(k)$ and $\tilde{b}(k)$.

where the starred summation symbol,

$$\sum^{\star} , \tag{2.45}$$

signals that only momenta in the effective reciprocal lattice (2.42) are involved. A notation that we will reiterate in the following.

We may now interpret the classical solutions of the previous paragraph as solutions of the Heiseberg equation for the operatorial ξ^x. The Fourier modes $\tilde{a}_k$ and $\tilde{b}_k$ become operators and the anticommutation relations (2.18) satisfied by ξ^x and $\xi_y^{\dagger}$ imply

$$[\tilde{a}_p, \tilde{a}_q^{\dagger}] = [\tilde{b}_p, \tilde{b}_q^{\dagger}] = \delta_{pq} ; \tag{2.46}$$

while other anticommutators vanish. To check this recall (B.5) and (2.37), by those we have

$$[\tilde{a}_p, \tilde{a}_q^{\dagger}] = \frac{2}{L} \sum_{xy} \frac{e^{-ipx+iqy}}{\sqrt{2\omega_p 2\omega_q}} [\xi^x, \xi_y^{\dagger}] \begin{cases} f_p f_q & x, y \text{ even} \\ g_p g_q & x, y \text{ odd} \\ \dots & \text{otherwise} \end{cases}$$

$$= \frac{2}{L\sqrt{2\omega_p 2\omega_q}} \left[f_p f_q \sum_{x \text{ even}} + g_p g_q \sum_{x \text{ odd}} \right] e^{-i(p-q)x}$$

$$= \frac{f_p f_q}{2\omega_p} \left(\delta_{pq} + \delta_{p,q+\pi} \right) + \frac{g_p g_q}{2\omega_p} \left(\delta_{pq} - \delta_{p,q+\pi} \right)$$

$$= \frac{f_p^2 + g_p^2}{2\omega_p} \left(\delta_{pq} + \delta_{p,q+\pi} \right) . \tag{2.47}$$

The π-shifted delta does not contribute[9] because $p, q \in [-\pi/2, +\pi/2[$ and the anticipated result is obtained. An analogous derivation carries over with $\tilde{b}$.

We now express the Hamiltonian (2.16) in terms of the monochromatic solutions $\tilde{a}_k^{\dagger}$ and $\tilde{b}_k^{\dagger}$ and show that these operators act by "creating" quanta of momentum k.

---

[9] Had we used a or b this would not be true, instead

$$[a_p, a_q^{\dagger}] = (\delta_{pq} + \delta_{p,q+\pi})/2 , \qquad [b_p, b_q^{\dagger}] = (\delta_{pq} - \delta_{p,q+\pi})/2 . \tag{2.48}$$

Once again the contributions of the two poles of Section 2.3A are intertwined.

Momentum space Hamiltonian. All the terms in Hamiltonian (2.16), namely

$$H = \frac{i}{2} \sum_x \left[\xi_{x+1}^\dagger \xi^x + \text{H.c.} \right] + m \sum_x (-1)^x \xi_x^\dagger \xi^x \ , \tag{2.49}$$

have the form $\xi_y^\dagger \xi^x$. For such an operator we have, by (2.38a),

$$\xi_y^\dagger \xi^x = \frac{1}{L} \sum_{qp} \frac{e^{-iqy+ipx}}{\sqrt{2\omega_q 2\omega_p}} \, \Theta(p,q) \ , \tag{2.50}$$

with

$$\Theta(p,q) = \Theta^\dagger(q,p) = \left[(f_q + g_q) a_q^\dagger + (f_q - g_q) b_{-q} \right] \left[(f_p + g_p) a_p + (f_p - g_p) b_{-p}^\dagger \right] \ . \tag{2.51}$$

Specializing this result to the kinetic terms,

$$\sum_x \xi_{x+1}^\dagger \xi^x = \frac{1}{L} \sum_{qp} \sum_x \frac{e^{-iq(x+1)+ipx}}{\sqrt{2\omega_q 2\omega_p}} \, \Theta(p,q) = \sum_k \frac{e^{-ik}}{2\omega_k} \, \Theta(k,k) \ . \tag{2.52}$$

Only the antiperiodic terms in $\Theta(k,k)$ survive the summation, recalling (2.35)–(2.37),

$$\Theta(k,k) = (f_k + g_k)^2 \, a_k^\dagger a_k + (f_k - g_k)^2 \, b_{-k} b_{-k}^\dagger + (f_k^2 - g_k^2)(a_k^\dagger b_{-k}^\dagger - b_{-k} a_k)$$

$$= 2\sin(k) \left(a_k^\dagger a_k - b_{-k} b_{-k}^\dagger \right) + 2m \left(a_k^\dagger b_{-k}^\dagger - b_{-k} a_k \right) + [\ldots] \tag{2.53}$$

where $[\ldots]$ are the periodic terms. For the mass term,

$$\sum_x (-1)^x \xi_x^\dagger \xi^x = \frac{1}{L} \sum_{qp} \sum_x \frac{e^{-iqx+ipx+i\pi x}}{\sqrt{2\omega_q 2\omega_p}} \, \Theta(p,q) = \sum_k \frac{1}{2\omega_k} \, \Theta(k, k+\pi) \ . \tag{2.54}$$

This time it is the periodic part that survives, namely

$$\Theta(k, k+\pi) = \left[(f_k - g_k) a_k^\dagger - (f_k + g_k) b_{-k} \right] \left[(f_k + g_k) a_k + (f_k - g_k) b_{-k}^\dagger \right]$$

$$= (f_k^2 - g_k^2)(a_k^\dagger a_k - b_{-k} b_{-k}^\dagger) + (f_k - g_k)^2 \, a_k^\dagger b_{-k}^\dagger - (f_k + g_k)^2 \, b_{-k} a_k$$

$$= 2m \left(a_k^\dagger a_k - b_{-k} b_{-k}^\dagger \right) - 2\sin(k) \left(a_k^\dagger b_{-k}^\dagger + b_{-k} a_k \right) + [\ldots] \ , \tag{2.55}$$

where $[\ldots]$ are the terms vanishing upon summation.

Putting everything together,

$$H = \sum_k \frac{1}{2\omega_k} \left[\frac{i}{2} e^{-ik}\, \Theta(k,k) + \text{H.c.} + m\, \Theta(k, k+\pi) \right]$$

$$= \sum_k \frac{1}{2\omega_k} \left[\sin(k)\, \Theta(k,k) + m\, \Theta(k, k+\pi) \right]$$

$$= \sum_k \frac{1}{2\omega_k} (2\sin^2(k) + 2m^2) \left(a_k^\dagger a_k - b_{-k} b_{-k}^\dagger \right)$$

$$= \sum_k \omega_k \left(a_k^\dagger a_k - b_k b_k^\dagger \right) \ . \tag{2.56}$$

The Hamiltonian is thus diagonalized by working in an eigenbasis of $a_k^\dagger a_k$ and $b_k b_k^\dagger$. Switching over to the effective Fourier modes and using anticommutator (2.46), the Hamiltonian can be rewritten as a positive semidefinite operator minus a constant,

$$H = \sum_k^\star \omega_k \left(\tilde{a}_k^\dagger \tilde{a}_k + \tilde{b}_k^\dagger \tilde{b}_k - 1 \right) \ . \tag{2.57}$$

The constant term incorporates both ultraviolet and infrared divergencies when the respective regulators are released[10] and makes the theory ill defined in the continuum limit. This is a manifestation of the problem of ordering of operators mentioned in Section 1.5. In the mass term of (2.49) we should have written,

$$(1 - C)\xi_x^\dagger \xi^x - C\xi^x \xi_x^\dagger = \xi_x^\dagger \xi^x - C \tag{2.59}$$

in place of $\xi^x \xi_x^\dagger$, with the constant C parametrizing our ignorance about the correct ordering. Using this constant we can cancel the problematic term in (2.57) and ensure the continuum limit is well defined[11]. More in general we say that an operator written in terms of the Fourier modes is well or *normal ordered* if all the a_k and b_k appear on the right of the $a_k^\dagger$ and $b_k^\dagger$. To achieve normal ordering the Fourier modes are exchanged as if they were classical variables [49].

In the end,

$$P^\mu = \sum_k^\star k^\mu \left(\tilde{a}_k^\dagger \tilde{a}_k + \tilde{b}_k^\dagger \tilde{b}_k \right) \ , \qquad k^\mu = (\omega_k, k) \ ; \tag{2.60}$$

---

[10] Recalling dispersion relation (2.29),

$$\sum_k^\star \omega(k) > \sum_k^\star m = \frac{mL}{2} \xrightarrow{L \to \infty} \infty \ , \qquad \sum_k^\star \omega(k) > \omega(\pi/2\ell) \sim \frac{1}{\ell} \xrightarrow{\ell \to 0} \infty \ . \tag{2.58}$$

[11] This is in fact a basic example of the renormalization procedure mentioned in Section 2.1 [66].

where $P^0 \equiv H$ and $P^1 \equiv P$ is the spatial momentum operator, clearly $[P^0, P^1] = 0$. The energy-momentum operators (2.60) mimics the one of free continuum quantum field theories and the usual results apply. By the usual anticommutators (2.46),

$$[P^\mu, \tilde{a}_k] = \sum_p [\tilde{a}_p^\dagger \tilde{a}_p, \tilde{a}_k] = -k^\mu \tilde{a}_k \ , \qquad [P^\mu, \tilde{b}_k] = -k^\mu \tilde{b}_k \ ; \qquad (2.61)$$

showing that $\tilde{a}_k$ and $\tilde{b}_k$ ($\tilde{a}_k^\dagger$ and $\tilde{b}_k^\dagger$) destroy (create) excitations of energy-momentum k^μ and unveiling the correspondence with two independent systems of anticommuting harmonic oscillators.

Fock space. Let $|0\rangle$ be the state with no "exchitation to destroy"[12],

$$\tilde{a}_k |0\rangle = \tilde{b}_k |0\rangle = 0 \quad \forall k \ , \qquad \langle 0|0\rangle = 1 \ . \qquad (2.62)$$

That is, $|0\rangle$ is the ground state of H and the (free theory) vacuum state $P^\mu |0\rangle = 0$. The *Fock space* of the theory is generated acting with $\tilde{a}_k^\dagger$ and $\tilde{b}_k^\dagger$ on this state,

$$|\bar{q}_N, \ldots, \bar{q}_1, p_M, \ldots, p_1\rangle := \tilde{b}_{q_N}^\dagger \cdots \tilde{b}_{q_1}^\dagger \ \tilde{a}_{p_M}^\dagger \cdots \tilde{a}_{p_1}^\dagger |0\rangle \ . \qquad (2.63)$$

States (2.63) are the lattice equivalent[13] of the single-particle and multi-particle states of Sections 1.1–1.2. Due to the properties of the creation and annihilation operators, they are automatically antisymmetrized and normalized as per (1.7), e.g.

$$\langle p|q\rangle = \langle 0| [\tilde{a}_p, \tilde{a}_q^\dagger] |0\rangle = \delta_{pq} \ , \qquad \langle \bar{p}|\bar{q}\rangle = \delta_{pq} \ . \qquad (2.64)$$

Particle wave packet states. In order to prepare a more physical state such as a momentum wave packet, a superposition is taken. For a single particle state,

$$|\phi\rangle = \sum_k^\star \phi(k) |k\rangle = \sum_k^\star \phi(k) \tilde{a}^\dagger(k) |0\rangle \ . \qquad (2.65)$$

Where $|\phi(k)|^2$ must be a probability distribution, so that

$$\langle \phi|\phi\rangle = \sum_k^\star |\phi(k)|^2 = 1 \ , \qquad \langle \phi|P_\mu|\phi\rangle = \sum_k^\star k_\mu |\phi(k)|^2 \ . \qquad (2.66)$$

---

[12] The existence of $|0\rangle$ is guaranteed by the fact that $\tilde{a}_k$ and $\tilde{b}_k$ satisfy the same canonical anticommutation relations of ξ^x and thus they admit the same representation; although here we label the states differently.

[13] As mentioned in Section 2.2, on the lattice Poincaré invariance is broken. Apart from this, the states constructed here are still energy-momentum eigenstates and hence are the direct analogue of the states in equations (1.4) and (1.6).

The prototypical $\phi(k)$ corresponds to a momentum space probability distribution $|\phi(k)|^2$ peaked in some momentum μ_k, and a position space $|\phi(x)|^2$ localized around a position μ_x. The obvious choice is a normal distribution[14], then

$$\phi(k; \mu_x, \mu_k, \sigma_k) = \mathcal{N} \exp\left(-\frac{(k - \mu_k)^2}{4\sigma_k^2} - ik\mu_x\right) ; \qquad (2.67)$$

where $\mathcal{N}$ is a normalization constant. Identical considerations apply to antiparticle $|\bar{k}\rangle$ wave packets. For a multi particle state an amplitude $\phi(p_1, \ldots, p_M, q_1, \ldots, q_N)$ is placed in front of (2.63). The normalization of the wave packet imposes

$$\sum_{\{p_i, q_j\}}^{\star} \sum_{\{\sigma_i\}}^{M} \sum_{\{\tau_j\}}^{N} \varepsilon_{\sigma_1 \ldots \sigma_M} \varepsilon_{\tau_1 \ldots \tau_N} |\phi(p_{\sigma_1}, \ldots, p_{\sigma_M}, q_{\tau_1}, \ldots, q_{\tau_N}])|^2 = 1 , \qquad (2.68)$$

where $\varepsilon_{\alpha_1 \ldots \alpha_K}$ is the Levi-Civita tensor. If the momenta of the particles are uncorrelated this factorizes in a product of single particle wave packets.

For our future purposes, it convenient to introduce a wave packet creation operator $\mathcal{A}^\dagger$ and write it in terms position space staggered fermion field $\xi_x^\dagger$. Recalling the expressions (2.39a) and (2.43) we have

$$\mathcal{A}^\dagger = \sum_k^{\star} \phi(k)\, \tilde{a}^\dagger(k) = \sum_x \tilde{\phi}(x)\, \xi^\dagger(x) = \sum_x \xi^\dagger(x) \sqrt{\frac{2}{L}} \sum_k^{\star} \phi(k) \frac{e^{+ikx}}{\sqrt{2\omega_k}} \begin{cases} f_k & x \text{ even} \\ g_k & x \text{ odd} \end{cases} ; \qquad (2.69)$$

which implicitly defines the position space amplitude $\tilde{\phi}(x)$. Recalling also (2.39b), the antiparticle wave packet creation operator $\mathcal{B}^\dagger$ is obtained from the previous equation exchanging f_k with g_k and substituting $\xi^\dagger$ with ξ, namely

$$\mathcal{B}^\dagger = \sum_k^{\star} \phi(k)\, \tilde{b}^\dagger(k) = \sum_x \tilde{\phi}(x)\, \xi(x) = \sum_x \xi(x) \sqrt{\frac{2}{L}} \sum_k^{\star} \phi(k) \frac{e^{+ikx}}{\sqrt{2\omega_k}} \begin{cases} g_k & x \text{ even} \\ f_k & x \text{ odd} \end{cases} . \qquad (2.70)$$

If in the above equations we set $\phi(k) = \phi(k; \mu_x, \mu_k, \sigma_k)$ as per (2.67), then $\tilde{\phi}(x)$ reads

$$\tilde{\phi}(x; \mu_x, \mu_k, \sigma_k) = \frac{\mathcal{N}}{\sqrt{L}} \sum_k^{\star} \frac{1}{\sqrt{\omega_k}} \exp\left(-\frac{(k - \mu_k)^2}{4\sigma_k^2} + ik(x - \mu_x)\right) \Xi(x, k) ; \qquad (2.71)$$

where $\Xi(x, k) = f_k$ for $\mathcal{A}^\dagger$ and even x, or for $\mathcal{B}^\dagger$ and odd x; otherwise $\Xi(x, k) = g_k$.

---

[14] Actually a truncated and discrete normal distribution since the lattice is a finite and discrete set.

2.3D Conserved Charges

The Hamiltonian action (1.63) associated to Hamiltonian (2.16), namely

$$S = \int \mathrm{d}t \left[\sum_x i\xi_x^\dagger \xi^x - H(\xi, \xi^\dagger) \right] , \tag{2.72}$$

is invariant under *particle number* global U(1) transformations

$$\xi^x \mapsto e^{-i\theta}\, \xi^x , \quad \theta \in \mathbb{R} . \tag{2.73}$$

The Noether conserved charge operator generating the symmetry is

$$Q = \sum_y \xi_y^\dagger \xi^y , \qquad [H, Q] = 0 ; \tag{2.74}$$

indeed,

$$i\theta[Q, \xi^x] = i\theta \sum_y \left(\xi_y^\dagger [\xi^y, \xi^x] - [\xi^x, \xi_y^\dagger]\xi^y \right) = -i\theta\xi^x = \delta\xi^x . \tag{2.75}$$

In analogy with the continuum case, this global conservation law is associated with a local continuity equation (in the lattice sense). Using the equation of motion (2.24) and its complex conjugate,

$$\frac{\mathrm{d}}{\mathrm{d}t}(\xi_x^\dagger \xi^x) = \dot{\xi}_x^\dagger \xi^x + \xi_x^\dagger \dot{\xi}^x = - \left[(\partial \xi_x^\dagger)\, \xi^x + \xi_x^\dagger\, (\partial \xi^x) \right] = -\tilde{\partial}(\xi_x^\dagger \xi^x) , \tag{2.76}$$

where ∂ is the central derivative and $\tilde{\partial}$ another finite difference derivative. Therefore,

$$\rho(x) = \xi_x^\dagger \xi^x , \qquad \frac{\mathrm{d}\rho}{\mathrm{d}t} + \tilde{\partial}\rho = 0 , \tag{2.77}$$

where $\rho(x)$ is the sought after *charge density*. However, due to the very definition of the staggered fermion field (2.13), the charge density (1.52) of the continuum theory is reproduced only by the sum of the contributions to $\rho(x)$ from two neighboring sites.

The expression of the total and local charges in terms of creation and annihilation operators is now derived and the normal order correction is evaluated. For $\rho(x)$ we can set $x = y$ in (2.50). Of the four terms in $\Theta(p, q)$ only

$$(f_q - g_q)(f_p - g_p)b_{-q}b_{-p}^\dagger \tag{2.78}$$

has to be reordered. Denoting with $\mathcal{N}(\rho(x))$ the normal ordered charge density,

$$\rho(x) - \mathcal{N}(\rho(x)) = \frac{1}{L} \sum_{qp} \frac{e^{i(p-q)x}}{\sqrt{2\omega_q 2\omega_p}} (f_q - g_q)(f_p - g_p)(b_{-q}b^\dagger_{-p} + b^\dagger_{-p}b_{-q})$$

$$= \frac{1}{L} \sum_{qp} \frac{e^{-i(p-q)x}}{\sqrt{2\omega_p 2\omega_q}} (b_q b^\dagger_p + b^\dagger_p b_q) \begin{cases} g_q g_p & x \text{ even} \\ f_q f_p & x \text{ odd} \end{cases}$$

$$= \frac{4}{L} \sum_{qp}^{\star} \frac{e^{-i(p-q)x}}{\sqrt{2\omega_p 2\omega_q}} \frac{\tilde{b}_q \tilde{b}^\dagger_p + \tilde{b}^\dagger_p \tilde{b}_q}{2} \begin{cases} g_q g_p & x \text{ even} \\ f_q f_p & x \text{ odd} \end{cases}$$

$$= \frac{1}{L} \sum_{k}^{\star} \frac{1}{\omega_k} \begin{cases} g_k^2 & x \text{ even} \\ f_k^2 & x \text{ odd} \end{cases} . \tag{2.79}$$

Here the symmetry properties (2.35) and (2.37) have been used extensively; in particular in the second step they allow to restrict the summation on the effective reciprocal lattice and exploit anticommutator (2.46). By construction $\langle 0|\mathcal{N}(\rho(x))|0\rangle = 0$. As a consequence, the expression (2.79) is also the vacuum expectation value of the unordered charge density. The two following limits hold:

$$\langle 0|\rho(x)|0\rangle \xrightarrow{m\to\infty} \begin{cases} 0 & x \text{ even} \\ 1 & x \text{ odd} \end{cases} , \qquad \langle 0|\rho(x)|0\rangle \xrightarrow{m\to 0} \frac{1}{2} ; \tag{2.80}$$

while for every mass value an half-filling condition is verified,

$$\langle 0|\rho(x) + \rho(x+1)|0\rangle = 1 . \tag{2.81}$$

These observations lead to an alternative expression for the normal ordered charge density that will be useful in the following:

$$\mathcal{N}(\rho(x)) = \xi_x^\dagger \xi^x - \frac{1 - (-1)^x}{2} - (-1)^x \nu , \quad \nu = \frac{1}{L} \sum_{k}^{\star} \frac{g_k^2}{\omega_k} ; \tag{2.82}$$

with the ν correction vanishing in large mass limit or when the continuum charge is recovered, summing over pairs of neighbouring sites.

In order to derive the expression of the total charge in momentum space we recall that the (appropriately normalized) Fourier transform is an isometry, therefore

$$Q = \sum_x \xi^\dagger(x)\xi(x) = \sum_k \xi^\dagger(k)\xi(k) . \tag{2.83}$$

According to (2.38a),

$$\xi(k) = \frac{(f_k + g_k)\, a_k + (f_k - g_k)\, b^\dagger_{-k}}{\sqrt{2\omega_k}}\ . \tag{2.84}$$

Via the usual symmetry and anticommutation properties (2.35), (2.37) and (2.46),

$$
\begin{aligned}
Q &= \sum_k \frac{1}{2\omega_k} \left[(f_k + g_k)\, a^\dagger_k + (f_k - g_k)\, b_{-k} \right] \left[(f_k + g_k)\, a_k + (f_k - g_k)\, b^\dagger_{-k} \right] \\
&= \sum_k \frac{1}{2\omega_k} \left[(f_k^2 + g_k^2)\, a^\dagger_k a_k + (f_k^2 - g_k^2)\, b_{-k} b^\dagger_{-k} \right] \\
&= \sum_k \left[a^\dagger_k a_k + b_k b^\dagger_k \right] = \sum_k^{\star} \left[\tilde{a}^\dagger_k \tilde{a}_k - \tilde{b}^\dagger_k \tilde{b}_k \right] + \frac{L}{2}\ ;
\end{aligned} \tag{2.85}
$$

where in the last step the half-filling normal ordering counter term has been isolated.

From now on Q and $\rho(x)$ will denote the normal ordered charge and charge density. In particular

$$Q = \sum_k^{\star} \left[\tilde{a}^\dagger_k \tilde{a}_k - \tilde{b}^\dagger_k \tilde{b}_k \right]\ , \qquad [H, Q] = 0\ , \qquad Q\,|0\rangle = 0\ . \tag{2.86}$$

The charge operator Q counts the difference between the number of *particles* (excitations of type a_k) and *antiparticles*[15] (b_k), which is a conserved quantity. In the light of this identification, the limits (2.80) are easily interpreted recalling those of f_k and g_k in (2.37). In particular, for $m \to \infty$ the particle (antiparticle) component of the general solution (2.38b) is supported on even (odd) sites.

The action of Q on field operators and the states they produce is the expected one:

$$[Q, \xi^\dagger_x] = [\xi^\dagger_y \xi^y, \xi^\dagger_x] = +\xi^\dagger_x\ , \qquad Q \xi^\dagger_x |0\rangle = [Q, \xi^\dagger_x]\,|0\rangle = +\xi^\dagger_x |0\rangle\ ; \tag{2.87}$$

(plus the opposite sign ones for ξ^x) meaning that $\xi^\dagger_x$ can either create a particle or destroy an antiparticle (vice versa for ξ^x). Similarly, in momentum space we have

$$Q\,|k\rangle = [Q, \tilde{a}^\dagger_k]\,|0\rangle = +\,|k\rangle\ , \qquad Q\,|\bar{k}\rangle = [Q, \tilde{b}^\dagger_k]\,|0\rangle = -\,|\bar{k}\rangle\ . \tag{2.88}$$

Multiple flavours. A theory of N staggered fermion flavours with degenerate mass is again described by Hamiltonian (2.16), only with ξ representing a colour multiplet $\{\xi^r\}_{r=1}^N$. The theory has a global U(N) symmetry, with ξ transforming in the fundamental representation. On top of the $\mathfrak{u}(1)$ conserved charge (2.77), there

---

[15] Notice that up to now there was no physical distinction between a_k and b_k operators.

are the $\mathfrak{su}(N)$ ones [87]. Up to ordering issues,

$$Q^a_{\mathfrak{su}(N)} = \sum_x \rho(x)_{\mathfrak{su}(N)} \;, \qquad \rho^a_{\mathfrak{su}(N)}(x) = \xi^\dagger_{x,r} \, (T^a)^r{}_s \, \xi^{x,s} \;. \tag{2.89}$$

2.4 Gauge Fields

Lattice gauge theories originate, analogously to the continuum case, from the requirement of the invariance of the action under internal group transformations specified independently at each lattice site. (In principle there could also be a time dependence but temporal gauge is here assumed.) The same geometric picture presented in the continuum case applies. Gauge degrees of freedom are introduced in order to compare matter fields evaluated at different lattice sites but, being the sites finitely separated, the transformation to be compensated is a finite group transformation. Thus, it is natural to replace as gauge degrees of freedom the (algebra valued) connection with (group valued) *comparators* $U_k(x) \equiv U(x + \ell\hat{k}, x)$. This formulation of the gauge theory in terms of compact valued degrees of freedom is called *compact* formulation. It is natural to regard the comparators as variables living on the link between two neighbouring lattice sites. In notations analogous to those of Section 1.3A, they transform as

$$U(x + \hat{k}, x) \mapsto V(g(x + \ell\hat{k})) \, U(x + \ell\hat{k}, x) \, V^\dagger(g(x)) \tag{2.90}$$

and can be thought of as the discrete equivalents of a continuous parallel transport along a standard straight path between adjacent sites. In fact, to make contact with the continuum description, we may associate a (canonically normalized) connection $A^a_k(x) \equiv A(x + \ell\hat{k}, x)$ to each link and write

$$U_k(x) = e^{g\ell A^a_k(x) T^a} \;. \tag{2.91}$$

We now introduce a representative of the electric field. In the continuum, the electric field was the conjugate momentum of the connection. This suggest to define the electric field $E^b_k(x)$ by,

$$\{A^a_i(x), E^b_j(y)\} = \sum_{z,k} \frac{\partial A^a_i(x)}{\partial A^c_k(z)} \frac{\partial E^b_j(y)}{\partial E^c_k(z)} = \delta_{xy}\delta_{ij}\delta^{ab} \;. \tag{2.92}$$

In the abelian theory this is still a valid choice. However, in the compact formulation the relevant bracket is the one with the comparator, namely

$$\{U_i(x), E_j(y)\} = \sum_{z,k} \frac{\partial e^{g\ell A_i(x)(-i)}}{\partial A_k(z)} \frac{\partial E_j(y)}{\partial E_k(z)} = \ell \, \delta_{xy}\delta_{ij}\, g(-i)U_i \;. \tag{2.93}$$

Thus E_k generate shifts in the algebra space and rotations (phase multiplications) in the group space. In the non-abelian case the derivative of the matrix exponential that would appear in (2.93) does not have a closed form. Instead of E_i^a it is convenient to introduce two sets of variables, L_j^a and R_j^a, defined as the generators of left and right group rotations [42, 89]:

$$\{U_i(x), L_j^a(y)\} = g\ell\, \delta_{xy}\delta_{ij}\, T^a U_i(x) \ , \quad \{U_i(x), R_j^a(y)\} = g\ell\, \delta_{xy}\delta_{ij}\, U_i(x)T^a \ . \quad (2.94)$$

Generators associated to different links have vanishing brackets; those associated to the same link realize the symmetry algebra. Indeed, omitting $x = y$ and $i = j$, Jacobi identity provides

$$
\begin{aligned}
\{U, \{L^a, L^b\}\} &= -\{L^a, \{L^b, U\}\} - \{L^b, \{U, L^a\}\} \\
&= -\{\{U, L^b\}, L^a\} + \{\{U, L^a\}, L^b\} \\
&= -g^2\ell^2 T^b T^a U + g^2\ell^2 T^a T^b U \\
&= +g^2\ell^2 f^{abc} T^c U \ .
\end{aligned}
\quad (2.95)
$$

Analogously (up to a sign) for right generators. Consequently,

$$\{L^a, L^b\} = g\ell f^{abc} L^c \ , \qquad \{R^a, R^b\} = -g\ell f^{abc} R^c \ , \qquad \{L^a, R^b\} = 0 \ . \quad (2.96)$$

In the $\ell \to 0$ limit both L_k^a and R_k^a reduce to the continuum electric field. In this limit, the nonabelian version of the bracket (2.93) becomes (again with $x = y$ and $i = j$ implicit)

$$
\begin{aligned}
\{U, E^a\} &= \frac{\partial \exp(g\ell A^b T^b)}{\partial A^a} = \lim_{\epsilon \to 0} \frac{\exp(g\ell A + g\ell\epsilon T^a) - \exp(g\ell A)}{\epsilon} \\
&= \left[\lim_{\epsilon \to 0} \frac{\exp(g\ell A + g\ell\epsilon T^a)\exp(-g\ell A) - 1}{\epsilon}\right] \exp(g\ell A) \\
&= \left[\lim_{\epsilon \to 0} \frac{g\ell A + g\ell\epsilon T^a - g\ell A + \mathcal{O}(\epsilon\ell^2)}{\epsilon}\right] U \\
&= g\ell\, T^a U + \mathcal{O}(\ell^2) \ ;
\end{aligned}
\quad (2.97)
$$

where Baker–Campbell–Hausdorff formula was used. Had we collected the comparator on the left the result would differ only in the $\mathcal{O}(\ell^2)$ terms, thus

$$E_k^a = L_k^a + \mathcal{O}(\ell) = R_k^a + \mathcal{O}(\ell) \ . \quad (2.98)$$

In the abelian case the above equalities are exact.

2.4A   Lattice Yang-Mills Theory

The ingredients introduced above allow to map the pure and matter coupled continuum Hamiltonian Yang-Mills theories to their lattice counterpart. The discussion that follows is kept at the classical level to allow for a direct comparison with the results of Subsection 1.4B. On the other hand, the quantization prescription of Subsection 1.5A encounters no obstacle on the lattice. This will be clear in a moment, when the theory of lattice quantum electrodynamics in two spacetime dimensions is presented.

Pure lattice Yang-Mills Hamiltonian.   With no matter fields, gauge invariants are appropriate combinations of L_i^a or R_i^a and Wilson loops, obtained concatenating comparators $U_i(x)$ along any closed lattice path. These are all valid Hamiltonian terms. In order to reproduce the continuum theory, we restrict to those arising from the discretization prescription applied to Hamiltonian (1.104), namely

$$H = \int \mathrm{d}\mathbf{x} \left[\frac{1}{2} \sum_{i,a} (E_i^a)^2 + \frac{1}{2} \sum_{i<j,a} (B_{ij}^a)^2 \right] . \tag{2.99}$$

Recalling (1.42) and the discussion that precedes[16],

$$\sum_a (B_{ij}^a)^2 = \sum_a (F_{ij}^a)^2 = \lim_{\epsilon \to 0} \frac{1}{g^2 D_V \epsilon^4} \left[d_V - \frac{W_{ij}(\epsilon) + W_{ij}^\dagger(\epsilon)}{2} \right] . \tag{2.100}$$

Reverting the limit ($\epsilon = \ell$) and neglecting a constant, this becomes a *plaquette* term:

$$W_{ij}(x;\ell) + W_{ij}^\dagger(x;\ell) = \operatorname{tr} U_j^\dagger(x) U_i^\dagger(x + \ell\hat{j}) U_j(x + \ell\hat{i}) U_i(x) + \text{H.c.} . \tag{2.101}$$

At finite spacing the plaquette introduces infinite additional tree-level terms compared to the continuum magnetic energy [102]. These start from next-to-leading order in ℓ and correspond to non-renormalizable or, in Wilson's language, irrelevant gluon self interactions. Setting $\ell = 1$, the lattice Yang-Mills Hamiltonian is [23, 42]

$$H = -\frac{1}{8D_V} \sum_x \operatorname{tr} \left[\sum_i L_i^2(x) + \frac{1}{g^2} \sum_{ij} U_j^\dagger(x) U_i^\dagger(x+\hat{j}) U_j(x+\hat{i}) U_i(x) + \text{H.c.} \right] , \tag{2.102}$$

where the left generators $L_i = L_i^a T^a$ have been used in place of the electric field[17].

---

[16] The coupling factor in the denominator compensates for the one in the exponent of the comparators in (2.91).

[17] Substituting L_i with R_i results in the same Hamiltonian, also at finite lattice spacing [42].

The discrete version of the Gauss law constraint (1.89) reads

$$\mathcal{G}^a(x) = \sum_k \left[R^a(x + \hat{k}, x) - L^a(x, x - \hat{k}) \right] \ . \tag{2.103}$$

It is the generator of the gauge transformations of the comparator; via (2.94)

$$
\begin{aligned}
\{ U_i(x), -\sum_y \theta^b(y)\mathcal{G}^b(y) \} &= \sum_{y,j} \theta^a(y) \Big[\{ U_i(x), L_j^b(y - \hat{j}) \} - \{ U_i(x), R_j^b(y) \} \Big] \\
&= (g\theta^b(x + \hat{i}) T^b) U_i(x) + U_i(x)(-g\theta^b(x) T^b) \ , \tag{2.104}
\end{aligned}
$$

which exponentiated yields exactly (2.90) with $V = \exp(g\theta^a T^a)$. Moreover,

$$
\begin{aligned}
\{ L_i^a(x), -\sum_y \theta^b(y)\mathcal{G}^b(y) \} &= \sum_{y,j} \theta^a(y) \{ L_i^a(x), L_j^b(y - \hat{j}) \} \\
&= g\theta^b(x + \hat{i}) f^{abc} L_i^c(x) \ . \tag{2.105}
\end{aligned}
$$

This shows that L_i^a (and analogously for R_i^a) transforms in the adjoint representation, like its continuum counterpart (1.103). For finite transformations we have

$$L_i \mapsto V(g(x + \hat{i})) \, L_i \, V^\dagger(g(x + \hat{i})) \ . \tag{2.106}$$

Together with the cyclic property of the trace, (2.90)–(2.106) prove the invariance of the Hamiltonian (2.102). We thus have a well defined gauge theory.

Matter coupled lattice Yang-Mills. We now couple the gauge theory to staggered fermion matter fields. The treatment of Section 2.3 is specialized to $1 + 1$ spacetime dimensions. We restrict to this setting, where there is no magnetic or plaquette term, and adopt the notation $U^{x+1}{}_x = U(x + 1, x)$ (similarly for the other variables living on the links). For a single fermion specie we gauge its particle number $G = \mathrm{U}(1)$ symmetry (2.73); for N flavours which we can, e.g., gauge the $G = \mathrm{SU}(N)$ symmetry subgroup.

The lattice minimal coupling consists in the insertion of a comparator $U^{x+1}{}_x$ in the hopping terms of the staggered fermion Hamiltonian (2.16):

$$\frac{i}{2} \sum_x \xi_{x+1}^\dagger \xi^x + \text{H.c.} \ \rightarrow \ \frac{i}{2} \sum_x \xi_{x+1}^\dagger U^{x+1}{}_x \xi^x + \text{H.c.} \ . \tag{2.107}$$

This substitution makes the hopping terms gauge invariant by construction as soon as we choose the representation $V(g)$ in the transformation law of the comparator (2.90) to be the one under which the matter fields transform. We now check that, among all the gauge invariant terms built out of comparators and matter fields, the

right hand side in (2.107) reproduces the covariant derivative term of the continuum Hamiltonian (1.106). Repeating backwards the steps that brought to the staggered fermion Hamiltonian (2.16),

$$\frac{i}{2}\sum_x \xi^\dagger_{x+1} U^{x+1}{}_x \xi^x + \text{H.c.} = (-i)\sum_x \xi^\dagger_x \left[\frac{(U^{x+1}{}_x)^\dagger \xi^{x+1} - (U^{x-1}{}_x)^\dagger \xi^{x-1}}{2} \right] . \quad (2.108)$$

Comparing this result with (1.23), the term in square brackets is recognized to be a central covariant derivative. Since (in temporal gauge) the minimal substitution does not interfere with the staggering procedure we conclude that the minimal coupling (2.107) provides the correct continuum limit.

Finally, the complete $d = 1$ matter coupled lattice Yang-Mills Hamiltonian reads

$$H = \frac{1}{2}\sum_{x,a} \left[(L^a)^{x+1}{}_x\right]^2 + \sum_x \left[\frac{i}{2}\xi^\dagger_{x+1} U^{x+1}{}_x \xi^x + \text{H.c.}\right] + m \sum_x (-1)^x \xi^\dagger_x \xi^x ; \quad (2.109)$$

while Gauss law receives a contribution from the matter current (2.73) or (2.89),

$$\mathcal{G}^a(x) = (R^a)^{x+1}{}_x - (L^a)^x{}_{x-1} - \rho^a(x) , \qquad \rho^a = ig\,\xi^\dagger_r (T^a)^r{}_s \xi^s , \quad (2.110)$$

like its continuum counterpart (1.107).

2.4B Lattice Schwinger Model

We now investigate in more detail the quantized compact lattice QED$_2$ or Schwinger model, namely the theory of a staggered fermion with U(1) gauge invariance. This model is arguably the simplest gauge invariant fermionic quantum field theory that can be written and thus provides an optimal test-bed for new numerical as well as analytical approaches to the study of gauge theories. Despite this simplicity, the model has an interesting phenomenology, e.g., the generation of a mass gap, as well as some features in common with chromodynamics, such as a confining behaviour [22, 59]. For these reasons the Schwinger model is the focus of the simulations implemented in this Thesis. Here we always take the fermion to be massive[18] but let us mention that the massless case has been solved exactly [9, 18].

The quantization prescription of Subsection 1.5A applies straightforwardly. Here we compute an explicit realization of the comparator and electric field operators, as previously done for the staggered fermion operators. To this aim, it is convenient to reabsorb the coupling factor appearing in the Poisson bracket (2.93) via $E \to gE$.

---

[18] The lattice description of massless particles presents some subtleties. The infrared cutoff always generates a non vanishing mass $\mathcal{O}(1/\ell L)$ as a finite volume artifact [102].

Before going in further detail, let us collect the defining ingredients of the theory.
These are

  (i) the link and site operators

$$U^{x+1}{}_x \text{ (unitary)}, \ E^{x+1}{}_x \text{ (Hermitian)} \qquad \text{and} \qquad \xi^x, \ \xi_x^\dagger \ ; \qquad (2.111)$$

 (ii) the Hilbert space

$$\mathscr{H} = \bigotimes_x \left(\mathscr{H}_{x-1,x} \ \otimes \mathscr{H}_x \right) \ , \qquad (2.112)$$

      namely a tensor product of local link (photon) and site (matter) Hilbert spaces;

(iii) the fundamental commutation and anticommutation relations

$$[U^{x+1}{}_x, E^{y+1}{}_y] = \delta_{xy} U^{x+1}{}_x \ , \qquad [\xi^x, \xi_y^\dagger] = \delta^x{}_y \ , \qquad (2.113)$$

      (other fundamental commutators vanish);

 (iv) the Hamiltonian

$$H = \frac{g^2}{2} \sum_x (E^{x+1}{}_x)^2 + \sum_x \left[\frac{i}{2} \xi_{x+1}^\dagger U^{x+1}{}_x \xi^x + \text{H.c.} \right] + m \sum_x (-1)^x \xi_x^\dagger \xi^x \ ; \ (2.114)$$

  (v) the physical state condition,

$$\mathcal{G}(x) \left| \Psi_{\text{phys}} \right\rangle = [E^{x+1}{}_x - E^x{}_{x-1} - \rho(x)] \left| \Psi_{\text{phys}} \right\rangle = 0 \ , \qquad (2.115)$$

      identifying the physical Hilbert subspace $\mathscr{H}_{\text{phys}}$.

Since electric field and comparator operators associated to different links commute
(rather than anticommuting), a representation of (2.113) on a single link is immedi-
ately extended to a representation on the whole chain. Then, leaving $x = y$ implicit
to lighten the notation, the commutator in (2.113) becomes

$$[U, E] = U \ . \qquad (2.116)$$

This shows that the electric field acts as a generator of phase rotations on the com-
parator but also that the comparator is a ladder (lowering) operator for the electric
field. An irreducible representation of (2.116) is clearly

$$E \left| \lambda \right\rangle = \lambda \left| \lambda \right\rangle \ , \qquad U \left| \lambda \right\rangle = \left| \lambda - 1 \right\rangle \ , \qquad \lambda = 0, \pm 1, \pm 2, \dots \ . \qquad (2.117)$$

This is not unique. There exist infinite other unitarily inequivalent representations
but these are all related to (2.117) simply by a shift in the electric field spectrum:

$E \rightarrow E + \delta\lambda$, $0 < \delta\lambda < 1$ [67]. Observe that the electric field has a *discrete spectrum*. Consequently, there cannot exist a generator of infiniteimal electric field translations; namely a connection operator A satisfying

$$[A, E] = i/g \ , \tag{2.118}$$

such that we could define a one-parameter family of operators $U(\beta) = e^{ig\beta A}$ obeying the commutator (2.116) for each $\beta \in \mathbb{R}$. An accidental consequence of this result is that the clash between Gauss law constraint and the canonical commuation relation encountered during the quantization of electromagnetism in the continuum, namely (1.118), is not present in the compact formulation of the lattice theory.

Let us stress that all the above properties are general results regarding the quantum mechanical commutation relations for angular variables [24, 67]. In our case, this commutation relation is a direct consequence of the compact formulation of the lattice gauge theory. In this formulation the fundamental degrees of freedom are a periodic variable (the comparator) and its quantized angular momentum (rescaled electric field) rather than a flat direction (connection) and its linear momentum (electric field) [24]. As just shown, the latter cannot even be implemented as an operator.

We now discuss some selected topics that are relevant for the implementation of numerical simulations of the Lattice Schwinger model dyanmics.

Physical subspace and normal order. The physical dynamics is contained in the gauge invariant sector of the Hilbert space, spanned by the states complying with Gauss law (2.115). If the normal ordering of the charge density derived for the theory of free staggered fermions should be performed also in the interacting theory, its relation with Gauss law must be adressed. Inserting the expression (2.82) of the normal ordered charge density in the definition of the Gauss operator we obtain

$$\mathcal{G}(x) = E^{x+1}{}_x - E^x{}_{x-1} - \xi_x^\dagger \xi^x + \frac{1 - (-1)^x}{2} + (-1)^x \nu \ . \tag{2.119}$$

Here we follow [60, 87, 89] and drop the ν correction; otherwise stated, we calibrate the normal order on the large mass limit case and define

$$\rho(x) = \xi_x^\dagger \xi^x - \frac{1 - (-1)^x}{2} \ . \tag{2.120}$$

Observe that the above modification is equivalent to a shift of the electric field,

$$E^{x+1}{}_x \rightarrow E^{x+1}{}_x - (-1)^x \nu/2 \ . \tag{2.121}$$

In the Hamiltonian (2.114) this shift amounts to

$$\sum_x (E^{x+1}{}_x)^2 \longrightarrow \sum_x (E^{x+1}{}_x - (-1)^x \nu/2)^2 = \sum_x (E^{x+1}{}_x)^2 - \nu \sum_x (-1)^x E^{x+1}{}_x + \text{const.}$$
(2.122)

The sum of the charge or the average of the electric field over pair of sites are unaffected by these operations.

Integrating out the electric field. We now show that, thanks to the Gauss law (2.115), an alternative descritpion of the theory which involves only the matter degrees of freedom is possible. This claim requires certain assumptions, the crucial one being that we are only interested in the gauge invariant properties of the system. Otherwise stated, we only aim to represent the states in $\mathscr{H}_{\text{phys}}$ and the action of the operators on this subspace. For the remainder of this discussion we denote with "$\approx$" an equality that is only required to hold on the physical Hilbert subspace $\mathscr{H}_{\text{phys}}$, e.g., $\mathcal{G}(x) \approx 0$.

Given an arbitrary site $z \in \Lambda$, for all $x > z$,

$$E^{x+1}{}_x \approx E^{x+1}{}_x - \sum_{y=z}^{x} \mathcal{G}(y) \approx \sum_{y=z}^{x} \rho(y) + E^z{}_{z-1} \ .$$
(2.123)

An analogous formula can be written for $x < z$. The action (on physical states) of all the electric field operators is determined in terms of the matter and $E^z{}_{z-1}$ degrees of freedom only. Substituting expression (2.123) in the Hamiltonian (2.114), the sole operators acting on the link local Hilbert spaces $\mathscr{H}_{x,x-1}$ ($x \neq z$) that are left are the comparators $U^x{}_{x-1}$, whose only dynamical role is to raise or lower the electric field $E^x{}_{x-1}$ value. Since the $E^x{}_{x-1}$ operators have been replaced with the right hand side of (2.123) we can remove $U^x{}_{x-1}$ from the Hamiltonian and represent all the physical states in the Hilbert space [99]

$$\mathscr{H}_{z-1,z} \bigotimes_x \mathscr{H}_x \ .$$
(2.124)

After this "integration" procedure, there is no longer a propagating gauge field (one degree of freedom per site) but only a single degree of freedom corresponding to $E^z{}_{z-1}$. Working with open boundaries, we can remove also $E^z{}_{z-1}$ via a boundary condition [96, 99] on the electric field; e.g., fixing its value on the leftmost link:

$$E^{x+1}{}_x \approx \sum_{y=1}^{x} \left[\xi_y^\dagger \xi^y - \frac{1 - (-1)^y}{2} \right] + \mathcal{E} \ , \qquad E^1{}_0 \approx \mathcal{E} \in \mathbb{R} \ .$$
(2.125)

With the electric field integrated out in this way, the dynamics of the Schwinger

model is specified by the Hamiltonian

$$H \approx \frac{g^2}{2} \sum_x \left[\sum_y^x \left(\xi_y^\dagger \xi^y - \frac{1 - (-1)^y}{2} \right) + \mathcal{E} \right]^2 + \sum_x \left[\frac{i}{2} \xi_{x+1}^\dagger \xi^x + \text{H.c.} \right] + m \sum_x (-1)^x \xi_x^\dagger \xi^x \,.$$

(2.126)

A few comments are due. In Section 1.3A we mentioned how gauge theories introduce a redundancy in the description of a physical system. Here, by explicitly solving Gauss law, we successfully removed the redundant degrees of freedom (together with gauge invariance) and reduced the dimension of the Hilbert space of the theory. However, notice that this comes at a price: Hamiltonian (2.126) contains *non-local* interaction terms. A second comment concerns the spectrum of the electric field on the physical subspace. Since the spectrum of $\xi_x^\dagger \xi^x$ is $\{0, 1\}$, (2.125) mandates that also the electric field is quantized in integer units [24]. The observation makes the representation of the link operators constructed in the previous pages more natural.

Photon Hilbert space truncation.   Despite the reduced number of degrees of freedom, the theory with the electric field integrated out is not particularly well suited for the application of tensor network methods or quantum simulation because of the non-local character of Hamiltonian (2.126). On the other hand, if we choose to keep the electric field explicit we run into the problem that the link Hilbert space constructed in (2.117) is *infinite dimensional*. No finite dimensional representation of commutation relation (2.116) can be realized in terms of an invertible U and an Hermitian E [86].[19] To make numerical simulations feasible the Hilbert of the theory space has to be *truncated*. Parametrizing the severity of the truncation it is then possible, at least in principle, to check the convergence of the results to an exact solution. The following paragraphs address the problem of how this truncation can be achieved, using the commutation relation (2.113) between the comparator and the electric field as a guiding principle.

A possible truncation strategy consists in introducing an upper bound Λ on the $|E|$ spectrum and consequently restricting the Hilbert space to the subspace

$$\mathscr{H}_{\text{trunc}} = \text{span} \left\{ |\lambda\rangle \, : \, |\lambda| \leq \Lambda \right\} \,.$$

(2.127)

The heuristic justification for this choice is the following. The contribution, e.g., to transition amplitudes, from configurations far from those explored by the classical

---

[19] Rewriting (2.116) as $UEU^{-1} = E + 1$ shows that it is incompatible with E having a bounded spectrum. This result can also be interpreted observing that the photon is a bosonic degree of freedom and in the Fock space of bosonic degrees of freedom a single momentum mode can have arbitrarily high occupation number [49].

trajectory is generally suppressed[20] [50, 67]. If the physics simulated involves, at the classical level, modest excitations of the electric field, then the states discarded in (2.127) should always have low occupations for Λ large enough. When the Hilbert space is truncated to $\mathscr{H}_{\text{trunc}}$ a new definition of $U\left|-\Lambda\right\rangle$ and $U^\dagger\left|+\Lambda\right\rangle$ has to be provided. Two possibilities are commonly considered in the literature.

The first [33, 44, 54, 58] is

$$U\left|-\Lambda\right\rangle = U^\dagger\left|+\Lambda\right\rangle = 0 \ . \tag{2.128}$$

With this approach the commutation relation (2.116) and thus gauge invariance are preserved exactly. The unitarity of U is lost but the restriction of U to $\left|-\Lambda\right\rangle^\perp$ is still an isometric operator. Theories obtained in this way, called *quantum link models*, identify the Hilbert space of a link with that of a *spin* degree of freedom of spin $S = \Lambda$. The electric field operator is mapped to a spin projection operator while U and $U^\dagger$ correspond to its lowering and raising operators respectively[21].

The second possibility [28, 29, 86, 93] consist in

$$U\left|-\Lambda\right\rangle = \left|+\Lambda\right\rangle \ , \quad U^\dagger\left|+\Lambda\right\rangle = \left|-\Lambda\right\rangle \ , \tag{2.129}$$

corresponding to a *cyclic* electric field $\lambda \in \mathbb{Z}_N$ with $N = 2\Lambda+1$. This choice preserves the unitarity of the comparator but violates the commutation relation (2.116)

$$[U, E]\left|-\Lambda\right\rangle = (-\Lambda)\left|+\Lambda\right\rangle - (+\Lambda)\left|+\Lambda\right\rangle = (1 - N)\,U\left|-\Lambda\right\rangle \ ; \tag{2.130}$$

and analogously for $U^\dagger$ on $\left|+\Lambda\right\rangle$. As a consequence, global or local U(1) transformations of the comparator can no longer be implemented, indeed

$$e^{-i\theta E}Ue^{i\theta E}\left|\lambda\right\rangle = \eta e^{i\theta}U\left|\lambda\right\rangle \ , \qquad \eta = \begin{cases} e^{-i\theta N}, & \lambda = -\Lambda \\ 1, & \lambda \neq -\Lambda \end{cases} \ . \tag{2.131}$$

On the other hand, if $\theta \in (2\pi/N)\mathbb{Z}$ the spurious η factor that shows up for $\lambda = \Lambda$ is canceled and we get a well defined transformation on the whole $\mathscr{H}_{\text{trunc}}$[22]. Hence U(1) gauge invariance is broken down to its finite subgroup generated by $e^{2\pi i/N}$ and the model becomes a discrete $\mathbb{Z}_N$ gauge theory. In the $N \to \infty$ limit, true compact

---

[20] This is particularly clear in the Euclidean path integral formulation of the quantum theory [83].

[21] At least, in the conventions adopted here, up to a different normalization of the matrix elements of raising and lowering operators with respect to the standard ones. See, e.g., in [67]

[22] Commutation relation (2.116) as well as its Hermitian conjugate still hold when restricted to the "bulk" of $\mathscr{H}_{\text{trunc}}$, generated by $\left|-\Lambda + 1\right\rangle, \left|-\Lambda + 2\right\rangle, \ldots, \left|+\Lambda - 1\right\rangle$. On this subspace continuous U(1) transformations can still be implemented, but the requirement $\left|\Psi\right\rangle \perp \left|\pm\Lambda\right\rangle$ is clearly not consistent with time evolution.

QED is recovered [17, 29]. For finite N, given that only a subset of the original U(1) gauge transformations is preserved, the subspace of gauge invariant states is enlarged. The physical state condition (2.115) becomes

$$\exp\left(-i\frac{2\pi}{N}\mathcal{G}(x)\right)|\Psi_{\text{phys}}\rangle = |\Psi_{\text{phys}}\rangle \; ; \tag{2.132}$$

and can be rewritten as a condition on the eigenvalues of the restriction of electric field and charge operators to the (truncated) physical subspace. Denoting an eigenvalue with the name of the corresponding operator, (2.132) implies

$$[E^{x+1}_{\;\;x} - E^{x}_{\;\;x-1} - \rho(x)]\;\text{mod}\; N = 0 \;, \tag{2.133}$$

where mod is the modulo operation[23]. Only the condition (2.132) is preserved by time evolution, while the U(1) Gauss law (2.115) is not.

For the simulations performed in this Thesis we adopt the cyclic electric field truncation scheme. Other than preserving the unitarity of the comparator, this choice will allow a simple estimation of the severity of the truncation taking place during the simulation. Despite this choice, both approaches have their own strengths and are routinely used in numerical studies (see, e.g., the references above).

Before proceeding, it should be mentioned that quantum link models have a straightforward generalization to nonabelian lattice gauge theories. Moreover, both the quantum link and $\mathbb{Z}_N$ models here introduced as a truncated version of compact quantum electrodynamics are of interest per se [29, 56].

Meson bound states.   In order to perform a scattering simulation, an initial free multi-particle state has to be prepared[24]. For free staggered fermions we have shown how to explicitly solve the spectrum of the theory and construct the asymptotic particle states introduced in Sections 1.1–1.2. In the massive Schwinger model the solution to this problem is no longer known. What can be safely argued is that the asymptotic states will not correspond to the charged fermions of the model. This is yet another consequence of Gauss law: hypothetical asymptotic charges would correspond to states of infinite electric field energy in the continuum limit. The linear rise of the Coulomb potential and the consequent confining force ("quark-trapping" [22, 59]) are typical of $1 + 1$ dimensional models. In the exactly solvable massless Schwinger model, all the asymptotic states are known to belong to the Fock space of a free massive boson [18, 59]. In the massive case an exact solution is not

---

[23] Given two numbers X, Y then X mod $Y = 0$ when X is a multiple of Y.

[24] At least approximately, given the finite time extent of the simulation.

available but "quark-trapping" still holds [22]. In the light of these observations, as candidate asymptotic scattering states, we look for charge neutral bound states.

The simplest guess for a *meson*[25] bound state with momentum k is

$$|k\rangle = c^\dagger(k) |\Omega\rangle = \sum_{qp}^{\star} \delta(p+q-k)\, \psi(p,q)\, \tilde{a}^\dagger(p)\tilde{b}^\dagger(q) |\Omega\rangle \ , \qquad (2.134)$$

where $|\Omega\rangle$ is the interacting vacuum, $\tilde{a}^\dagger(p)$ and $\tilde{b}_k^\dagger(q)$ are the fermion and antifermion creation operators of the free theory and $c^\dagger(k)$ is a tentative meson creation operator. Together with $P|\Omega\rangle = 0$, the transformation properties of $\tilde{a}^\dagger(p)$ and $\tilde{b}_k^\dagger(q)$ under space translations[26] ensure that the state $|k\rangle$ is a momentum eigenstate, $P|k\rangle = k|k\rangle$. However, unless further conditions are imposed on $\psi(p,q)$, $|k\rangle$ is not an Hamiltonian eigenstate (and thus not a proper stable bound state). The bound state problem is intimately non-perturbative but it is possible to formulate and solve an approximate version of such conditions by treating the Coulomb potential as a classical field [78]. Nonetheless, the number of sites available in our numerical lattice simulations may not even allow to resolve the internal structure $\psi(p,q)$ of the bound state. For this reason we just point out that, as a first approximation, a physically sensible ansatz for $\psi(p,q)$ is obtained requiring that the fermion and antifermion are centered in close real space positions ($\bar{x}$ and $\bar{y}$) and have similar momenta. Assuming that $q-p$ follows a normal distribution centered in zero and of standard deviation λ_k, the previous requirements suggest

$$\psi(p,q) \propto \exp\left[-\frac{(q-p)^2}{4\lambda_k^2} - i(p\bar{x} - q\bar{y})\right] = \exp\left[-\frac{(q-p)^2}{4\lambda_k^2} - ik\mu_x - i(q-p)\frac{\lambda_x}{2}\right] .$$
$$(2.138)$$

Here the meson center of mass position μ_x and string length λ_x parameters have

---

[25] This name is chosen in analogy with the mesons of quantum chromodynamics. In both cases the bound state is a composed by a fermion in the fundamental representation of the gauge group and an antifermion in the conjugate representation.

[26] In a lattice theory ($\ell = 1$) with staggered fermions, space translation symmetries $x \to x + 2n$ ($n \in \mathbb{Z}$) are implemented by integer powers of $\exp(-2iP)$. Inserting

$$e^{2iP}\xi(x)\, e^{-2iP} = \xi(x-2) \qquad (2.135)$$

in the expression (2.39a) of $\tilde{a}^\dagger(k)$ yields

$$e^{2i\ell P}\tilde{a}^\dagger(k)\, e^{-2i\ell P} = e^{2ik}\tilde{a}^\dagger(k) \ ; \qquad (2.136)$$

analogously for $\tilde{b}^\dagger(k)$. Then

$$e^{2i\ell P}\delta(p+q-k)\tilde{a}^\dagger(p)\tilde{b}^\dagger(q)\, e^{-2i\ell P} = \delta(p+q-k)e^{2i(p+q)}\tilde{a}^\dagger(p)\tilde{b}^\dagger(q) \ ; \qquad (2.137)$$

proving that (2.134) produces excitations of momentum k.

been introduced, they read

$$\mu_x = (\bar{x} + \bar{y})/2 \; , \qquad \lambda_x = \bar{y} - \bar{x} \; . \tag{2.139}$$

As observed in the discussion of the theory of free staggered fermions, the physical states are momentum wave packets. Independently from the explicit form of $\psi(p, q)$, we can define a meson wave packet creation operator $\mathcal{C}^\dagger$ as

$$\mathcal{C}^\dagger = \sum_k^\star \phi(k) c^\dagger(k) = \sum_{qp}^\star \phi(p + q) \, \psi(p, q) \, \tilde{a}^\dagger(p) \tilde{b}^\dagger(q) \; ; \tag{2.140}$$

where $\phi(k)$ is the momentum space wave packet amplitude, typically a Gaussian. Introducing a new function $\phi(p, q) = \phi(p + q)\psi(p, q)$ and inserting the expressions (2.39a) and (2.39b) of the Fourier mode operators in terms of the position space staggered fermion operators, $\mathcal{C}^\dagger$ becomes

$$\mathcal{C}^\dagger = \sum_{qp}^\star \phi(p, q) \, \tilde{a}^\dagger(p) \tilde{b}^\dagger(q) = \sum_{xy}^\star \tilde{\phi}(x, y) \, \xi^\dagger(x) \xi(y) \; . \tag{2.141}$$

This equation implicitly defines $\tilde{\phi}(x, y)$, analogously to (2.69)–(2.71).

For simplicity, in the numerical simulations reported in Chapter 4 the fermion and antifermion within a meson are produced completely uncorrelated. With this choice, a meson wave packet can be prepared by means of the fermion and antifermion wave packet creation operators (2.69) and (2.70). We use the same momentum space normal probability distribution for both wave packets but, to center them in different real space positions $\bar{x}$ and $\bar{y}$, the amplitudes are shifted by a phase. In the end, our factorized meson wave packet creation operator reads,

$$\begin{aligned}
\mathcal{C}^\dagger = \mathcal{A}^\dagger \mathcal{B}^\dagger &= \sum_{qp}^\star \phi(p; \bar{x}, \mu_k, \sigma_k) \, \tilde{a}^\dagger(p) \, \phi(q; \bar{y}, \mu_k, \sigma_k) \, \tilde{b}^\dagger(q) \\
&= \sum_{xy} \tilde{\phi}(x; \bar{x}, \mu_k, \sigma_k) \, \xi^\dagger(x) \, \tilde{\phi}(y; \bar{y}, \mu_k, \sigma_k) \, \xi(y) \; .
\end{aligned} \tag{2.142}$$

All the approximations we have introduced here are not a priori justified. Nevertheless, as far as scattering processes are concerned, a partial justification can be put forward. The result of using (2.142) to produce a meson wave packet should mostly amount to the introduction of some internal excitation in the bound state. As long as this excitation is not too strong, we still expect to observe meaningful scattering processes. More specifically, we hope that the states we prepare are still bound enough to survive until the collision. The simulations reported in Chapter 4 show that, in the coupling regime that has been explored, this is the case. More

importantly, in Chapter 4 we show how bound states with correlated fermion and antifermion of type (2.138) can be prepared[27].

Dressing of creation and annihilation operators.   All the creation operators in the previous paragraph violate Gauss law and thus do not produce gauge invariant states. In order to obtain physical states the fermion and antifermion creation operators $\tilde{a}_k^\dagger$ and $\tilde{b}_k^\dagger$ have to be appropriately combined with electric field raising $(U^x{}_{x-1})^\dagger$ and lowering $U^x{}_{x-1}$ operators respectively. This is achieved writing them in terms the position space fields $\xi_x^\dagger$ and ξ^x, as per (2.39a) and (2.39b), and making the replacements

$$\xi_x^\dagger \to \xi_x^\dagger \prod_{y>x} (U^y{}_{y-1})^\dagger \; , \qquad \xi^x \to \xi^x \prod_{y>x} U^y{}_{y-1} \; . \tag{2.143}$$

With these substitutions Gauss law is preserved by increasing (decreasing) the electric field in all the links following the site in which a positive (negative) charge has been created. Notice that to preserve the value of the electric field at the boundary of the chain we must always act with a charge neutral operator[28], namely with both a $\xi_x^\dagger$ and a ξ^y. This is, by construction, the case of all the creation operators of the previous section. Given $x < y$, recalling the unitarity of the comparator (2.111),

$$\xi_x^\dagger \xi^y \to \xi_x^\dagger \xi^y \prod_{z>x} \prod_{w>y} (U^z{}_{z-1})^\dagger U^w{}_{w-1} = \xi_x^\dagger \xi^y \prod_{x \le z < y} (U^{z+1}{}_z)^\dagger \; ; \tag{2.144}$$

similarly for $y < x$, with $(U^{z+1}{}_z)^\dagger$ replaced by $U^{z+1}{}_z$.

---

[27] The only reason why these are not in the reported simulations is that the related code has not been implemented yet.

[28] This is simply a restatement of the observation that the asymptotic states of the Schwinger model are charge neutral.

3

Tensor Networks

In this Chapter the many-body problem is formulated and the entanglement entropy is defined, motivating the introduction of some concepts from tensor network theory. An efficient representation of many-body states and operators is illustrated, together with two algorithms implementing a ground state search and time evolution. These tools are essential for the development of the simulations presented in Chapter 4.

3.1 Many-Body Problem

In Chapter 2 it has been discussed how lattice quantum field theories are many-body quantum mechanical systems. The many-body problem, namely the study of several interacting quantum degrees of freedom, is encountered in a wide range of scientific fields [85, 87]. Among these, the numerical simulation of high energy physics is just an example. In this Section we present some general features of many-body systems and introduce the concept of entanglement. The latter is at the foundation of an important class of numerical techniques, introduced in the next Section, that allow to attack many-body problems efficiently.

The Hilbert space of an L-body system is the tensor product of L single-body or *local* Hilbert spaces,

$$\mathscr{H} = \mathscr{H}_1 \otimes \cdots \otimes \mathscr{H}_L \ . \tag{3.1}$$

The single-body constituents of the system can be any quantum degree of freedom. Here we label them with a position index $x = 1, \ldots, L$ in analogy with the case of lattice quantum field theory, where each degree of freedom represent the local state of a field on a lattice site[1]. Chosen a *local basis* $\{|\alpha_x\rangle\}$ for each $\mathscr{H}_x$ space, a state $|\psi\rangle \in \mathscr{H}$ can be represented by a rank-L complex tensor $\psi_{\alpha_1 \alpha_2 \ldots \alpha_L}$ via

$$|\psi\rangle = \sum_{\alpha_1 \alpha_2 \ldots \alpha_L} \psi_{\alpha_1 \alpha_2 \ldots \alpha_L} |\alpha_1\rangle \otimes |\alpha_2\rangle \otimes \cdots \otimes |\alpha_L\rangle \ . \tag{3.2}$$

Let us assume for simplicity that all the local Hilbert spaces have dimension d. Then

---

[1] Here, to lighten the notation, we neglect the distinction between site and link degrees of freedom.

$\dim \mathscr{H} = d^L$ independent coefficients have to be specified in order to identify the state $|\psi\rangle$. This exponential growth of the Hilbert space dimension with the system size makes many-body problems extremely challenging to attack numerically. To give a quantitative idea, consider a small chain of $L = 160$ two-level bodies, an example are the lattices of 160 staggered fermions sites that will be considered in the next Chapter. Storing the coefficients $\psi_{\alpha_1 \alpha_2 \dots \alpha_L}$ representing the state of such a system requires an enormous amount of memory, about 10^{40} gigabytes.

Mean field and beyond. The crucial observation in overcoming the above obstacle is that not all the states in the Hilbert space $\mathscr{H}$ have the same physical relevance. Usually the description of physical phenomena involves only an exponentially small portion of the exponentially large Hilbert space $\mathscr{H}$ [80, 87]. A key step in the investigation of many-body systems is the development of methods that target directly the relevant portion of $\mathscr{H}$. As an example, the assumption at the basis of *mean field theory* is that a good approximate description of a many-body system can be achieved considering only states that factorize as

$$|\psi\rangle = |\psi_1\rangle \otimes \cdots \otimes |\psi_L\rangle \ ; \tag{3.3}$$

namely, neglecting the correlations between the components of the system. In this way, each of the $|\psi_x\rangle$ is specified separately and only Ld coefficients are needed to represent the overall state of the system. The complexity of the problem has been thus reduced from exponential to linear in the system size. However, the mean field ansatz is an uncontrolled and not always justified approximation. In order to show how it can be improved, let us consider a two-body system AB with Hilbert space

$$\mathscr{H}_{\mathrm{AB}} = \mathscr{H}_{\mathrm{A}} \otimes \mathscr{H}_{\mathrm{B}} \ , \qquad d_{\mathrm{A}} \equiv \dim \mathscr{H}_{\mathrm{A}} \leq d_{\mathrm{B}} \equiv \dim \mathscr{H}_{\mathrm{B}} \ . \tag{3.4}$$

Given two bases $\{|\alpha\rangle\}$ and $\{|\beta\rangle\}$ of $\mathscr{H}_{\mathrm{A}}$ and $\mathscr{H}_{\mathrm{B}}$ respectively, we can represent a normalized state $|\psi_{\mathrm{AB}}\rangle \in \mathscr{H}_{\mathrm{AB}}$ of AB as

$$|\psi_{\mathrm{AB}}\rangle = \sum_{\alpha,\beta}^{d_{\mathrm{A}},d_{\mathrm{B}}} \psi_{\alpha\beta} |\alpha\rangle \otimes |\beta\rangle \tag{3.5}$$

Via a singular value decomposition (SVD) $\psi_{\alpha\beta}$ can be written as a matrix product:

$$\psi_{\alpha\beta} = \sum_k^{d_{\mathrm{A}}} S_{\alpha k} V_{kk} D_{k\beta} \ , \tag{3.6}$$

with S and D unitary and V diagonal with non-negative entries $V_{kk} = \lambda_k \geq 0$, called *singular values* (SVs), that we assume to be listed in descending order. Equivalently,

$$|\psi_{AB}\rangle = \sum_{\alpha,\beta}^{d_A,d_B} \sum_k^{d_A} \lambda_k (S_{\alpha k} |\alpha\rangle) \otimes (D_{k\beta} |\beta\rangle) = \sum_k^{d_A} \lambda_k |k_A\rangle \otimes |k_B\rangle \ . \tag{3.7}$$

Here $\{|k_A\rangle = \sum_\alpha S_{\alpha k} |\alpha\rangle\}$ is a new orthonormal basis of $\mathscr{H}_A$ and the analogously defined $\{|k_B\rangle\}$ can be completed to an orthonormal basis of $\mathscr{H}_B$. Typically, for non-random states and in particular for states describing physical configurations, there is a strong hierarchy in the singular values. We can exploit this fact to discard some of them, e.g., the ones below an arbitrary precision ϵ, and reduce the dimensionality of the matrices involved in (3.6) and (3.7). Denoting with χ the number of singular values left, called bond dimension, the introduced approximation reads

$$|\psi_{AB}^{\text{trunc}}\rangle = \frac{1}{\mathcal{N}} \sum_k^\chi \lambda_k |k_A\rangle \otimes |k_B\rangle \ , \qquad \mathcal{N} = \sqrt{\sum_k^\chi \lambda_k^2} \ ; \tag{3.8}$$

where $\mathcal{N}$ enforces the normalization of the state. Notice that setting $\chi = 1$ we recover the mean field ansatz. Consequently, varying the precision ϵ, we can interpolate between the mean field and exact representations in a controlled way [87, 95]. It can be proven [11, 91] that the approximation (3.8) is also the optimal one in the sense that, for fixed $M_{\alpha\beta}$ rank, $M_{\alpha\beta} = \sum_k^\chi S_{\alpha k} V_{kk} D_{k\beta}$ minimizes the 2-norm

$$\left\| \psi_{\alpha\beta} - M_{\alpha\beta} \right\| \ . \tag{3.9}$$

We now give a possible generalization of the above compression procedure to the many-body case. As is now explained, this is mostly a matter of reshufflings tensor indices. Consider the state $\psi_{\alpha_1\alpha_2\ldots\alpha_L}$ in (3.2). We can identify α_1 with the index α in (3.6) and fuse all the other indices in a single index $\beta = 2, \ldots, d^L$; perform an SVD; eventually truncate; adsorb the V_{kk} matrix in the definition of $D_{k\beta}$; and finally split again the index β. The procedure is then repeated, this time $\{k, \alpha_2\}$ is identified with α and the indices on the right of α_2 with β. Proceeding iteratively, the many-body wave function $\psi_{\alpha_1\alpha_2\ldots\alpha_L}$ is decomposed in a product of L tensors[2] [80, 87]

$$\psi_{\alpha_1\alpha_2\ldots\alpha_L} = \sum_{k_1 k_2\ldots k_L} S_{\alpha_1}^{k_1} S_{\alpha_2}^{k_1 k_2} \cdots S_{\alpha_{L-1}}^{k_{L-2} k_{L-1}} D_{\alpha_L}^{k_{L-1}} \ , \tag{3.10}$$

where we moved up the contracted indices $k_x = 1, \ldots, \chi_x$ to better distinguish them from the external indices $\alpha_x = 1, \ldots, \dim \mathscr{H}_x$. The right hand side of (3.10) is the

---

[2] Despite their common name, the $S_{\alpha_x}^{k_x-1 k_x}$ are different tensors for different values of x. We adopt the convention that tensors are identified not only by their name but also by their indices.

matrix product state representation of $|\psi\rangle$ and provides a first example of tensor network ansatz. A more systematic discussion of tensor network methods is given in the next Section. Here we just point out that the procedure outlined above, namely the construction of a matrix product states out of a rank-L tensor is only a formal procedure. In practice, matrix product states are often used to study systems whose state cannot even be stored in its exact representation. Rather than providing an exact state and rewriting it in matrix product state form, the algorithms presented in the next Section assume that a faithful tensor network representation of the state of interest with sufficiently low bond dimensions exists. To understand why this is often the case we introduce the concept of entanglement.

Entanglement entropy. The efficiency of the compressions (3.8) and (3.10) depends heavily on how rapidly the singular values decrease. Let us focus on the two-body case. If in the decomposition (3.7) there is only one non-vanishing singular value the state $|\psi_{AB}\rangle$ is said to be *separable* and the mean field representation is exact. Generally this is not the case and $|\psi_{AB}\rangle$ is said to be an *entangled* state. To quantify the achievable compression we need a measure of entanglement. Namely, a measure of how far from the separable case $|\psi_{AB}\rangle$ is and how much the configurations of the subsystems A and B are correlated.

To this aim, consider again the decomposition (3.7). Notice that, unless $|\psi_{AB}\rangle$ is separable, we cannot associate two wave functions, $|\psi_A\rangle$ and $|\psi_B\rangle$, to the subsystems A and B. Indeed, the wave function is not the most general description of the state of a quantum system. In the following we refer to states that admit a wave function representation, e.g., $|\psi_{AB}\rangle$, as *pure states*. In systems that interact with an environment, such as the subsystems A and B, the state generally consists of a statistical mixture of pure states $\{|\psi_n\rangle\}$, each associated with a classical probability or population p_n. We refer to these configurations as *mixed states*. Mixed states are conveniently described in terms of a *density matrix* ρ, defined as

$$\rho = \sum_n p_n |\psi_n\rangle\langle\psi_n| \ , \qquad \sum_n p_n = 1 \ . \tag{3.11}$$

The density matrix is Hermitian, positive semidefinite, has unit trace and satisfies

$$\text{tr}(\rho^2) \leq 1 \ . \tag{3.12}$$

Inequality (3.12) is saturated if and only if ρ represents a pure state $|\psi\rangle$, in which case the density matrix is the projector $|\psi\rangle\langle\psi|$. Given a density matrix ρ, the scalar

$$S(\rho) = -\text{tr}(\rho \log \rho) \ ; \tag{3.13}$$

is called *Von-Neumann entropy* of ρ. Notice it vanishes for pure states, such as $|\psi_{\mathrm{AB}}\rangle$ and also the wave functions $|\psi_{\mathrm{A}}\rangle$ and $|\psi_{\mathrm{B}}\rangle$ when $|\psi_{\mathrm{AB}}\rangle$ is separable. The important point is that, having introduced the density matrix, we can now associate a density matrix ρ_{A} (ρ_{B}) to the subsystem A (B) also when $|\psi_{\mathrm{AB}}\rangle$ is not separable. As we now motivate, $S(\rho_{\mathrm{A}})$ provides a good entanglement measure for the pure state $|\psi_{\mathrm{AB}}\rangle$.

Recalling (3.7), the density matrix representation of $|\psi_{\mathrm{AB}}\rangle$ is

$$\rho_{\mathrm{AB}} = |\psi_{\mathrm{AB}}\rangle\langle\psi_{\mathrm{AB}}| = \sum_{i,j} |i_{\mathrm{A}} i_{\mathrm{B}}\rangle \, \lambda_i \lambda_j^* \, \langle j_{\mathrm{A}} j_{\mathrm{B}}| \ ; \tag{3.14}$$

with $|i_{\mathrm{A}} i_{\mathrm{B}}\rangle = |i_{\mathrm{A}}\rangle \otimes |i_{\mathrm{B}}\rangle$. The *reduced density matrix* for the subsystem A is simply the partial trace of ρ_{AB} over the subsystem B,

$$\rho_{\mathrm{A}} = \sum_{\beta} \langle\beta|\rho_{\mathrm{AB}}|\beta\rangle = \sum_{i,j,k} \langle k_{\mathrm{B}}|i_{\mathrm{A}} i_{\mathrm{B}}\rangle \, \lambda_i \lambda_j^* \, \langle j_{\mathrm{A}} j_{\mathrm{B}}|k_{\mathrm{B}}\rangle = \sum_k \lambda_k^2 |k_{\mathrm{A}}\rangle\langle k_{\mathrm{A}}| \ , \tag{3.15}$$

and the squared singular values are interpreted as populations. Together with the analogous result for ρ_{B}, (3.15) yields

$$S(\rho_{\mathrm{A}}) = S(\rho_{\mathrm{B}}) = -\operatorname{tr}(\rho_{\mathrm{A}} \log \rho_{\mathrm{A}}) = -\sum_k \lambda_k^2 \log \lambda_k^2 \ . \tag{3.16}$$

This quantity is called the *entanglement entropy* of the pure state $|\psi_{\mathrm{AB}}\rangle$ of the bipartite system AB [94]. It vanishes if $|\psi_{\mathrm{AB}}\rangle$ is separable and has the maximum possible value when all the λ_k coefficients are equal. As a consequence, it provides a good estimate of how difficult it is to compress $|\psi_{\mathrm{AB}}\rangle$ or, otherwise stated, how much information the state contains.

For a many-body pure state, the above discussion defines an entanglement entropy for every bipartition of the system. A "typical" pure state in the Hilbert space has an entanglement entropy between large enough subregions that scales like the volume of the subregions [94]. On the other hand, low-energy eigenstates of gapped Hamiltonians with *local* interactions have been proven to satisfy *area laws* [80, 87, 94]. These assert that the entanglement entropy of a region tends to scale as the size of the boundary of the region and not as its volume; in particular it is constant in one dimensional systems [65]. Area laws are the profound explanation for the efficiency of tensor network ansatze in describing the low-energy properties of physical systems: they target directly the relevant, low-entanglement, portion of the Hilbert space [80].

3.2   Tensor Network Methods

A *tensor network* (TN) is a collection of tensors and contraction rules. Although we do not use it here, there exist a particularly convenient *diagrammatic notation* for TNs [95]. A TN is represented by a graph in which a node corresponds to a tensor and the edges attached to it represent its indices. In particular dangling edges are uncontracted indices while edges that connect two nodes denote a contraction.

As just discussed, many-body computations typically involve huge tensors; TN methods allow to break these huge tensors in smaller ones while accommodating as much information as possible with the available resources. Here an overview of some concepts from tensor network theory, relevant for the development of the Thesis, is put forward. A detailed presentation can be found in [71, 80, 94, 95].

3.2A   Ansatze

We now introduce TN ansatze for the representation of states and operators. Together with the TN algorithms outlined in the next Section, they constitute the building blocks of most of the work presented in Chapter 4. In the following we always assume that repeated indices are contracted.

Matrix Product State.   The *Matrix Product State* (MPS) ansatz is one of the most successful TN representations of one-dimensional many-body pure states [95]. It encodes the coefficients $\psi_{\alpha_1\alpha_2\ldots\alpha_L}$ as a product of matrices M_{α_x},

$$|\psi\rangle = M_{\alpha_1}^{k_0 k_1} M_{\alpha_2}^{k_1 k_2} \cdots M_{\alpha_{L-1}}^{k_{L-2}k_{L-1}} M_{\alpha_L}^{k_{L-1}k_L} |\alpha_1\alpha_2\ldots\alpha_L\rangle \ . \tag{3.17}$$

The k_x are called *bond* or *virtual* indices and their dimension χ_x is the local *bond dimension*. The α_x are *physical* indices and run over the local Hilbert space basis. The boundary matrices are vectors, $\chi_0 = \chi_L = 1$, so that the contraction of the virtual indices always produces a scalar. The trivial indices k_0, k_L are introduced just to uniformize the MPS layout; at least working with open boundary conditions. Although we do not use them in numerical simulations, with periodic boundaries it is natural to treat k_0 and k_L as proper virtual indices and contract them.

The space spanned by MPS is dense in the sense that, in principle, every Hilbert space vector can be represented using an exponentially large (in L) bond dimension. For fixed uniform bond dimension χ, an MPS naturally realizes the one-dimensional area law as the entanglement entropy for every bipartition is bounded by $\log \chi$ [80]. Notice also that the tensors in (3.10) satisfy by construction the isometric condition

$$S^{*\,l_1}_{\ \alpha_1} S^{k_1}_{\alpha_1} = \delta^{k_1 l_1} \ , \qquad S^{*\,k_{j-1}l_j}_{\ \ \alpha_j} S^{k_{j-1}k_j}_{\alpha_j} = \delta^{k_j l_j} \quad \text{for } j < L \ . \tag{3.18}$$

Given an MPS it is always possible to enforce this or similar isometric conditions exploiting the invariance of the network under the local invertible transformations

$$M_{\alpha_x} \to M_{\alpha_x} Y^{-1} \ , \qquad M_{\alpha_{x+1}} \to Y M_{\alpha_{x+1}} \ ; \qquad (3.19)$$

where Y is an invertible $\chi_x \times \chi_x$ matrix. Chosen a site x, via a sequence of transformations (3.19) it is possible to impose [94, 95]

$$\prod_{y<x} M^{*k_{y-1}l_y}_{\alpha_y} M^{k_{y-1}k_y}_{\alpha_y} = \delta^{k_{x-1}l_{x-1}} \ , \qquad \prod_{z>x} M^{*l_{z-1}k_z}_{\alpha_z} M^{k_{z-1}k_z}_{\alpha_z} = \delta^{k_x l_x} \ . \qquad (3.20)$$

This is known as *mixed canonical form* of the MPS. It reduces the evaluation of the norm of the MPS $\langle \psi | \psi \rangle$ to the complete contraction of the $M^{k_{x-1}k_x}_{\alpha_x}$ tensor with its conjugate, namely to an $\mathcal{O}(1)$ operation in the system size. Similarly for expectation values of local operators with support on the site x. Finally, the site around which the isometrization is performed can be moved quite efficiently [71].

Matrix Product Operator.   Another tensor network ansatz emerging naturally when MPSs are employed is the *Matrix Product Operator* (MPO) [69]. It is used to represent many-body operators as

$$O = w^{k_0} W^{k_0 k_1}_{\alpha_1 \beta_1} W^{k_1 k_2}_{\alpha_2 \beta_2} \cdots W^{k_{L-1} k_L}_{\alpha_L \beta_L} w^{k_L} |\alpha_1 \alpha_2 \dots \alpha_L \rangle\langle \beta_1 \beta_2 \dots \beta_L | \ . \qquad (3.21)$$

The main difference with the MPS ansatz is that there are both ingoing and outgoing physical indices. The vectors w^{k_0} and w^{k_L} are here introduced in order to have a uniform bulk. In the MPOs considered in this Thesis they are always

$$[w^{k_0}] = \begin{bmatrix} 1 & 0 & 0 & 0 \end{bmatrix} \ , \qquad [w^{k_L}] = \begin{bmatrix} 0 & 0 & 0 & 1 \end{bmatrix}^T \qquad (3.22)$$

An important result is that all local short range interactions can be represented *exactly* as an MPO with small bond dimension [94]. The MPO representation of the free staggered fermions and lattice Schwinger model Hamiltonians, as well as of the fermion, antifermion and meson wave packet creation operators, are given in Chapter 4.

3.2B   Algorithms

Two crucial operations for the simulation of scattering processes in lattice gauge theories and, more in general, for the investigation of quantum systems, are:

(i) determining of the ground state, to prepare the initial wave packets;

(ii) evolving the prepared state, to compute transition amplitudes.

Here we present the working principles of two algorithms that implement the above

tasks; we disregard technical details and efficiency issues.

The simulations presented in Chapter 4 are based on the *Tensor Network Python* (TeNPy) library [94] implementation of these algorithms.

Ground state search.   Many interesting properties of a quantum mechanical system can be deducted studying it low-energy eigenstates. The MPS representation of these states can be computed with an extremely efficient variational algorithm: the *Density Matrix Renormalization Group* (DMRG) algorithm [94, 95]. DMRG relies on the MPO representation of the Hamiltonian to recasts the global energy optimization problem in a sequence of *local* optimizations of the MPS tensors with respect to local effective Hamiltonians.

The optimization problem for the ground state is encoded by the Lagrangian [95]

$$\mathscr{L}(\{M^{k_{x-1}k_x}_{\alpha_x}, M^{*\,k_{x-1}k_x}_{\alpha_x}\}) = \langle\psi|H|\psi\rangle - \lambda(\langle\psi|\psi\rangle - 1) \ , \tag{3.23}$$

where the variables with respect to which we optimize are the MPS tensors as well as the Lagrange multiplier λ, enforcing the normalization of the state. Ideally, given an initial guess or random MPS we should optimize all its tensors simultaneously. In practice this is not efficient or even viable [80], so we use as variational space the coefficients of a single tensor at time, while keeping the others, called environment, fixed. Imposing the stationarity of $\mathscr{L}$ with respect to the tensor $M^{*\,k_{x-1}k_x}_{\alpha_x}$ provides

$$\tilde{H}^{k_{x-1}k_x l_x l_{x+1}}_{\alpha_x\beta_x} M^{l_x l_{x+1}}_{\beta_x} - \lambda M^{k_{x-1}k_x}_{\alpha_x} = 0 \tag{3.24}$$

where the effective Hamiltonian $\tilde{H}$ for M_{α_x} results from the contraction of the Hamiltonian MPO with all the other MPS tensors and their conjugates. Moreover, we assumed that the MPS is in the mixed canonical form (3.20) to simplify the derivative of $\langle\psi|\psi\rangle$ with respect to $M^*_{\alpha_x}$ [71]. Once the sets of indices α_x, k_x, k_{x+1} and β_x, l_x, l_{x+1} are fused in two single indices, (3.24) becomes an ordinary eigenvalue problem. The lowest eigenstate can be found via standard algorithms (e.g., Lanczos) together with its eigenvalue λ_0, providing the current ground state energy estimate.

The update of $M^{k_{x-1}k_x}_{\alpha_x}$ changes the effective problem for the other tensors. The algorithm sweeps over the tensors iteratively, performing local optimizations until the desired convergence of λ_0 or some other global observable is reached [94]. Once a ground state $|\Psi_0\rangle$ has been found, the next excited state can be computed adding a term $\lambda' \langle\Psi_0|\Psi\rangle$ to the Lagrangian (3.23). The extremization with respect to the multiplier λ' imposes $|\Psi\rangle$ is orthogonal to the ground state. Proceeding iteratively a few low-energy eigenstates can be determined.

The DMRG implementation used in our simulations updates two neigbouring tensors

at a time. In this version, an initial contraction of the two tensors and a final SVD to split back the optimized tensor have to be performed. The SVD allows the algorithm to grow the bond dimension as required by the chosen precision [94].

Time evolution. Suppose an Hamiltonian H and an initial state $|\psi(0)\rangle$ in MPS form are given. The Schrödinger time evolution (1.112) of $|\psi(0)\rangle$, namely

$$|\psi(t)\rangle = U(t) |\psi(0)\rangle = e^{-iHt} |\psi(0)\rangle \;, \tag{3.25}$$

can be determined using the *Time Evolving Block Decimation* (TEBD) algorithm [94, 95]. TEBD assumes that the Hamiltonian contains at most nearest-neighbour interactions[3], i.e. it can be written as a sum of two-site operators of the form

$$H = \sum_x H^{[x,x+1]} = \sum_x H^{\alpha_x \alpha_{x+1}}_{\beta_x \beta_{x+1}} |\beta_x \beta_{x+1}\rangle\langle\alpha_x \alpha_{x+1}| \;. \tag{3.26}$$

The starting point of the algorithm consists in isolating the Hamiltonian terms corresponding to even and odd bonds, namely

$$H = H_{\text{even}} + H_{\text{odd}} = \sum_{x \text{ even}} H^{[x,x+1]} + \sum_{x \text{ odd}} H^{[x,x+1]} \;. \tag{3.27}$$

In general H_{even} and H_{odd} do not commute one with the other. Nonetheless, each is a sum of commuting operators. Consequently, their exponentials factorize exactly:

$$\exp\left(-itH_{\text{even}}\right) = \prod_{x \text{ even}} \exp\left(-itH^{[x,x+1]}\right) = \prod_{x \text{ even}} U^{[x,x+1]}(t) \;. \tag{3.28}$$

Identically for odd bonds. The (small) matrices $U^{[x,x+1]}$ can be evaluated exactly. In order to compute the exponential of $H_{\text{even}} + H_{\text{odd}}$, the TEBD algorithm splits the time interval t in small steps δt and relies on a Suzuki-Trotter decomposition [45]. Let X and Y be two non commuting operators, the second-order Suzuki-Trotter decomposition reads

$$e^{\delta t(X+Y)} = e^{\delta t X/2} e^{\delta t Y} e^{\delta t X/2} + \mathcal{O}(\delta t^3) \;; \tag{3.29}$$

there exist higher order variants as well.

Without going into the implementation details [94], notice that acting with $U^{[x,x+1]}$ on the MPS tensors $M^{k_{x-1}k_x}_{\alpha_x}$ and $M^{k_x k_{x+1}}_{\alpha_{x+1}}$ merges them in a single bigger tensor. The MPS representation is recovered applying an SVD and truncating the singular

---

[3] In the presence of slightly longer range interactions a nearest-neighbour Hamiltonian can be recovered by fusing groups of neighbouring sites in a single, bigger, local Hilbert space.

values below the desired precision[4]. Notice also that, generally, the update increases the entanglement entropy (and thus χ_x) at the bond between sites x and $x+1$ [94].

The error sources of the algorithm are the truncation of the singular values and the Trotterization. Specifically, a Suzuki-Trotter decomposition of order M introduces an error $\mathcal{O}(t\delta t^M)$ on the final state $|\psi(t)\rangle$ [94].

---

[4] The unitarity of the transformation (up to the final truncation error) ensures that it can be performed in a way that preserves the canonical form of the MPS [94].

4

Scattering Simulations

In this Chapter the numerical simulations are presented. These involve the kinematics of the theory of free staggered fermions and the scattering of mesons in the lattice Schwinger model. For each class of simulations we first give an overview of the ingredients required and then report and comment the obtained results.

All the numerical values reported in the Chapter are in lattice units[1]. The simulations based on tensor network methods rely on the TeNPy library [94].

4.1 Free Staggered Fermions

The theory of free staggered fermions is an ideal setting to test the numerical codes developed. This is particularly simple working with an exact representation of the many-body Hilbert space $\mathscr{H}$. By exact representation we mean that a basis for $\mathscr{H}$ is chosen and the coefficients defining the states and operators in that basis are stored in memory as complex arrays (exactly, up to the machine floating-point precision). However, due to the exponential increase of the Hilbert space dimension with the system size, only small[2] lattices can be studied with an exact representation. The achievable number of sites does not allow to produce wave packets with positions and momenta localized enough to study the free kinematics with sufficient precision. For this reason a MPS implementation has been undertaken. Its main features are now summarized, before presenting the outcome of some simulations.

In our tensor network based implementations we always work with open boundary conditions. We use the local occupation number $\xi_x^\dagger \xi^x$ eigenbasis for the site Hilbert spaces $\mathscr{H}_x$, $x = 1, \ldots, L$. The staggered fermion operators are constructed according to the Jordan-Wigner representation (2.22). Let us recall the non-vanishing matrix elements of the single-site operators involved,

$$\langle 1|\sigma^+|0\rangle = 1 \ , \qquad \langle 0|\sigma^-|1\rangle = 1 \ , \qquad \langle 1|n|1\rangle = 1 \ . \tag{4.1}$$

---

[1] This is consistent because we do not study the continuum limit of our simulations. However, care is required when comparing the parameters of simulations involving different lattice sizes.

[2] Up to 22 sites with the available amount of RAM memory (16 GB) and using sparse matrices.

In terms of these operators, the free staggered fermion Hamiltonian (2.16) reads

$$H = \frac{i}{2} \sum_x \left(\sigma^+_{x+1} \sigma^-_x - \sigma^+_x \sigma^-_{x+1} \right) + m \sum_x (-1)^x n_x \ , \tag{4.2}$$

where the x subscript of the single-site operators denotes the site on which they act, tensor products with the identity on the other sites are implied as usual. A direct computation reveals that the MPO representation (3.21) of (4.2) is built by the tensors

$$[W_H^{k_{x-1} k_x}] = \begin{bmatrix} 1 & \sigma^+ & \sigma^- & m(-1)^x\, n \\ 0 & 0 & 0 & -i/2\, \sigma^- \\ 0 & 0 & 0 & +i/2\, \sigma^+ \\ 0 & 0 & 0 & 1 \end{bmatrix} . \tag{4.3}$$

Here and in all the representations of MPOs that follow the matrix entries are labeled by the virtual indices k_{x-1}, k_x. We omit the physical indices α_x, β_x that would be attached to each matrix entry, as well as the site index x.

In order to prepare the initial states for simulations of the free kinematics, also the fermion and antifermion wave packet creation operators (2.69) and (2.70) have to be implemented. In terms of the operators (4.1) they read

$$\mathcal{A}^\dagger = \sum_x \tilde{\phi}(x) \left[\prod_{y<x} (-1)^{n_y} \right] \sigma^+_x \ , \qquad \mathcal{B}^\dagger = \sum_x \tilde{\phi}(x) \left[\prod_{y<x} (-1)^{n_y} \right] \sigma^-_x \ . \tag{4.4}$$

Despite the non-local Jordan-Wigner strings, these operators admit a simple MPO representation with

$$[W_{\mathcal{A}^\dagger}^{k_{x-1} k_x}] = \begin{bmatrix} (-1)^n & \tilde{\phi}(x)\, \sigma^+ \\ 0 & 1 \end{bmatrix} \ , \qquad [W_{\mathcal{B}^\dagger}^{k_{x-1} k_x}] = \begin{bmatrix} (-1)^n & \tilde{\phi}(x)\, \sigma^- \\ 0 & 1 \end{bmatrix} \ . \tag{4.5}$$

In our simulations we use as amplitude $\tilde{\phi}(x)$ the $\tilde{\phi}(x; \mu_x, \mu_k, \sigma_k)$ in (2.71), namely a wave packet centered in μ_x in position space and corresponding to a normal probability distribution with mean μ_k and standard deviation σ_k in momentum space.

Simulation scheme. We simulate the free propagation of two wave packets for various fermion masses and wave packets parameters. For each wave packet, the momentum and position space amplitudes are evaluated numerically from the input parameters m, μ_x, μ_k and σ_k. The wave packets probability distributions and the expected peak trajectories based on the wave packet group velocity (2.29) are de-

picted in a preview plot, before any resource heavy computation is performed. An example is shown in Figure 4.1.
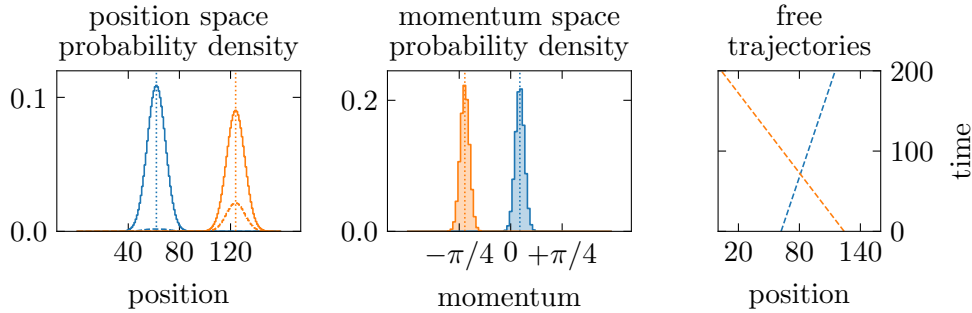
Figure 4.1: Preview of two $m = 0.5$ fermion wave packets on a 160 sites lattice, and of their expected trajectories up to $t = 200$. The wave packets are centered in positions $\mu_x = 62$ and 124 and momenta $\mu_k \pm \sigma_k = +0.14 \pm 0.07$ and -0.7 ± 0.07 respectively. In the position space plot, $\left|\tilde{\phi}(x)\right|^2$ corresponds to the solid curve on even sites and to the dashed curve on odd sites. For antifermions the two are exchanged, as per (2.71). The Fourier transform automatically satisfies the uncertainty principle.

From now on we will often refer to fermion and antifermion wave packets simply as fermion or antifermion. Once the wave packet parameters are chosen we proceed with the actual simulation, which consists of the following steps:

(i) determine the model ground state $|0\rangle$ via DMRG, exploiting the MPO representation (4.3) of the Hamiltonian;

(ii) prepare the initial state $|\Psi(0)\rangle$ by applying to $|0\rangle$ a sequence of creation MPOs (4.5), one for each wave packet;

(iii) compute its time evolution $|\Psi(t)\rangle = e^{-itH} |\Psi(0)\rangle$ via TEBD, using the nearest neighbour form (4.2) of the Hamiltonian.

During the evolution, the particle number charge density and the entanglement entropy associated to every bipartition of the chain (bond entropy) are sampled at regular intervals. In all the plots of this Chapter the charge density is summed over pairs of neighbouring sites to reproduce that of the continuum theory.

Results: free kinematics. We consider a chain of size $L = 160$ and different values of the mass parameter $m = 0.5, 0.7, 0.9$. For each mass we prepare an initial state of two fermions with different momenta, as those shown in Figure 4.1. The simulations of their propagation are shown in Figure 4.2. The MPS singular values are truncated at $\epsilon = 10^{-4.5}$ and a fourth order Trotter decomposition with $\delta t = 0.05$ is used for TEBD.
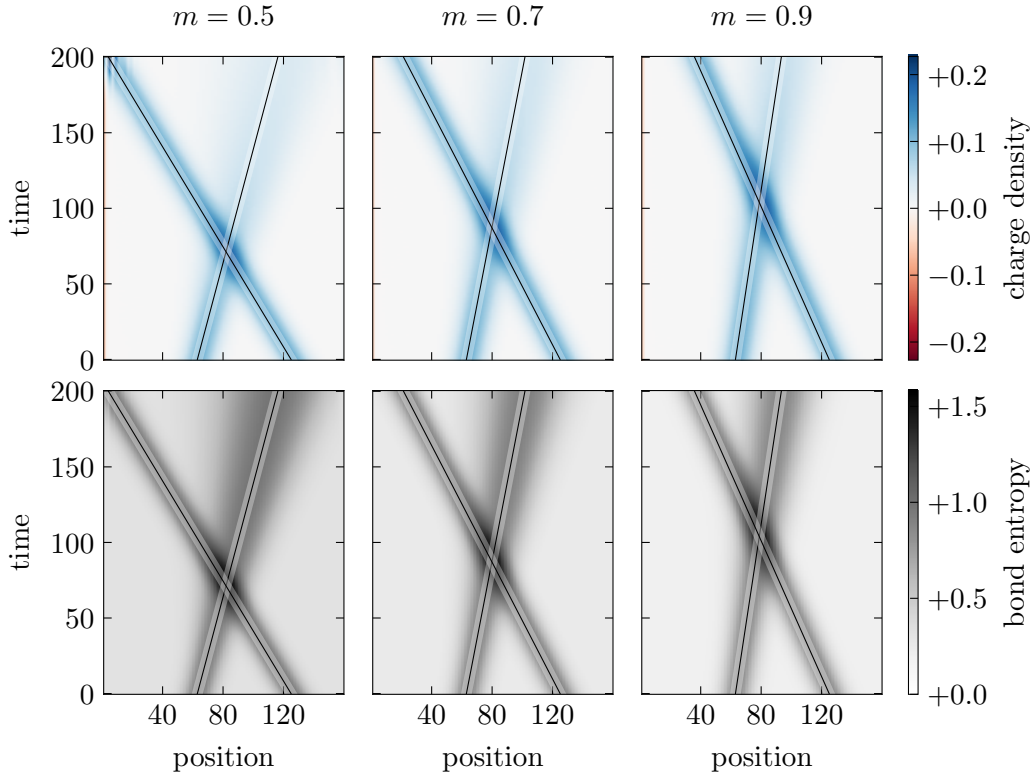
Figure 4.2: Particle number charge density and bond entropy during the free propagation of the two fermions of Figure 4.1. The straight lines in overlay are the trajectories of the wave packet peak predicted by the group velocity. Different columns correspond to different masses, $m = 0.5, 0.7, 0.9$ from left to right.

We observe that the propagation reproduces the behaviour expected for a free theory. Both fermions appear to follow their free trajectory and no sign of interaction or entanglement generation is present. The explanation of this fact is particularly simple in terms of the momentum space dynamics. It has been shown, see (2.60), that the Hamiltonian is diagonal in momentum space. As illustrated in Figure 4.1, the initial wave packets have well separated support in momentum space and thus evolve independently, but the same holds also for each momentum mode inside a single wave packet. Indeed, no entanglement is generated at all by the dynamics. There is however a spreading of the wave packets and of their initial internal entanglement. The spreading is more pronounced for light and slow fermions in agreement with the non linearity of the group velocity in the momentum and in particular with the fast rise of the group velocity of light particles near zero momentum (see Figure 2.1).

Together with the low entanglement of the initial state, the absence of entanglement

generation makes MPS simulations of the free theory extremely efficient. The maximum MPS bond dimension is constant during the simulation and corresponds to about 20 for a minimum singular value $\epsilon = 10^{-4.5}$.

4.2   Massive Schwinger Model

We simulate the Schwinger model dynamics with two of the approaches presented in Subsection 2.4B. Their numerical implementation is now discussed in more detail.

4.2A   Integrated Electric Field and Exact Representation

In the first approach we exploit the integration of the electric field degrees of freedom to reduce the dimension of the Hilbert space and opt for its exact representation. Nevertheless, similar memory limitations to the ones discussed for the exact representation of the free theory are present.

We work with open boundary conditions, fix the electric field at the left of the chain to zero and integrate out all the remaining link degrees of freedom by enforcing the Gauss law constraint. With this operation the many-body Hilbert space $\mathscr{H}$ is the one of the free theory. Working in the local occupation eigenbasis, the single-site operators are the ones of the free theory, defined in (4.1). The electric field is expressed as

$$E^{x+1}{}_{x} = \sum_{y=1}^{x} \left[n_y - \frac{1 - (-1)^y}{2} \right] \; ; \tag{4.6}$$

while the Hamiltonian (2.126) becomes

$$H = \frac{g^2}{2} \sum_{x} \left[\sum_{y}^{x} \left(n_y - \frac{1 - (-1)^y}{2} \right) \right]^2 + \frac{i}{2} \sum_{x} \left[\sigma_{x+1}^+ \sigma_x^- - \sigma_x^+ \sigma_{x+1}^- \right] + m \sum_{x} (-1)^x n_x \; . \tag{4.7}$$

To further reduce the dimensionality of $\mathscr{H}$ we restrict our analysis to a charge q sector[3]

$$\mathscr{H}_q = \{ |\Psi\rangle \in \mathscr{H}_{\text{phys}} : Q |\Psi\rangle = q |\psi\rangle \} \; , \qquad Q = \sum_{x} n_x - L/2 \; . \tag{4.8}$$

The consistency of this operation with time evolution is guaranteed by charge conservation $[H, Q] = 0$. Observing that $Q + L/2$ is the total occupation number, by a

---

[3]   The justification for considering only charge eigenstates comes from the electric charge superselection rule, which is yet another consequence of Gauss law [55, 77].

simple combinatorial argument the dimension of the charge q sector is

$$\dim \mathscr{H}_q = \begin{pmatrix} L \\ q + L/2 \end{pmatrix} . \tag{4.9}$$

Chosen a total charge q, via a recursive algorithm we identify all the local occupation eigenstates in $\mathscr{H}$ that have total charge q and use them as a basis of $\mathscr{H}_q$. Finally, we compute the matrix elements of the operators used in the simulation in this basis. The observables, such as the Hamiltonian, the charge density and the electric field, are operators that map each charge sector into itself[4]. Conversely, by (2.87), the staggered fermion operators ξ^x and $\xi_x^\dagger$ that appear in the creation and annihilation operators map a charge sector into a different one. It follows that two bases, related to different values of q, are involved in the computation of their matrix elements.

Simulation scheme. Some simulations of the dynamics of an excited fermion-antifermion pair have been carried out and are reported in Figure 4.3. Despite the different implementation, the workflow is similar to the one used for the free theory, namely:

(i) find the interacting ground state $|\Omega\rangle$, which we assume to be in the charge zero sector, via standard numerical routines;

(ii) apply to $|\Omega\rangle$ a fermion and an antifermion wave packet creation operators from the free theory (4.4);

(iii) evolve the prepared state, using a standard numerical algorithm that computes the action of a matrix exponential on a vector [70].

Results: fermions confinement. We consider a chain of size $L = 24$, fix the mass parameter $m = 0.9$ and perform simulations for various coupling strengths $g = 0.2, 0.4, 0.6, 1.0$. We prepare an initial state consisting of a fermion and an antifermion with opposite momenta, pointing one away from the other. Their propagation is shown in Figure 4.3.

We observe that the reciprocal attraction bends the trajectories and confines the fermion-antifermion pair in an oscillatory motion, whose period depends on the value of the coupling[5]. Despite the outgoing momenta, no "asymptotic" well separated fermion and antifermion are observed. Indeed, in hindsight, the usage of the words fermion and antifermion to describe the content of the initial state is improper: as discussed in Subsection 2.4B there are no such isolated charged particles in the

---

[4] That is, they commute with Q, in accordance with the charge superselection rule [77].

[5] Actually, in the $g = 0.20$ case the wave packets approach the boundaries. In order for the simulation to be completely trusted it should be repeated on a longer chain.
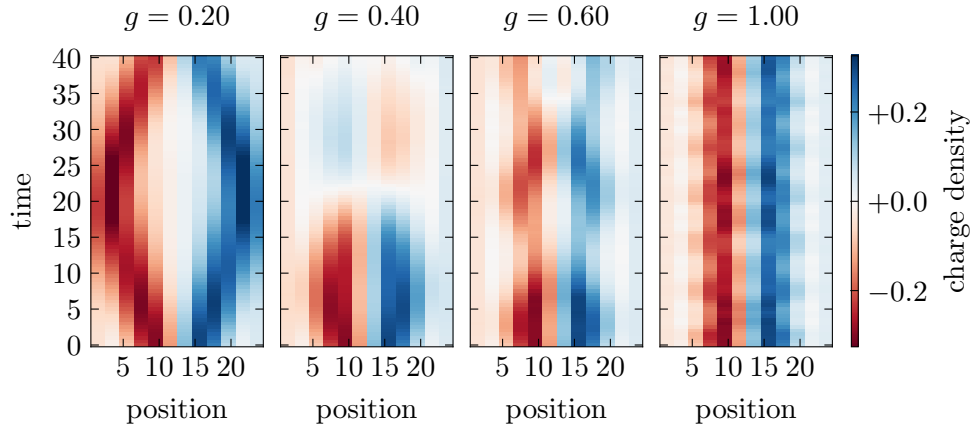
Figure 4.3: Dynamics of a fermion and an antifermion initially pointing one away from the other, for different values of the coupling. In all the simulations $m = 0.9$ and the momenta are $\mu_k \pm \sigma_k = \pm 0.5 \pm 0.2$

Schwinger model. The initial state is thus better qualified as an excited fermion-antifermion bound state. Here we prepared the initial state pretending to ignore the confining properties of the model but ended up obtaining a (very circumstantial) evidence of confinement. The limited achievable lattice sizes (24 sites) preclude a quantitative study of the confining properties of the model, which is anyhow beyond the scope of this Thesis. In the following, we take for granted that the correct asymptotic particle states are the charge neutral mesons discussed in Subsection 2.4B and focus on the study of meson-meson scattering processes.

The limited number of available lattice sites in the just discussed implementation does not allow for the preparation of an initial state of two well localized mesons, left aside the simulation of their dynamics. In order to study this problem, we need to reformulate it within a tensor network approach.

4.2B $\mathbb{Z}_N$ Model and Matrix Product State Representation

The second approach to the simulation of the Schwinger model is based on the $\mathbb{Z}_N$ gauge model ($N = 2\Lambda + 1$, $\Lambda = 1, 2, 3$), originating from a cyclic electric field truncation scheme, and on a MPS representation of the sate of the system.

In addition to the fermion local Hilbert spaces $\mathscr{H}_x$, located on the sites of the chain, the link Hilbert spaces $\mathscr{H}_{x,x+1}$ and the related operators have to be represented. In

the electric field eigenbasis, the link operators are defined by

$$E\left|\Lambda\right\rangle = \Lambda\left|\Lambda\right\rangle \ , \qquad U\left|\Lambda\right\rangle = \begin{cases} \left|+\Lambda\right\rangle \ , & \Lambda = -\Lambda \\ \left|\Lambda - 1\right\rangle \ , & \text{otherwise} \end{cases} . \tag{4.10}$$

In terms of the operators (4.1) and (4.10), the Hamiltonian reads

$$H = \frac{g^2}{2}\sum_x (E^{x+1}{}_x)^2 + \frac{i}{2}\sum_x \left[\sigma^+_{x+1}U^{x+1}{}_x\sigma^-_x - \sigma^+_x(U^{x+1}{}_x)^\dagger\sigma^-_{x+1}\right] + m\sum_x (-1)^x n_x \ . \tag{4.11}$$

In order to have a nearest-neighbour Hamiltonian, as required by TEBD, we group the Hilbert spaces of a site and of the subsequent link together[6]

$$\mathscr{H}_x \otimes \mathscr{H}_{x,x+1} \to \tilde{\mathscr{H}}_x \ . \tag{4.12}$$

The operators defined on $\mathscr{H}_x$ and $\mathscr{H}_{x,x+1}$ are extended to operators on $\tilde{\mathscr{H}}_x$ by taking their Kronecker product with an identity on $\mathscr{H}_{x,x+1}$ and $\mathscr{H}_x$ respectively. With this grouping, the tensors of the Hamiltonian MPO are similar to the free ones:

$$[W_H^{k_{x-1}k_x}] = \begin{bmatrix} 1 & \sigma^+ U^\dagger & \sigma^- U & (-1)^x m\,n + g^2/2\,E^2 \\ 0 & 0 & 0 & -i/2\,\sigma^- \\ 0 & 0 & 0 & +i/2\,\sigma^+ \\ 0 & 0 & 0 & 1 \end{bmatrix} . \tag{4.13}$$

Our proposal of a meson wave packet consisting of uncorrelated fermion and antifermion pairs can be prepared dressing the free theory wave packet creation operators (4.4) according to (2.143). The fermion wave packet creation operator becomes

$$\mathcal{A}^\dagger = \sum_x \tilde{\phi}(x) \left[\prod_{y<x}(-1)^{n_y}\right] \sigma^+_x \left[\prod_{y\geq x}(U^{y+1}{}_y)^\dagger\right] \ , \tag{4.14}$$

whose MPO representation is in terms of

$$[W_{\mathcal{A}^\dagger}^{k_{x-1}k_x}] = \begin{bmatrix} (-1)^n & \tilde{\phi}(x)\,\sigma^+ U^\dagger \\ 0 & U^\dagger \end{bmatrix} . \tag{4.15}$$

Analogously for the antifermion case $\mathcal{B}^\dagger$. These are the MPOs that we use to prepare the initial state in all the simulation shown in the following pages. As done for

---

[6] Notice that this operation is not generally convenient when working with MPOs only.

the free theory simulations, as $\tilde{\phi}(x)$ we use the amplitude $\tilde{\phi}(x; \mu_x, \mu_k, \sigma_k)$ in (2.71), corresponding to a normal momentum space distribution.

Although not implemented in the simulations shown here, we found an MPO representation of the generic dressed meson wave packet creation operator (2.141), namely of

$$
\mathcal{C}^\dagger = \sum_{xy} \tilde{\phi}(x,y) \left[\prod_{z<x} (-1)^{n_z} \right] \sigma_x^+ \left[\prod_{z\geq x} (U^{z+1}{}_z)^\dagger \right] \left[\prod_{z<x} (-1)^{n_z} \right] \sigma_x^- \left[\prod_{z\geq x} U^{z+1}{}_z \right] .
$$
(4.16)

In order to derive the MPO representation of this operator, it is convenient to rewrite it in a different form. Using the commutation between operators that act on different sites, $(-1)^{2n} = 1$ and the unitarity of the comparator

$$
\mathcal{C}^\dagger = \sum_{xy} \tilde{\phi}(x,y) \begin{cases} n_x , & x = y \\ \sigma_x^+ \left[\displaystyle\prod_{x\leq z<y} (-1)^{n_z} (U^{z+1}{}_z)^\dagger \right] \sigma_y^- , & x < y \\ \sigma_x^+ \left[\displaystyle\prod_{y\leq z<x} (-1)^{n_z} (U^{z+1}{}_z) \right] \sigma_y^- , & x > y \end{cases} ;
$$
(4.17)

recalling also $(-1)^n \sigma^- = \sigma^-$ and $\sigma^+ (-1)^n = \sigma^+$,

$$
\mathcal{C}^\dagger = \sum_{xy} \tilde{\phi}(x,y) \begin{cases} n_x , & x = y \\ \sigma_x^+ (U^{z+1}{}_z)^\dagger \left[\displaystyle\prod_{x<z<y} (-1)^{n_z} (U^{z+1}{}_z)^\dagger \right] \sigma_y^- , & x < y \\ \sigma_y^- (U^{z+1}{}_z) \left[\displaystyle\prod_{y<z<x} (-1)^{n_z} (U^{z+1}{}_z) \right] \sigma_x^+ , & x > y \end{cases} .
$$
(4.18)

Finally, the $W_{\mathcal{C}^\dagger}$ tensors of the MPO representation of this operator are shown in Figure 4.4. These tensors have a virtual index of dimension $L + 2$, a fact that might make the contraction with an MPS quite resource heavy for long chains. However, the MPO can be compressed, numerically [71] or analytically, by discarding the rows and columns related to irrelevant amplitudes, $f_y \ll 1$. The relevance of this MPO comes from the fact that all the approximations we made in the preparation of our meson states are contained in the functional form of $\tilde{\phi}(x,y)$. If a more precise guess for the amplitude $\tilde{\phi}(x,y)$ is available, it suffices to plug it in the tensors in Figure 4.4.

With the introduced tools, various simulations of meson-meson scatterings have been performed. Except for the different operators involved, the simulations follow the

$$
\begin{bmatrix}
1 & \sigma^-U & & & f_L\,\sigma^+U^\dagger & \cdots & f_{x+1}\,\sigma^+U^\dagger & f_x\,n \\
 & (-1)^n U & & & & & & f_{x-1}\,\sigma^- \\
 & & \ddots & & & & & \vdots \\
 & & & (-1)^n U & & & & f_1\,\sigma^- \\
 & & & & (-1)^n U^\dagger & & & \\
 & & & & & \ddots & & \\
 & & & & & & (-1)^n U^\dagger & \\
 & & & & & & & \sigma^- \\
 & & & & & & & 1
\end{bmatrix}
$$

Figure 4.4: Meson wave packet creation MPO tensors. For the $W^{k_{x-1}k_x}$ tensor, $f_y = \tilde{\phi}(x,y)$. Empty entries represent null operators.

same workflow of the free theory ones. During the simulation, together with the charge density and the bond entropy we measure also the expectation value of the electric field, which we always average over pairs of neighbouring sites in the plots shown below.

Scattering for different couplings. Some meson-meson scatterings for fixed mass and initial wave packet parameters but different coupling strengths have been simulated in the $\mathbb{Z}_7$ Schwinger model[7] on a lattice with 80 sites. The results are shown in Figures 4.5 and 4.6. For comparison, we also report the evolution predicted by the free theory[8]. In all the simulations of this paragraph the MPS singular values are truncated at 5×10^{-5} and a fourth order Trotter decomposition with $\delta t = 0.0625$ is used for TEBD.

For the weak coupling $g = 0.08$ the scattering trajectories approach the free ones. Conversely, in the stronger $g = 0.20$ case we observe a clear repulsion of the two mesons which starts even before the two mesons have completely penetrated one into the other. The intermediate case is more enigmatic: it seems that a (likely unstable)

---

[7] See the following paragraphs for a justification of the choice $N = 7$.

[8] This is obtained using the MPS code from the free theory, the same result can be obtained setting $g = 0$ in the the Schwinger model code.
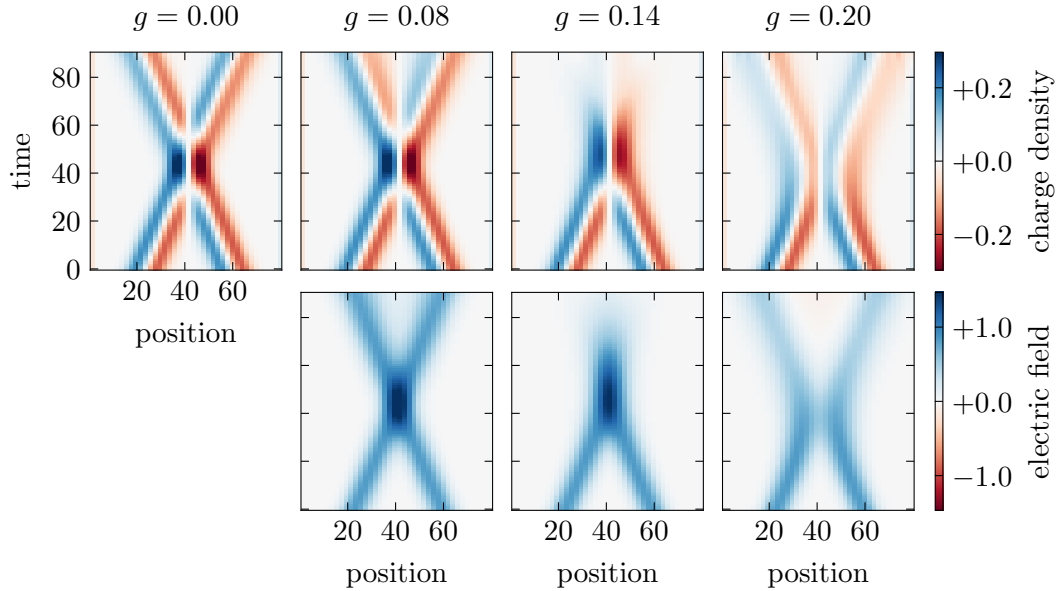
Figure 4.5: Charge density and electric field during a meson-meson scattering, for different values of the coupling. The mass is $m = 0.9$. The fermion and antifermion wave packets have $\mu_k \pm \sigma_k = \pm 0.80 \pm 0.15$.

intermediate state is produced. However, the final product(s) of the collision are not clearly distinguishable from the above plot, we will return on this case below.
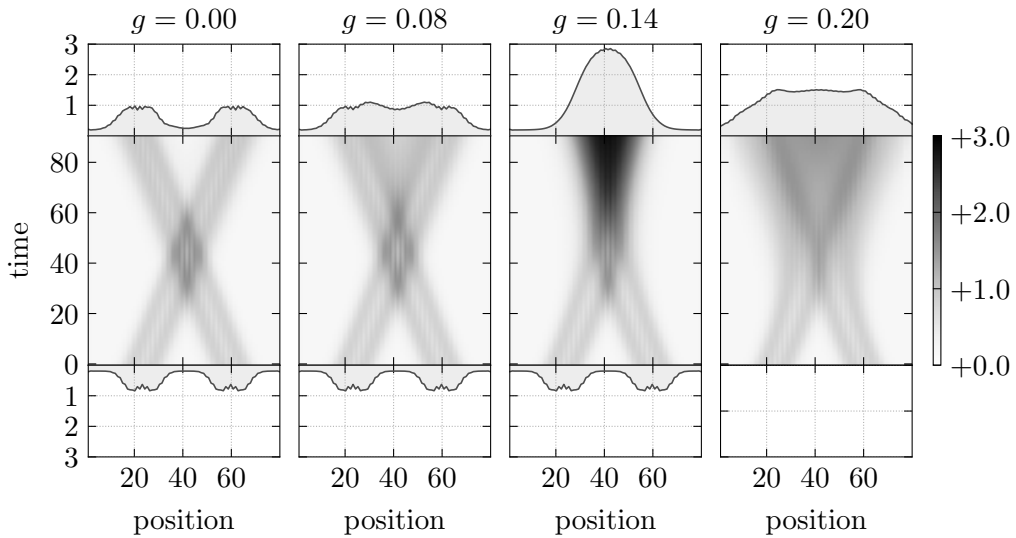
Figure 4.6: Bond entropy during the same simulations of Figure 4.5. The top and bottom plots show the entanglement entropy profile at the initial and final time.

Another interesting quantity we have monitored during these simulations is the entanglement entropy, shown in Figure 4.6. The absence of entanglement between the fermion and antifermion constituents of a single meson is an artifact of the factorization of the meson amplitude in a pair of uncorrelated fermion and antifermion amplitudes. We observe that, as soon as the interaction is turned on, some entanglement is generated between the final products of the collision. This entanglement generation is the most apparent difference between the free and $g = 0.08$ cases. The intermediate coupling case $g = 0.14$ is again peculiar and requires further investigation.
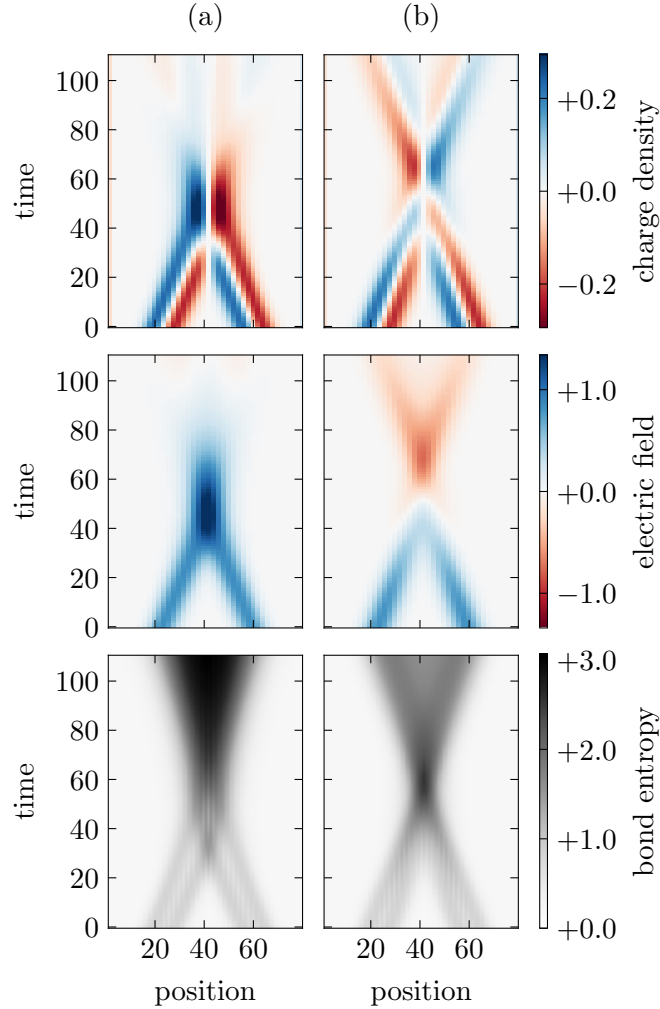
Figure 4.7: Scattering of mesons with different momenta for $g = 0.14$. Momenta are $\mu_k \pm \sigma_k = \pm 0.80 \pm 0.15$ (left) and $\pm 0.45 \pm 0.15$ (right). The remaining parameters are the ones of the simulations in Figure 4.5.

We simulated its evolution for a longer time. The result is plotted in Figure 4.7 (a). From the final part of the evolution it seems that the outcome of the collision is a superposition of different possible products with similar associated probabilities; further investigations are anyway required for this case. We also simulated a scattering of a pair of mesons with lower momenta and same value of all the other parameters. The phenomenology, shown in Figure 4.7 (b) is quite different: the products of the collision are clearly also two mesons, but their polarization is inverted with respect to the one of the incoming mesons.

Another case that we consider is that of two oppositely polarized mesons. We do this for the stronger coupling $g = 0.20$ and report the results in Figure 4.8 (b). For comparison in Figure 4.8 (a) we report also the scattering for aligned meson polarizations from the previous simulations. The prominent difference between the two processes is a stronger entanglement generation in the case of antialigned mesons.
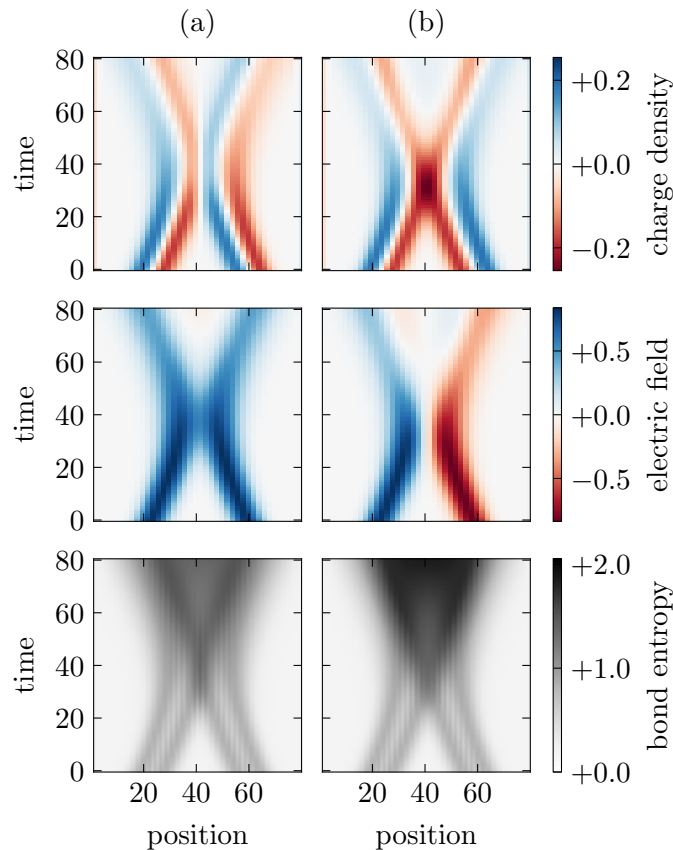
Figure 4.8: Scattering of mesons with aligned or antialigned polarizations for $g = 0.20$. The other parameters are identical to those of Figure 4.5.

Convergence and truncation of the MPS singular values. In order to validate all the above results it is important to verify the convergence of the simulations with the minimum singular value (SV) threshold ϵ. This has been done for the simulation with the strongest coupling in Figure 4.5. We choose this case because, on very general grounds, stronger interactions induce stronger correlations (slower SV decay) and thus the effects of the truncation are expected to be more severe. The parameters of the model are $m = 0.9$, $g = 0.20$ and $N = 7$. The lattice size is $L = 80$. All simulations use a fourth order Trotter decomposition with $\delta t = 0.05$ and terminate at $t = 80$, corresponding to a final Trotterization error of about 5×10^{-4}. The convergence is qualitatively depicted in Figure 4.9.
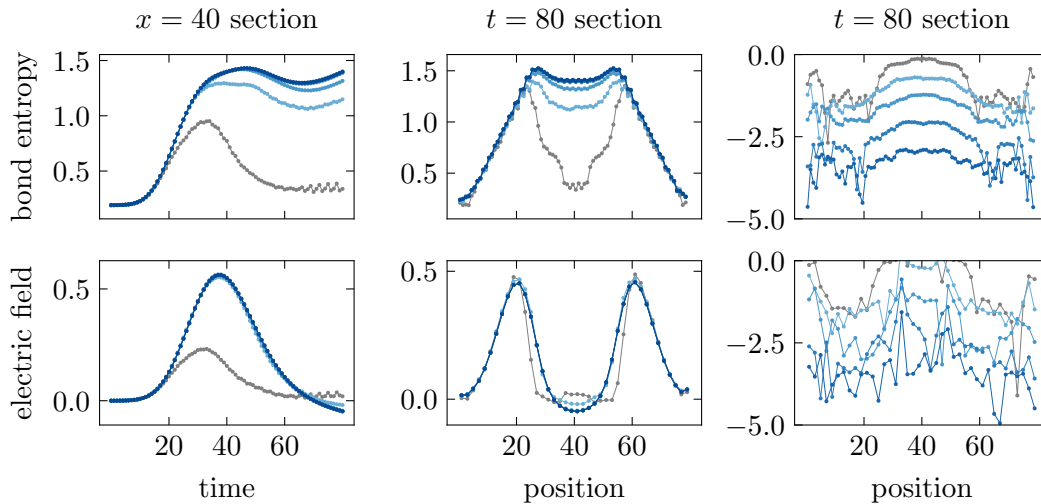
Figure 4.9: Convergence of the simulations with the SV cutoff ϵ, namely: $\epsilon = 10^{-3}$ (grey line) and $\epsilon = 10^{-3.5}, 10^{-4}, \ldots, 10^{-5.5}$ (progressively darker shades of blue). The first row is concerned with the bond entropy, the second with the electric field. Left column: time evolution of the midchain values of the above quantities; center column: their profile at the end of the simulation; rightmost column: logarithm of the relative deviations of the results in the previous column with respect to the result X^* corresponding to the smallest SV: $\log_{10}(|X/X^* - 1|)$.

A more quantitative study of the convergence is carried out using the value of the midchain entanglement entropy S_{mid} at the end of the simulation as a reference quantity. Its expected value S^*_{mid} is extrapolated by means of a power law fit of S_{mid} as a function of the SV threshold ϵ. Afterwards, we computed the relative deviations
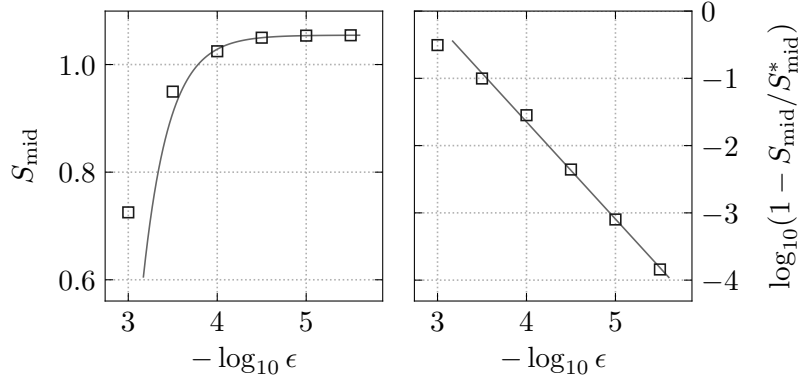
Figure 4.10: Convergence of the final midchain entropy with the SV cutoff. Left: midchain entanglement at $t = 80$ and weighted interpolation (weight $1/\epsilon^2$) via $S_{\mathrm{mid}}(\epsilon) = A\epsilon^B + S_{\mathrm{mid}}^*$. Right: logarithm of the relative deviations from S_{mid}^* and linear fit. The outlier simulation $\epsilon = 10^{-3}$ is ignored in both interpolations.

$\delta(\epsilon)$ from S_{mid}^*, namely

$$\delta(\epsilon) = \left| \frac{S_{\mathrm{mid}} - S_{\mathrm{mid}}^*}{S_{\mathrm{mid}}^*} \right| = 1 - S_{\mathrm{mid}}/S_{\mathrm{mid}}^* \ . \tag{4.19}$$

A linear interpolation of $\log_{10} \delta(\epsilon)$ as a function of $-\log_{10} \epsilon$ is shown in Figure 4.10. For ϵ small enough, the relative precision is found to scale as

$$\delta(\epsilon) \sim 10^{4.5 \pm 0.2} \epsilon^{1.45 \pm 0.04} \ . \tag{4.20}$$

We conclude that the simulations show a good convergence in the SV cutoff.

With our implementation we have been able to reach a precision in the measure of the midchain entanglement of $10^{-4} \sim 10^{-3}$ but the scaling (4.20) suggests that it should be possible to improve this value. However, the time required by the simulation increases with its precision. For our runs it ranges from $\mathcal{O}(10\ \mathrm{hours})$ for $\epsilon = 10^{-4}$, to $\mathcal{O}(100\ \mathrm{hours})$ for $\epsilon = 10^{-5.5}$. While this is still a reasonable amount of time, more efficient implementations are to be pursued if a relevant improvement in the precision is required. Very efficient tensor network simulations of lattice gauge theories can be achieved exploiting gauge redundancy of the theory and, at the same time, preserving the locality of the interaction [82]. Another important remark concerns the behaviour of the MPS bond dimension during the simulations. After the two mesons have started interacting entanglement generation takes place and results in a linear increase of maximum bond dimension χ_{max} with time, shown in
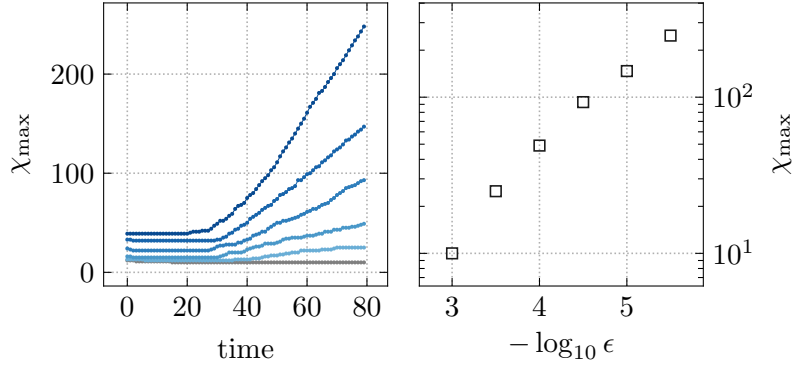
Figure 4.11: Maximum bond dimension χ_{max} at each time stamp (left) and of the whole simulation (right) for different SV cutoffs, namely: $\epsilon = 10^{-3}$ (grey line) and $\epsilon = 10^{-3.5}, 10^{-4}, \ldots, 10^{-5.5}$ (progressively darker shades of blue).

Figure 4.11. The consequent slowdown of the time evolution eventually causes the simulation to break down [94]. This behaviour is in stark contrast with what had been observed in the simulations of the free theory, where χ_{max} was found to be constant.

Truncation of the electric field. Another important simulation parameter is the number N of electric field levels resulting from the truncation procedure. It has been shown [79] that $N = 3$ gives already an excellent approximation of the exact ground state of the (massless) Schwinger model. For dynamical processes the answer is likely to depend significantly on the specific process under investigation. Here we focus on the meson-meson scatterings in Figures 4.5–4.6 and, more precisely, on the weakest coupling case $g = 0.08$. At a first analysis, this case appeared to be the most demanding one in terms of the number of link levels required. The interpretation is twofold: for weaker coupling it is energetically less unfavourable to excite states with high electric field, and the compenetration between the two mesons is more pronounced. This results in a high probability of finding at least two charges of the same sign on the same side of a bipartition of the chain. According to the Gauss law of the untruncated model, such a configuration should have a maximum electric field of at least 2, questioning the validity of an $N = 3$ truncation for scattering processes. As we now show, $N = 5$ turned out to be insufficient either.

The analysis that follows is based on the Schwinger model Gauss law (2.119)

$$\mathcal{G}(x) \, |\Psi_{\text{phys}}\rangle = 0 \; , \qquad \mathcal{G}(x) = E^{x+1}{}_x - E^x{}_{x-1} - \sigma_x^+ \sigma_x^- + \frac{1 - (-1)^x}{2} \; . \qquad (4.21)$$

As discussed in Subsection 2.4B the cyclic truncation scheme returns a $\mathbb{Z}_N$ gauge theory, whose gauge invariant states are only required to satisfy the original Gauss law modulo N, as per (2.133). If our aim was that of studying the $\mathbb{Z}_N$ lattice gauge theory, we should treat all these states as physical. Since here the $\mathbb{Z}_N$ model is introduced as an approximation of the U(1) theory, we still regard the states not satisfying the U(1) Gauss law as unphysical. On the other hand, these states can be generated by the dynamics of the $\mathbb{Z}_N$ theory and even by our meson creation operators. When a configuration that cannot be represented exactly with the available number of electric field levels is generated, the U(1) Gauss law is violated. We conclude that, even if there is no way of consistently imposing the physical state condition, we can easily check for its violation monitoring the expectation value of the U(1) Gauss law. If the truncated model is a good approximation of the exact theory, we expect the state of the system $|\Psi\rangle$ to always contain a small fraction of Gauss law violating configurations and thus to yield a small $\langle\Psi|\mathcal{G}(x)|\Psi\rangle$. If this is not the case we conclude that more link levels are needed.

The expectation value of the Gauss law in $\mathbb{Z}_3$, $\mathbb{Z}_5$ and $\mathbb{Z}_7$ simulations of a meson-meson scattering with $m = 0.9$, $g = 0.08$ are shown in Figure 4.12 (in two colour scales). The singular values are truncated at 10^{-5}. According to the convergence behaviour in[9] Figure 4.10 the truncation error should be $\mathcal{O}(10^{-3})$. An error of the same magnitude comes from the $\delta t = 0.05$ fourth order Trotter decomposition.

While the simulated values of N are too few to study a convergence of some observable, the obtained results still allow to draw some conclusions. In all the simulations a violation of Gauss law is observed but in the $N = 7$ case the violation is below the precision of the simulation $\mathcal{O}(10^{-3})$, as is clear from the plot in the second row. Observe that for $N = 3$ Gauss law is badly violated even by the preparation of the meson states; for $N = 5$ a significant violation takes place when the tails of the meson wave packets start to compenetrate.

---

[9] Actually, those results are referred to the strong coupling case. In the weak coupling case the convergence might be slightly different but the orders of magnitude are likely to be the same.
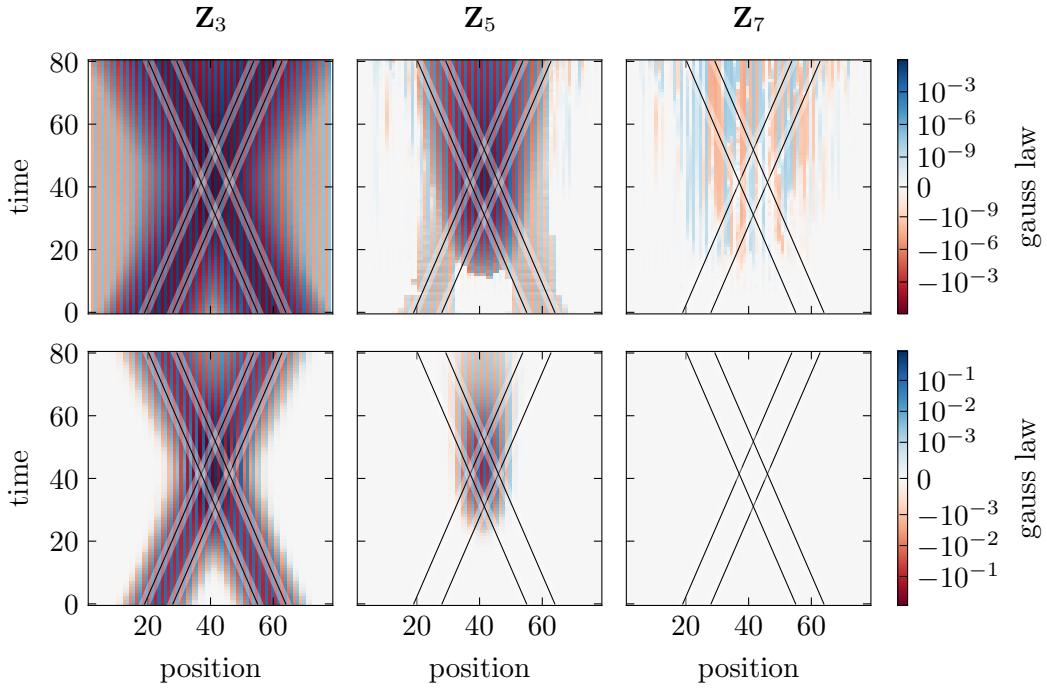
Figure 4.12: Gauss law violation (expectation value) in $\mathbb{Z}_3$, $\mathbb{Z}_5$ and $\mathbb{Z}_7$ simulations of a weak coupling meson-meson scattering. The colour scale is linear for $-\delta < \langle \mathcal{G} \rangle < +\delta$ and logarithmic outside, with $\delta = 10^{-9}$ for the plots in the first row and $\delta = 10^{-3}$ for the second. The alternating sign is due to the usage of staggered fermions and $\rho = \sigma_x^+ \sigma_x^- - (x \bmod 2)$. The free peak trajectories are shown in overlay to help locating the space-time region where the Gauss law violation takes place.

Conclusion and Outlook

We presented an idealized description of a scattering process and we specialized it to a recipe for the lattice computation of S-matrix elements. We reviewed the classical Hamiltonian description of $1 + d$ dimensional abelian and nonabelian continuum gauge theories, deriving the Gauss law constraint and discussing how it should be treated upon quantization. We then focused on Hamiltonian lattice theories, introducing a possible lattice description of Dirac fermions fields, namely staggered fermions, and gave a unified presentation of the compact formulation of abelian and nonabelian gauge theories. We solved the quantum theory of free staggered fermions in $1+1$ dimensions and showed that it reproduces the features of its continuum counterpart. The solution we found allowed us to construct creation operators for free fermion wave packets. The generalization to higher space dimensions is straightforward. We then studied the theory of quantum electrodynamics in $1 + 1$ dimensions, also known as Schwinger model. We presented some strategies to approximate the theory using a finite dimensional Hilbert space: the integration of the electric field, the quantum link models and the $\mathbb{Z}_N$ gauge theories. Some of these apply also in higher space dimensions or to nonabelian gauge theories. We identified the asymptotic states of the theory as meson bound states and discussed how such states can be prepared, with different degrees of approximation.

We studied tensor network methods for the numerical simulation of quantum manybody problems, specifically matrix product states and operators. Exploiting them, we verified our solution of the free theory by simulating the kinematics of some free fermion wave packets. Afterwards, we simulated some scattering processes in the Schwinger model using two approaches. We first integrated out the gauge field degrees of freedom which, however, was not efficient enough to observe meaningful scatterings. On the contrary, tensor network methods allowed us to explore these processes. We backed up this claim by reporting the outcome of some proof of principle scattering simulations of the collision between two mesons, and by studying their numerical convergence. We were able to reproduce different behaviours for different coupling strengths. These ranged from a qualitatively almost free propagation to a manifest repulsion. We monitored the entanglement entropy during the scattering and observed that, in contrast with the free theory, the interaction always generates entanglement between the final products of the collision. We gave a preliminary characterization of the minimum N required for a $\mathbb{Z}_N$ simulation of meson-meson scatterings.

A possible follow up of this work consists in its generalization to non abelian theories and, maybe, to higher space dimensions. Another outlook concerns the improvement of the modelling of the initial meson states. Some possibilities in this direction have already been hinted in this Thesis. Apart from the introduction of these and other additional features, it should be stressed that the tools developed with this work already allow for the investigation of some interesting phenomena in the lattice Schwinger model. We thus conclude that it might be worth to perform new simulations in a systematic way, varying the model or initial wave packets parameters. Finally, it should be possible to increase the lattice size and, eventually, study the continuum and thermodynamic limits of the obtained results. If this turns out to be too demanding in terms of computational resources, we mentioned that there is room for significant optimizations in our tensor network codes. The implementation of more efficient simulations provides yet another potential future continuation of this work.

A

Fermions in 1 + 1 Dimensions

According to Wigner [3], particles are classified on the basis of their transformation law under spacetime (and eventually internal, but we ignore these here) symmetries. We now review [50] the possibilities in $1 + 3$ spacetime dimensions and analyze the differences arising in $1 + 1$ dimensions.

First of all, we shall be more precise about what is meant by spacetime symmetries. In Section 1.1 we identified these with the Poincaré group, however, it turned out [7, 8, 12] that among Lorentz transformations only those that do not change the orientation of space or time are exact symmetries of nature. These belong to its identity component, the restricted Lorentz group $\mathrm{SO}^+(1, d)$. In this Thesis invariance under space inversions is also assumed, but it can be implemented separately because

$$\mathrm{O}(1, d) \cong \{1, \mathcal{P}, \mathcal{T}, \mathcal{PT}\} \ltimes \mathrm{SO}^+(1, d) \tag{A.1}$$

where $\mathcal{P}$ and $\mathcal{T}$ are parity and time-reversal.

All is left to do is to study the representations of the restricted Poincaré group $\mathrm{ISO}^+(1, d)$. As a prerequisite, its Lie algebra is

$$[M_{\mu\nu}, M_{\rho\sigma}] = \eta_{\mu\rho} M_{\nu\sigma} - \eta_{\mu\sigma} M_{\nu\rho} - \eta_{\nu\rho} M_{\mu\sigma} + \eta_{\nu\sigma} M_{\mu\rho} \tag{A.2a}$$

$$[M_{\mu\nu}, P_\rho] = \eta_{\mu\rho} P_\nu - \eta_{\nu\rho} P_\mu \tag{A.2b}$$

$$[P_\mu, P_\nu] = 0 \tag{A.2c}$$

with $d(d + 1)/2$ independent $M_{\mu\nu} = -M_{\nu\mu}$ generating Lorentz transformations in a neighborhood of the group identity and $1 + d$ momenta P_μ generating translations.

The unitary irreducible representations can be found by the method of induced representations [3], now informally summarized for completeness. Notice that, since the (restricted) Lorentz and Poincaré groups are not compact, their nontrivial unitary representations will be infinite dimensional.

Firstly, the unitary irreps of the translation group are characterized. These are in

correspondence with the (generalized) eigenvectors of the four-momentum operator,

$$\hat{U}(a)\,|p\sigma\rangle = e^{-ia^\mu \hat{P}_\mu}\,|p\sigma\rangle = e^{-ia^\mu p_\mu}\,|p\sigma\rangle \ ; \tag{A.3}$$

labeled by $p^\mu \in \mathbb{R}^{1,d}$ and a *finite*[1] index σ for the (p-independent) degeneracy. Secondly, the orbits of $\mathrm{SO}^+(1,d)$ in p^μ space are identified. Exponentiating (A.2b) $\hat{P}^\mu$ is seen to transform in the fundamental representation of the Lorentz group and so do its eigenvectors[2]. Consequently, the orbits are labeled by the invariants $m^2 = p^\mu p_\mu$ and, for $m \geq 0$, by $\mathrm{sgn}\,p_0$. A unitary representation of the whole $\mathrm{ISO}^+(1,d)$ is obtained appropriately "gluing together" the spaces generated by $|p\sigma\rangle$ corresponding to momenta p_μ in a given orbit. Thirdly, the action of $\mathrm{SO}^+(1,d)$ on each orbit is factorized as follows. Chosen a representative momentum k_μ, any $\Lambda \in \mathrm{SO}^+(1,d)$ can be decomposed in a standard transformation $\overline{\Lambda}_p$ that maps[3] $|k\sigma\rangle$ in $|p\sigma\rangle$ and a transformation W of the *isotropy group* or *little group*, leaving k_μ invariant

$$\hat{U}(\Lambda)\,|p\sigma\rangle = \hat{U}(\Lambda)\,\hat{U}(\overline{\Lambda}_p)\,|k\sigma\rangle = \hat{U}(\overline{\Lambda}_{\Lambda p})\,\hat{U}(\overline{\Lambda}_{\Lambda p}^{-1}\Lambda\overline{\Lambda}_p)\,|k\sigma\rangle = \hat{U}(\overline{\Lambda}_{\Lambda p})\,\hat{U}(W)\,|k\sigma\rangle \ . \tag{A.4}$$

Lastly, the possible $\hat{U}(W)$, furnishing a representation of the little group, have to be investigated. The physical orbits fall in three different classes, ($m > 0$, $p^0 > 0$), ($m^2 = 0$, $p^0 > 0$) and $p^\mu = 0$, each with its own little group. For concreteness, let us focus on the first case. As representative momentum we may take $k^0 = m$, $k^i = 0$. The associated little group is the rotation group $\mathrm{SO}(d)$ which is compact and thus has finite dimensional unitary irreps $D_{\sigma\tau}(W)$, validating the requirement that the degeneracy index is finite. Analogous results hold for the other two classes of orbits. In particular $p^\mu = 0$ (assumed to be degeneracy-free) is identified with the vacuum state $|0\rangle$ of the theory, corresponding to the absence of particles rather than a single particle state. It is trivially invariant under the whole $\mathrm{ISO}^+(1,d)$.

The classification of the unitary irreps of the Poincaré group has thus been reduced to the simpler problem of finding the unitary irreps of the rotation group. Yet to discuss is the construction of projective representations. In [3] Wigner proved that every projective unitary representation of the restricted Poincaré group in four spacetime dimensions comes from an ordinary one of its covering group $\mathrm{SL}(2,\mathbb{C}) \ltimes \mathbb{R}^{1,3}$. The above derivation goes on unchanged, except for the little groups which are replaced with their double covers, e.g., $\mathrm{SO}(3)$ is replaced by $\mathrm{Spin}(3) \cong \mathrm{SU}(2)$, giving rise to half-integer quantum numbers. Their unitary irreps are labeled by spin $j \in \mathbb{N}/2$ (for the $m > 0$) case and helicity $j \in \mathbb{Z}/2$ ($m = 0$). Finally, the *spin-statistic* theorem

---

[1]   This reasonable requirement is because we want (1.115) to hold for a finite number of quantum fields. Eventual continuous degeneracies are considered unphysical.

[2]   Explicitly, $\hat{P}^\mu \hat{U}(\Lambda)\,|p\sigma\rangle = \hat{U}(\Lambda)\,\hat{U}^\dagger(\Lambda)\,\hat{P}^\mu \hat{U}(\Lambda)\,|p\sigma\rangle = \hat{U}(\Lambda)\,\Lambda^\mu{}_\nu \hat{P}^\nu\,|p\sigma\rangle = \Lambda^\mu{}_\nu p^\nu\,\hat{U}(\Lambda)\,|p\sigma\rangle$.

[3]   Eventually redefining the degeneracy index such a Λ can always be found.

[13, 50] states that, in order to preserve causality, fields that correspond via (1.115) to irreps of even (odd) $2j$ have to commute (anticommute) at separated spacetime points, thus satisfying bosonic (fermionic) statistic.

In *two spacetime dimensions* the intrinsically projective representations emerge in a different way but these do not admit a physical interpretation as particles [51]. On the other hand the little groups encountered in ordinary representations, such as SO(1), are trivial whence, properly speaking, there is *no such thing as spin* and all fields are scalars [39]. Nevertheless, the restricted Lorentz group still possesses integer and half-integer quantum number representations. Most importantly, fields in these representations still obey commutation and anticommutation relations respectively [39, 72]. In light-cone coordinates,

$$x^{\pm} = x^0 \pm x^1 \;, \quad \eta = \mathrm{d}x^+ \, \mathrm{d}x^- \;; \tag{A.5}$$

the defining representation of $\mathrm{SO}^+(1,1)$ consists of the boost matrices

$$\Lambda_\xi = \begin{bmatrix} e^{+\xi} & 0 \\ 0 & e^{-\xi} \end{bmatrix} = e^{\xi M_{01}} \;, \qquad M_{01} = \begin{bmatrix} +1 & 0 \\ 0 & -1 \end{bmatrix} \tag{A.6}$$

parametrized by the rapidity ξ. It is clearly reducible; the irreducible representations are labeled by $j \in \mathbb{R}$ and read

$$D^j : \Lambda_\xi \overset{\sim}{\longmapsto} e^{j\xi} \;. \tag{A.7}$$

Among these, the ones with $j \in \mathbb{Z}/2$ correspond to commuting or anticommuting fields [39]. Now, (A.6) shows that under parity $\xi \to -\xi$; if $\mathcal{P}$ is to be implemented, irreps consist of either D^0 or pairs of opposite j representations $D^j \oplus D^{-j}$ that get exchanged by $\mathcal{P}$. For $j = 1$ the vector representation (A.6) is recovered; $j = 1/2$ is instead the Dirac spinor[4]. Indeed, in two spacetime dimensions a possible choice of gamma matrices verifying (1.43) is

$$\gamma_0 = \begin{bmatrix} 0 & 1 \\ 1 & 0 \end{bmatrix} \;, \quad \gamma_1 = \begin{bmatrix} 0 & -1 \\ 1 & 0 \end{bmatrix} \quad \leadsto \quad \Sigma_{01} = \frac{1}{2}\gamma_0\gamma_1 = \frac{1}{2}\begin{bmatrix} +1 & 0 \\ 0 & -1 \end{bmatrix} \;, \tag{A.8}$$

providing a boost generator which is half of the one of vectors (A.6), as expected. From (A.8) it is also clear that the Dirac spinorial representation embeds a parity transformation implemented by means of γ_0.

---

[4] Contrary to what happens in $d = 3$ where inequivalent finite-dimensional representations of the Lorentz group induce inequivalent unitary representations of the Poincare group, all these different j representations correspond to the same (up to the mass $\hat{P}^2$) Poincaré representation [39].

B

Staggered Functions

Consider the piecewise (staggered) function

$$\varphi\colon \{1, 2, \ldots, 2N\} \to \mathbb{C} \,, \quad x \mapsto \begin{cases} \chi^{\mathrm{E}}(x) & x \text{ even} \\ \chi^{\mathrm{O}}(x) & x \text{ odd} \end{cases} \,. \tag{B.1}$$

An expression for its discrete Fourier transform $\mathcal{F}$ can be obtained rewriting φ as

$$\varphi(x) = \varphi^{\mathrm{E}}(x) + \varphi^{\mathrm{O}}(x) = \frac{1 + (-1)^x}{2}\chi^{\mathrm{E}}(x) + \frac{1 - (-1)^x}{2}\chi^{\mathrm{O}}(x) \,; \tag{B.2}$$

and applying the discrete convolution theorem [48]

$$\varphi(k) = \varphi^{\mathrm{E}}(k) + \varphi^{\mathrm{O}}(k) = \left\{ \mathcal{F}\left[\frac{1 + (-1)^x}{2}\right] * \mathcal{F}[\chi^{\mathrm{E}}] + \mathcal{F}\left[\frac{1 - (-1)^x}{2}\right] * \mathcal{F}[\chi^{\mathrm{O}}] \right\}(k) \,, \tag{B.3}$$

with $k \in (\pi/N)\{-N, -N+1, \ldots, N-1\}$. Observing that

$$1 = e^{i0x} = \sum_k e^{ikx}\delta(k) \,, \qquad (-1)^x = e^{i\pi x} = \sum_k e^{ikx}\delta(k + \pi) \tag{B.4}$$

and thus

$$\frac{1}{2N} \sum_{\substack{x \text{ even} \\ x \text{ odd}}} e^{-ikx} = \mathcal{F}\left[\frac{1 \pm (-1)^x}{2}\right](k) = \frac{\delta(k) \pm \delta(k + \pi)}{2} \,; \tag{B.5}$$

the convolutions are trivial

$$\varphi^{\mathrm{E}}(k) = \frac{\chi^{\mathrm{E}}(k) + \chi^{\mathrm{E}}(k + \pi)}{2} \,, \qquad \varphi^{\mathrm{O}}(k) = \frac{\chi^{\mathrm{O}}(k) - \chi^{\mathrm{O}}(k + \pi)}{2} \,. \tag{B.6}$$

Notice the completely general behaviour under $k \to k + \pi$,

$$\varphi^{\mathrm{E}}(k + \pi) = +\varphi^{\mathrm{E}}(k) \,, \qquad \varphi^{\mathrm{O}}(k + \pi) = -\varphi^{\mathrm{O}}(k) \,; \tag{B.7}$$

we refer to these stating φ^{E} (φ^{O}) is π-periodic (π-antiperiodic) or π-shift even (odd).

Bibliography

[1] P. Jordan and E. Wigner, "Über das Paulische äquivalenzverbot", Zeitschrift für Physik **47**, 631–651 (1928) `10.1007/BF01331938`.

[2] P. A. M. Dirac, *The Principles of Quantum Mechanics* (Clarendon Press, 1930).

[3] E. Wigner, "On Unitary Representations of the Inhomogeneous Lorentz Group", Annals of Mathematics **40**, 149–204 (1939) `10.2307/1968551`.

[4] P. G. Bergmann, "Non-Linear Field Theories", Physical Review **75**, 680–685 (1949) `10.1103/PhysRev.75.680`.

[5] P. A. M. Dirac, "Generalized Hamiltonian Dynamics", Canadian Journal of Mathematics **2**, 129–148 (1950) `10.4153/CJM-1950-012-1`.

[6] C. N. Yang and R. L. Mills, "Conservation of Isotopic Spin and Isotopic Gauge Invariance", Phys. Rev. **96**, 191–195 (1954) `10.1103/PhysRev.96.191`.

[7] T. D. Lee and C. N. Yang, "Question of Parity Conservation in Weak Interactions", Physical Review **104**, 254–258 (1956) `10.1103/PhysRev.104.254`.

[8] C. S. Wu, E. Ambler, R. W. Hayward, D. D. Hoppes, and R. P. Hudson, "Experimental Test of Parity Conservation in Beta Decay", Physical Review **105**, 1413–1415 (1957) `10.1103/PhysRev.105.1413`.

[9] J. Schwinger, "Gauge Invariance and Mass. II", Physical Review **128**, 2425–2429 (1962) `10.1103/PhysRev.128.2425`.

[10] P. W. Anderson, "Plasmons, Gauge Invariance, and Mass", Physical Review **130**, 439–442 (1963) `10.1103/PhysRev.130.439`.

[11] R. M. Johnson, "On a theorem stated by eckart and young", Psychometrika **28**, 259–263 (1963) `10.1007/BF02289573`.

[12] J. H. Christenson, J. W. Cronin, V. L. Fitch, and R. Turlay, "Evidence for the 2π decay of the K_2^0 meson", Physical Review Letters **13**, 138–140 (1964) `10.1103/PhysRevLett.13.138`.

[13] R. F. Streater and A. S. Wightman, *PCT, Spin and Statistics, and All That* (W. A. Benjamin, 1964).

[14] S. Coleman and J. Mandula, "All Possible Symmetries of the S Matrix", Physical Review **159**, 1251–1256 (1967) `10.1103/PhysRev.159.1251`.

[15] S. L. Adler, "Axial-Vector Vertex in Spinor Electrodynamics", Phys. Rev.
      177, 2426–2438 (1969) `10.1103/PhysRev.177.2426`.

[16] J. S. Bell and R. Jackiw, "A PCAC puzzle: $\pi 0 \rightarrow \gamma\gamma$ in the σ-model", Il
      Nuovo Cimento A (1965-1970) **60**, 47–61 (1969) `10.1007/BF02823296`.

[17] J. Schwinger, *Quantum Kinematics and Dynamics* (W. A. Benjamin, 1970).

[18] J. H. Lowenstein and J. A. Swieca, "Quantum electrodynamics in two dimen-
      sions", Annals of Physics **68**, 172–195 (1971) `10.1016/0003-4916(71)90246-`
      `6`.

[19] M. E. Fisher and M. N. Barber, "Scaling Theory for Finite-Size Effects in the
      Critical Region", Phys. Rev. Lett. **28**, 1516–1519 (1972) `10.1103/PhysRevLett.`
      `28.1516`.

[20] K. G. Wilson, "Confinement of quarks", Phys. Rev. D **10**, 2445–2459 (1974)
      `10.1103/PhysRevD.10.2445`.

[21] A. A. Belavin, A. M. Polyakov, A. S. Schwartz, and Y. S. Tyupkin, "Pseu-
      doparticle solutions of the Yang-Mills equations", Physics Letters B **59**, 85–87
      (1975) `10.1016/0370-2693(75)90163-X`.

[22] S. Coleman, R. Jackiw, and L. Susskind, "Charge shielding and quark confine-
      ment in the massive schwinger model", Annals of Physics **93**, 267–275 (1975)
      `https://doi.org/10.1016/0003-4916(75)90212-2`.

[23] J. Kogut and L. Susskind, "Hamiltonian formulation of Wilson's lattice gauge
      theories", Phys. Rev. D **11**, 395–408 (1975) `10.1103/PhysRevD.11.395`.

[24] T. Banks, L. Susskind, and J. Kogut, "Strong-coupling calculations of lattice
      gauge theories: $(1 + 1)$-dimensional exercises", Phys. Rev. D **13**, 1043–1053
      (1976) `10.1103/PhysRevD.13.1043`.

[25] C. G. Callan, R. F. Dashen, and D. J. Gross, "The structure of the gauge
      theory vacuum", Phys. Lett. B **63**, 334–340 (1976) `10.1016/0370-2693(76)`
      `90277-X`.

[26] L. Susskind, "Lattice fermions", Phys. Rev. D **16**, 3031–3039 (1977) `10.1103/`
      `PhysRevD.16.3031`.

[27] M. Creutz, "Quantum electrodynamics in the temporal gauge", Annals of
      Physics **117**, 471–483 (1979) `10.1016/0003-4916(79)90365-8`.

[28] S. Elitzur, R. B. Pearson, and J. Shigemitsu, "Phase structure of discrete
      Abelian spin and gauge systems", Physical Review D **19**, 3698–3714 (1979)
      `10.1103/PhysRevD.19.3698`.

[29] D. Horn, M. Weinstein, and S. Yankielowicz, "Hamiltonian approach to $z(n)$ lattice gauge theories", Physical Review D **19**, 3715–3731 (1979) `10.1103/PhysRevD.19.3715`.

[30] J. B. Kogut, "An introduction to lattice gauge theory and spin systems", Rev. Mod. Phys. **51**, 659–713 (1979) `10.1103/RevModPhys.51.659`.

[31] N. E. Bralic, "Exact computation of loop averages in two-dimensional Yang-Mills theory", Phys. Rev. D **22**, 3090–3103 (1980) `10.1103/PhysRevD.22.3090`.

[32] C. Itzykson and J. B. Zuber, *Quantum Field Theory*, International Series In Pure and Applied Physics (McGraw-Hill, New York, 1980).

[33] D. Horn, "Finite matrix models with continuous local gauge invariance", Physics Letters B **100**, 149–151 (1981) `10.1016/0370-2693(81)90763-2`.

[34] L. H. Karsten and J. Smith, "Lattice fermions: Species doubling, chiral invariance and the triangle anomaly", Nucl. Phys. B **183**, 103–140 (1981) `10.1016/0550-3213(81)90549-6`.

[35] H. B. Nielsen and M. Ninomiya, "A no-go theorem for regularizing chiral fermions", Phys. Lett. B **105**, 219–223 (1981) `10.1016/0370-2693(81)91026-1`.

[36] L. Castellani, "Symmetries in constrained hamiltonian systems", Annals of Physics **143**, 357–371 (1982) `https://doi.org/10.1016/0003-4916(82)90031-8`.

[37] R. P. Feynman, "Simulating physics with computers", International Journal of Theoretical Physics **21**, 467–488 (1982) `10.1007/BF02650179`.

[38] D. Friedan, "A proof of the Nielsen-Ninomiya theorem", Commun. Math. Phys. **85**, 481–490 (1982) `10.1007/BF01403500`.

[39] P. Yip, "Spinors in two dimensions", J. Math. Phys. **24**, 1206–1212 (1983) `10.1063/1.525798`.

[40] R. Jackiw, "Topological investigations of quantized gauge theories", in *Current algebra and anomalies*, edited by S. B. Treiman, R. Jackiw, B. Zumino, and E. Witten (WORLD SCIENTIFIC, 1985), pp. 211–359, `10.1142/0131`.

[41] S. B. Treiman, R. Jackiw, B. Zumino, and E. Witten, *Current Algebra and Anomalies* (WORLD SCIENTIFIC, 1985), `10.1142/0131`.

[42] A. M. Polyakov, *Gauge Fields and Strings* (Harwood Academic Publishers, 1987).

[43] H. Kleinert, *Gauge Fields in Condensed Matter* (WORLD SCIENTIFIC, 1989), `10.1142/0356`, eprint: `https://www.worldscientific.com/doi/pdf/10.1142/0356`.

[44] P. Orland and D. Rohrlich, "Lattice gauge magnets: Local isospin from spin", Nuclear Physics B **338**, 647–672 (1990) `10.1016/0550-3213(90)90646-U`.

[45] M. Suzuki, "General theory of fractal path integrals with applications to many-body theories and statistical physics", Journal of Mathematical Physics **32**, 400–407 (1991) `10.1063/1.529425`, eprint: `https://doi.org/10.1063/1.529425`.

[46] M. Henneaux and C. Teitelboim, *Quantization of Gauge Systems* (Princeton University Press, Aug. 1994).

[47] A. Wipf, "Hamilton's formalism for systems with constraints", in Canonical Gravity: From Classical to Quantum, edited by J. Ehlers and H. Friedrich, Lecture Notes in Physics (1994), pp. 22–58, `10.1007/3-540-58339-4_14`, eprint: `https://arxiv.org/abs/hep-th/9312078v3`.

[48] W. L. Briggs and V. E. Henson, *The DFT: An Owners' Manual for the Discrete Fourier Transform* (SIAM, Jan. 1995).

[49] M. E. Peskin and D. V. Schroeder, *An Introduction To Quantum Field Theory* (Avalon Publishing, Oct. 1995).

[50] S. Weinberg, *The Quantum Theory of Fields*, Vol. 1 (Cambridge University Press, 1995), `10.1017/CBO9781139644167`.

[51] S. K. Bose, "Projective representations of the 1+1-dimensional Poincaré group", Journal of Mathematical Physics **37**, 2376–2387 (1996) `10.1063/1.531516`.

[52] R. Haag, *Local Quantum Physics: Fields, Particles, Algebras*, Theoretical and Mathematical Physics (Springer Berlin Heidelberg, 1996), `10.1007/978-3-642-61458-3`.

[53] S. Weinberg, "What is Quantum Field Theory, and What Did We Think It Is?", in Conceptual foundations of quantum field theory. Proceedings, Symposium and Workshop, Boston, USA, March 1-3, 1996 (Mar. 1996), pp. 241–251, arXiv:`hep-th/9702027`.

[54] S. Chandrasekharan and U.-J. Wiese, "Quantum link models: A discrete approach to gauge theories", Nucl. Phys. B **492**, 455–471 (1997) `10.1016/S0550-3213(97)80041-7`.

[55] J. Kijowski, G. Rudolph, and A. Thielmann, "Algebra of Observables and Charge Superselection Sectors for QED on the Lattice", Communications in Mathematical Physics **188**, 535–564 (1997) `10.1007/s002200050178`.

[56] B. B. Beard, R. C. Brower, S. Chandrasekharan, D. Chen, A. Tsapalis, and U. .-J. Wiese, "D-theory: field theory via dimensional reduction of discrete variables", Nuclear Physics B - Proceedings Supplements, Proceedings of the XVth International Symposium on Lattice Field Theory **63**, 775–789 (1998) `10.1016/S0920-5632(97)00900-6`.

[57] R. Gupta, "Introduction to Lattice QCD", (1998), arXiv:`hep-lat/9807028` `[hep-lat]`.

[58] R. Brower, S. Chandrasekharan, and U.-J. Wiese, "QCD as a quantum link model", Physical Review D **60**, 094502 (1999) `10.1103/PhysRevD.60.094502`.

[59] E. Abdalla, M. C. B. Abdalla, and K. D. Rothe, *Non-Perturbative Methods in 2 Dimensional Quantum Field Theory*, 2nd (WORLD SCIENTIFIC, 2001), `10.1142/4678`.

[60] T. Byrnes, *Density Matrix Renormalization Group: A New Approach to Lattice Gauge Theory* (timbyrnes, 2003).

[61] B. S. DeWitt and B. S. DeWitt, *The Global Approach to Quantum Field Theory* (Oxford University Press, 2003).

[62] J. B. Kogut and M. A. Stephanov, "The Phases of Quantum Chromodynamics: From Confinement to Extreme Environments", in (Cambridge University Press, Dec. 2003) Chap. 6 The Hamiltonian version of lattice gauge theory.

[63] S. Chandrasekharan and U.-J. Wiese, "An Introduction to Chiral Symmetry on the Lattice", Prog. Part. Nucl. Phys. 53 (2004) 373-418, `10.1016/j.ppnp.2004.05.003` (2004) `10.1016/j.ppnp.2004.05.003`, arXiv:`hep-lat/0405024v1` `[hep-lat]`.

[64] T. H. Hansson, V. Oganesyan, and S. L. Sondhi, "Superconductors are topologically ordered", Annals of Physics **313**, 497–538 (2004) `10.1016/j.aop.2004.05.006`.

[65] M. B. Hastings, "An area law for one-dimensional quantum systems", Journal of Statistical Mechanics: Theory and Experiment **2007**, P08024–P08024 (2007) `10.1088/1742-5468/2007/08/P08024`.

[66] D. Tong, *Quantum Field Theory* (2007).

[67] K. Konishi and G. Paffuti, *Quantum Mechanics: A New Introduction* (Oxford University Press, Oxford, New York, Mar. 2009).

[68] U.-J. Wiese, "An introduction to lattice field theory", (2009).

[69] B. Pirvu, V. Murg, J. I. Cirac, and F. Verstraete, "Matrix product operator representations", New Journal of Physics **12**, 025012 (2010) `10.1088/1367-2630/12/2/025012`.

[70] A. H. Al-Mohy and N. J. Higham, "Computing the Action of the Matrix Exponential, with an Application to Exponential Integrators", SIAM Journal on Scientific Computing **33**, 488–511 (2011).

[71] U. Schollwöck, "The density-matrix renormalization group in the age of matrix product states", Annals of Physics, January 2011 Special Issue **326**, 96–192 (2011) `10.1016/j.aop.2010.09.012`.

[72] M. B. Green, J. H. Schwarz, and E. Witten, *Superstring Theory: Volume 1, Introduction: 25th Anniversary Edition*, 2012.

[73] D. B. Kaplan, "Chiral Symmetry and Lattice Fermions", (2012), arXiv:`0912.2560`.

[74] "The Oxford Handbook of Philosophy of Physics", in, edited by R. Batterman, Oxford Handbooks (Oxford University Press, Oxford, New York, Mar. 2013) Chap. 6 Effective Field Theories.

[75] E. Fradkin, *Field Theories of Condensed Matter Physics* (Cambridge University Press, Feb. 2013).

[76] P. Schindler, D. Nigg, T. Monz, J. T. Barreiro, E. Martinez, S. X. Wang, S. Quint, M. F. Brandl, V. Nebendahl, C. F. Roos, M. Chwalla, M. Hennrich, and R. Blatt, "A quantum information processor with trapped ions", New Journal of Physics **15**, 123012 (2013) `10.1088/1367-2630/15/12/123012`.

[77] F. Strocchi, *An Introduction to Non-Perturbative Foundations of Quantum Field Theory*, International Series of Monographs on Physics (Oxford University Press, Oxford, New York, Feb. 2013).

[78] P. Hoyer, "Bound states – from QED to QCD", in (2014), arXiv:`1402.5005` `[hep-ph]`.

[79] S. Kühn, J. I. Cirac, and M.-C. Bañuls, "Quantum simulation of the Schwinger model: A study of feasibility", Physical Review A **90**, 042305 (2014) `10.1103/PhysRevA.90.042305`.

[80] R. Orús, "A practical introduction to tensor networks: Matrix product states and projected entangled pair states", Annals of Physics **349**, 117–158 (2014) `10.1016/j.aop.2014.06.013`.

[81] E. Rico, T. Pichler, M. Dalmonte, P. Zoller, and S. Montangero, "Tensor Networks for Lattice Gauge Theories and Atomic Quantum Simulation", Phys. Rev. Lett. **112**, 201601 (2014) `10.1103/PhysRevLett.112.201601`.

[82] P. Silvi, E. Rico, T. Calarco, and S. Montangero, "Lattice Gauge Tensor Networks", New J. Phys. **16**, 103015 (2014) `10.1088/1367-2630/16/10/103015`, arXiv:`1404.7439`.

[83] M. S. Swanson, *Path Integrals and Quantum Processes* (Courier Corporation, Feb. 2014).

[84] U.-J. Wiese, "Towards quantum simulating QCD", Nucl. Phys. A, QUARK MATTER 2014 **931**, 246–256 (2014) `10.1016/j.nuclphysa.2014.09.102`.

[85] P. Coleman, *Introduction to Many-Body Physics* (Cambridge University Press, Nov. 2015).

[86] S. Notarnicola, E. Ercolessi, P. Facchi, G. Marmo, S. Pascazio, and F. V. Pepe, "Discrete Abelian Gauge Theories for Quantum Simulations of QED", Journal of Physics A: Mathematical and Theoretical **48**, 30FT01 (2015) `10.1088/1751-8113/48/30/30FT01`.

[87] M. Dalmonte and S. Montangero, "Lattice gauge theory simulations in the quantum information era", Contemp. Phys. **57**, 388–412 (2016) `10.1080/00107514.2016.1151199`.

[88] E. A. Martinez, C. A. Muschik, P. Schindler, D. Nigg, A. Erhard, M. Heyl, P. Hauke, M. Dalmonte, T. Monz, P. Zoller, and R. Blatt, "Real-time dynamics of lattice gauge theories with a few-qubit quantum computer", Nature **534**, 516–519 (2016) `10.1038/nature18318`.

[89] E. Zohar, J. I. Cirac, and B. Reznik, "Quantum Simulations of Lattice Gauge Theories using Ultracold Atoms in Optical Lattices", Reports on Progress in Physics **79**, 014401 (2016) `10.1088/0034-4885/79/1/014401`.

[90] M. C. Bañuls, K. Cichy, J. I. Cirac, K. Jansen, S. Kühn, and H. Saito, "Towards overcoming the Monte Carlo sign problem with tensor networks", EPJ Web of Conferences **137**, 04001 (2017) `10.1051/epjconf/201713704001`.

[91] I. Bengtsson and K. Zyczkowski, *Geometry of Quantum States: An Introduction to Quantum Entanglement* (Cambridge University Press, Aug. 2017).

[92] H. Bernien, S. Schwartz, A. Keesling, H. Levine, A. Omran, H. Pichler, S. Choi, A. S. Zibrov, M. Endres, M. Greiner, V. Vuletic, and M. D. Lukin, "Probing many-body dynamics on a 51-atom quantum simulator", Nature **551**, 579–584 (2017) `10.1038/nature24622`.

[93] E. Ercolessi, P. Facchi, G. Magnifico, S. Pascazio, and F. V. Pepe, "Phase transitions in Z_n gauge models: Towards quantum simulations of the Schwinger-Weyl QED", Physical Review D **98**, 074503 (2018) `10.1103/PhysRevD.98.074503`.

[94] J. Hauschild and F. Pollmann, "Efficient numerical simulations with tensor
      networks: tensor network python (tenpy)", SciPost Phys. Lect. Notes 5, `10.
      21468/SciPostPhysLectNotes.5` (2018) `10.21468/SciPostPhysLectNotes.
      5`, arXiv:1805.00055v4 `[cond-mat.str-el]`.

[95] S. Montangero, *Introduction to Tensor Network Methods: Numerical simula-
      tions of low-dimensional many-body quantum systems* (Springer International
      Publishing, 2018), `10.1007/978-3-030-01409-4`.

[96] D. Tong, *Gauge theory* (2018).

[97] M. C. Bañuls, R. Blatt, J. Catani, A. Celi, J. I. Cirac, M. Dalmonte, L.
      Fallani, K. Jansen, M. Lewenstein, S. Montangero, C. A. Muschik, B. Reznik,
      E. Rico, L. Tagliacozzo, K. Van Acoleyen, F. Verstraete, U.-J. Wiese, M.
      Wingate, J. Zakrzewski, and P. Zoller, "Simulating Lattice Gauge Theories
      within Quantum Technologies", (2019).

[98] T. Felser, P. Silvi, M. Collura, and S. Montangero, "Two-dimensional quantum-
      link lattice Quantum Electrodynamics at finite density", (2019).

[99] C. Nagele, J. E. Cejudo, T. Byrnes, and M. Kleban, "Flux unwinding in the
      lattice Schwinger model", Physical Review D **99**, 094501 (2019) `10.1103/
      PhysRevD.99.094501`.

[100] J. Preskill, "Simulating quantum field theory with a quantum computer", in
      Proceedings of The 36th Annual International Symposium on Lattice Field
      Theory — PoS(LATTICE2018), Vol. 334 (May 2019), p. 024, `10.22323/1.
      334.0024`.

[101] A. Smith, M. S. Kim, F. Pollmann, and J. Knolle, "Simulating quantum many-
      body dynamics on a current digital quantum computer", npj Quantum Infor-
      mation **5**, 106 (2019) `10.1038/s41534-019-0217-0`.

[102] A. Maas, *Lattice quantum field theory, Lecture in SS 2020 at the KFU Graz*
      (2020).

[103] S. V. Mathis, G. Mazzola, and I. Tavernelli, "Toward scalable simulations of
      Lattice Gauge Theories on quantum computers", arXiv:2005.10271 [cond-mat,
      physics:hep-lat, physics:quant-ph] (2020).

[104] S. Notarnicola, M. Collura, and S. Montangero, "Real-time-dynamics quan-
      tum simulation of $(1 + 1)$-dimensional lattice QED with Rydberg atoms",
      Physical Review Research **2**, 013288 (2020) `10.1103/PhysRevResearch.2.
      013288`.